Aus der Klinik und Poliklinik für Neurochirurgie
Direktor: Prof. Dr. med. H. W. S. Schroeder
Aus dem Institut für Pharmakologie
Direktor Prof. Dr. rer. nat. Mladen Tzvetkov
der Universitätsmedizin der Ernst-Moritz-Arndt-Universität Greifswald

Influence of ACT-209905 on glioblastoma growth *in vitro*

Inauguraldissertation zur Erlangung des akademischen Grades
Doktor der Wissenschaften in der Medizin
(Dr. med.)
an
der Universitätsmedizin
der Universität Greifswald

vorgelegt von: Yong Xiao
geboren am 21.10.1982
in Liaoning, V.R. China

Dekan: Prof. Dr. med. Karlhans Endlich

1. Gutachter: Prof. Dr. med. Henry Schroeder

2. Gutachter: Prof. Dr. med. Bernhard H. Rauch

3. Gutachter: Prof. Dr. rer. nat. Anke C. Fender

Ort, Raum: Greifswald (online defense)

Tag der Disputation: 24.08.2020

Table of contents

List of figures

List of tables

1 Summary

The glioblastoma multiforme (GBM) not only presents the most common tumor of the central nervous system in adults, it is also the most aggressive brain tumor. Although patients suffering from GBM standardly receive a combination of multiple treatments including surgery, radiotherapy and chemotherapy, its prognosis is still poor with a median survival time of only 12-15 months. Therefore, new and effective treatment methods are urgently needed.

A signaling molecule which is both involved in proliferation, migration and invasion of a broad range of healthy and malignant cells is the lipid mediator sphingosine-1-phosphate (S1P). Previous studies have confirmed that sphingosine-1-phosphate (S1P) receptor 1 (S1PR1) is involved in the regulation of proliferation, invasion, metastasis, vascular maturation and angiogenesis of GBM cells, and is closely related to the occurrence and development of tumors. Thus, ACT-209905 (provided by Actelion Pharmaceuticals) as a selective S1PR1 modulator was applied to gain insights into the molecular processes activated by S1PR1 in GBM cells using two human (LN18, U87MG) and one murine (GL261) GBM cell line.

In our in vitro cell viability analyses, we found that ACT-209905 significantly reduced viability of LN18 cells in a concentration dependent manner. A combined administration of ACT-209905 with S1PR2 inhibitors (Compound 16, Compound 16ME – both provided by ONO Pharmaceuticals, and JTE-013 – commercially available) showed a stronger effect than the single administration demonstrating that both S1PR1 and S1PR2 are involved in growth of GBM cells and may interact with each other. Our results also demonstrated that ACT-209905 can induce apoptosis in GBM cells since caspase 3 activity was induced by the S1PR1 modulator which might therefore play an important role in inhibiting the proliferation of GBM cells. Further, we found a significant inhibitory effect of ACT-209905 on the migration and invasion of LN18 and U87MG GBM cells arguing for a participation of S1PR1 signaling in migration and invasion of GBM cells, too. Stimulation of S1P receptors results in the activation of several kinases such as AKT1 and ERK1/2, correspondingly our immunoblot analyses showed a strong activation of both kinases by S1P which was reduced by ACT-209905 in LN18 cells but not in GL261 cells suggesting that different pathways are activated

by S1P in these GBM cell lines. Further studies have to be performed to clarify the role of AKT1 and ERK1/2 in the inhibitory effects of ACT-209905 on GBM proliferation, migration and invasion.

Currently, GBM stem cells are discussed as a reason for resistance against the radiochemotherapy and the recurrence of the tumor. Our immunoblot analyses showed that Nestin and CD133, two marker proteins for GBM stem cells, were higher expressed in GBM cells treated with ACT-209905 compared to control or S1P treated LN18 cells. Further investigations in the future might contribute to the elucidation of an involvement of the S1P receptors in the stem cell behavior of GBM cells. Paradoxically to the up-regulation of CD133 and Nestin by ACT-209905, treatment of LN18 stem-like neurospheres with ACT-209905 showed a significant cytotoxic effect of the compound which was even more pronounced in the stem-like neurosphere cells compared to the adherent parental LN18 cells.

Overall, the studies of this work improve our understanding of the complex mechanisms of S1P signaling in GBM cells and might drive the development of its pharmacological modulation as a new therapeutic principle in GBM. Furthermore, an extended knowledge about the molecular effects of ACT-209905 on GBM cells will broaden the understanding for possible future applications and clinical indications.

2 Introduction

2.1 Overview of glioblastoma multiforme

Glioblastoma multiforme (GBM) is the most common malignant tumor of the central nervous system in adults, accounting for 35.26% – 60.9% of intracranial tumors [1-3]. It is classified by the World Health Organization (WHO) into WHO grade IV by their latest intracranial tumor grading standard. GBM represents an astrocytic tumor being highly aggressive and invasive to the healthy brain tissue, and thus it can often not be completely removed by surgery. The symptoms of GBM depend on the location of the tumor and may include persistent headaches, seizures, vision changes, nausea, vomiting, loss of appetite, speech difficulties, changes in mood and behavior, energy, cranial nerve defects and motor- or paresthesia. The exact cause of GBM development is not clear, and most occur by chance without any genetic factors [4]. However, hereditary diseases such as neurofibromatosis and tuberous sclerosis are susceptibility diseases which are associated with a higher risk to suffer from glioma, and some oncogenes are discussed to be involved in the development of the disease [5-11].

Glioma mainly spreads in the central nervous system resulting in less distant metastasis. Only the bone metastasis of oligodendroglioma is reported in this case [13]. Enhanced magnetic resonance imaging (MRI) is a common method for diagnosing gliomas such as GBM [14].

The current standard therapy of GBM is gross total resection of the contrast enhanced MRI parts of the tumor followed by adjuvant radiochemotherapy with temozolomid. However, the tumor is often already spread in distant brain areas and is not surgically removable in total resulting in a rapid relapse of the tumor [15-19]. Although the treatment of GBM has continuously improved in the fields of nursing, surgical resection, radiotherapy and chemotherapy, its prognosis has not been substantially improved. The median survival time is still only 12 – 15 months [20-22]. By now, treatment methods fail to provide a complete cure for glioma, and because of its lack of specificity against target cells toxic side effects can cause secondary damage to healthy tissues and organs. Overall, the survival rate of GBM patients is not raised significantly after surgery. For example, Tumor-treating fields (TTF) is the first intervention in a decade leading to an improved survival in patients with newly

diagnosed GBM and was recently approved by the U.S. Food and Drug Administration (FDA) for use in combination with temozolomide [23,24]. The Phase III trial's data show that TTF plus chemotherapy after first disease recurrence prolonged overall survival of GBM patients, but only for 3 months (11.8 vs 9.2 months) [25]. Therefore, exploring more effective GBM comprehensive treatment methods has become a hot topic in medical research.

2.2 Role of Sphingosine-1-Phosphate in tumor biology

2.2.1 Overview of Sphingosine-1-Phosphate Signaling

Sphingosine-1-phosphate (S1P) is a bioactive lipid with several important physiological functions. It is widely found in body fluids and cells such as blood, lymph, red blood cells, neutrophils and platelets [26]. S1P is formed by the metabolism of sphingomyelin by the action of sphingomyelinase leading to the formation of ceramide which is which is further processed to sphingosine by the enzyme ceramidase. Sphingosine is then phosphorylated by the sphingosine kinase (Sphk) isoenzymes 1 and 2 giving rise to S1P [27]. SphK1 is mainly present in the cytoplasm, while SphK2 is primarly found in the nucleus [28]. Due to the differences in the distribution of SphK isoforms in various tissues and cells, S1P is produced in a specific microenvironment and activates its cell surface receptors (sphingosine-1-phosphate receptors, S1PRs) in an autocrine or paracrine manner. Five different sphingosin-1-phosphate receptors (S1PR1-5) are known which regulate a variety of biological functions such as cell growth, survival, exercise, differentiation, anti-apoptosis, angiogenesis, maturation as well as production of cytokines and chemical factors [29, 30]. In addition, S1P can also act as a second messenger to act directly within the cell to mediate a variety of biological effects [31]. S1P can be dephosphorylated by S1P phosphatases 1 and 2 to form sphingosine, or it can be irreversibly decomposed into phosphatidylethanolamine and hexadecenal by S1P lyase (S1PL). This maintains the dynamic balance of S1P in the human physiological environment [32,33].

2.2.2 Pathways by which S1P influences tumor growth

S1P plays an important role in the formation, transformation and progression of various malignant tumors, and can regulate tumor cell proliferation, apoptosis and angiogenesis [34].

Therefore, S1P has been increasingly recognized as an important carcinogen in recent years, involving a variety of cancer categories, including breast cancer, colorectal cancer, kidney cancer, lung cancer, melanoma, ovarian cancer as well as glioblastoma [35]. The S1P receptors (S1PR) seem to be key players in the involvement of progression of these tumor types. Interestingly, the intracellular secondary messenger function of S1P and the continuously activated signaling pathways are also thought to be a key to regulating cellular processes during cancer pathology. Although several studies have revealed the biological function of S1P, determining the specific mechanisms involved in a particular cancer type is more challenging. This is most likely due to the complex nature of the S1P signaling system, cell type-specific effects, abundance or deficiency of specific S1P receptors dependent on the cell type, and changes in the intracellular environment [36].

S1P can regulate the growth and apoptosis of tumor cells and stimulates angiogenesis, which is the result of its biological interaction with different S1PRs. S1PRs belong to the G protein-coupled receptor family. As mentioned above, five subtypes of S1PRs (1-5) have been found, of which S1PR1-3 are ubiquitously expressed in several tissues, while S1PR4 and S1PR5 are primarily expressed in blood cells and cells of the central nervous system. Further, all five S1PRs (cytoplasmic, and/or nuclear) are widely distributed in benign and/or malignant tissues of multiple systems/organs [37]. However, each S1PR subtype is different from the others in its systemic distribution, subcellular localization, and difference in the expression level between benign and malignant tissues [37]. An overlapping function and an ability of some opposite effects are peculiarities of these receptors. However, the role of the individual receptor subtype depends on the activation of the respective downstream effector proteins, in particular coupling to respective G-proteins [38]. For instance, S1PR1, S1PR2 and S1PR5 signal via Gi/o. S1PR2 and S1PR3 activate Gq, and S1PR2, S1PR3, and S1PR5 bind with G12/13. These Gα proteins stimulate the Ras/extracellular signal-regulated kinase (ERK), phosphoinositide 3-kinase (PI3K)/AKT, and Rho/ Ras homolog gene family (RhoA) kinase (ROCK) signaling pathways [39]. In addition, S1PR1 couples via a Gi-protein to multiple effector pathways, including phospholipase C (PLC), adenylate cyclase, and Ras/MAPK (Ras GTPase/mitogen-activated protein kinase). For example, S1P is known to stimulate tumor cell proliferation and migration through binding to S1PR1 whereas S1PR4 can promote the terminal differentiation of macrophages, mediate T cell immune responses,

and activate S1PR5 to inhibit the migration of brain glial cells [40-44]. Studies have also shown that S1P binds to S1PR1 and S1PR3, which promotes tumor growth and metastasis. In contrast, binding of S1P to S1PR2 can inhibit tumor growth and metastasis [45, 46].

Several studies have confirmed changes in S1P levels, as well as the involvement of their receptors and metabolic enzymes in many types of cancer pathophysiology. S1P levels in animal models of intestinal tumorigenesis, associated with decreased expression of S1P lyase (SPL) and decreased enzyme activity, was seen to increase compared to other local tissues [47,48]. In human ovarian cancer patients, S1P is elevated in plasma and malignant ascites [49,50]. High expression levels of S1PR1, S1PR3 and the S1P-producing enzyme SphK1 have also been reported in breast cancer patients [51-55]. Overexpression of SphK1 also has been observed in several tumor types of animal and xenograft models compared to respective normal tissues, including rat colon adenocarcinoma and mouse leukemia models, as well as human breast, lung and colon tumors [56]. Increased proliferation and decreased apoptosis are associated with high SphK1 expression in mouse breast cancer cells [57]. S1P, the SphK1/2 and the receptors S1PR1-3 and S1PR5 are involved in cell survival and growth, and are overexpressed in many tumors including glioblastoma. Elevated levels of S1P were found in GBM compared with non-malignant brain tissue. Studies have shown that the expression of SphK1 affects the survival of patients with glioblastoma, but the role of SphK1/2 and the receptors S1PR1-3 and S1PR5 has not been fully understood in the pathogenesis and progression of glioblastoma [58-62].

2.2.3 S1P signaling in Glioblastoma multiforme

In the brain, neurons and astrocytes are able to synthesize and release S1P, which is also the source of extracellular S1P [63]. In addition, it has been reported in the literature that GBM cells can also secrete S1P [64]. Recent studies have shown that S1P has high levels in GBM tissues, and S1P is involved in the proliferation, differentiation, survival and migration of tumor cells, and can also affect the survival of GBM stem cells [62, 63]. There are also reports that indicate high levels of SphK1 expression are closely associated with shorter survival times in GBM patients [59,67]. Our *in vitro* laboratory experiments found that S1P can affect the migration and invasion of GBM cells [62], and that S1PR1 and S1PR2 are associated with survival of GBM patients.

There is no definite evidence to support the involvement of S1P signaling in GBM, but many studies have shown that it plays an important role in the regulation of proliferation, invasion and migration of GBM cells [reviewed in 68]. Elevated expression levels of S1PR1, S1PR2, S1PR3 and S1PR5 can be detected in human GBM tumor tissues [62,69,70]; Further, the expression of S1PR1, S1PR2 and S1PR3 was also increased in GBM cells compared with healthy brain tissue, but only S1PR1 and S1PR2 were significantly associated with patient survival [62,69]. In C6 rat glioma cells, S1PR2 plays a major role for S1P-induced shape changes, while S1PR1 and S1PR3 show synergistic effects [71]. However, research from Quint and colleagues has shown that S1PR5 is also an important factor affecting the prognosis of patients with GBM [72].

S1PR1-5 is coupled with Gi/o, and S1PR2 and S1PR3 are coupled with Gq [73]. S1PR1 is not but the other S1PRs are coupled with G12/13. When coupled with Gi/o, S1PRs activate downstream phospholipase C (PLC), Ras, and Phosphatidylinositol-3-kinase (PI3K). PLC regulates cell chemotaxis by activating downstream Ca^{2+} and protein kinase C (PKC). Ras regulates cell proliferation by activating downstream extracellular signal regulated kinase (ERK). PI3K affects cell survival and motility by activating downstream protein kinases (Proteinkinase B, Akt) and Rac, respectively. When S1PRs are coupled to Gq, the downstream PLC can be activated to precipitate the chemotaxis of downstream Ca^{2+} and PKC regulatory cells. When G12/13 is activated by S1PRs, the downstream Rho is activated to regulate the anti-migratory performance of the cells [74, 75]. S1PR1 uses Gi proteins to join with a variety of effector pathways, including phospholipase C (PLC), adenylate cyclase, and Ras/MAPK (Ras GTPase/mitogen-activated protein kinase). In GBM, S1P activates multiple signaling pathways in parallel, including mitogen-activated extracellular signal-regulated kinase (MAPK/ERK), protein kinase C (PKC), Ca2+ signaling via PLC, and phospholipase D (PLD) [76-78].

The significant role of S1PR modulators in inhibiting or delaying tumor cell proliferation and metastasis has been given more and more attention by researchers, which has opened up new ways to approach the treatment of GBM and provided new considerations. Future research will reveal if S1P-based treatment options are effective against GBM in patients and whether they show better safety and tolerance.

2.3 S1PR1 and ACT-209905 – an S1PR1 modulator

S1PR1 was the first S1PR to be discovered and is still the most studied S1PR. S1PR1 is widely expressed in tissue cells of various organs and can be found in different parts of the cell, such as the nucleus, cytoplasm, cell membrane, and cytoplasm. During embryonic development, S1PR1 is highly expressed in the blood vessels and nervous system, which is particularly important for the normal development of the vasculature. In adult tissues, S1PR1 is highly expressed in the lung, brain and immune organs (such as the marginal zone of the spleen) [79]. S1PR1 is biologically diverse and an important lymphocyte surface receptor that can effectively promote lymphocyte blood entry [80]. At the same time, S1PR1 is closely related to various immune system diseases such as autoimmune encephalomyelitis, autoimmune diabetes, arthritis and colitis, and participates in affecting many aspects of the immune system [81].

Current research shows that tumor cells can promote tumor development through S1PR1 signaling pathways, and increased S1PR1 expression can promote tumor proliferation, invasion and metastasis. For example, activation of the S1PR1 promoter can induce the expression of endogenous S1PR1 in bladder tumor cells of MB49 mice, thereby promoting tumor proliferation and invasion [82]. Furthermore, increasing the expression of S1PR1 in renal cell G401 cells and changing the balance of S1PR1/S1PR2 expression causes active G401 cells to acquire metastatic properties [83]. Silencing the expression of S1PR1 in tumor endothelial cells by small interfering RNA or antagonizing the activity of S1PR1 by antibodies can inhibit tumor growth [84]. Liu et al. [85] showed that silencing the S1PR1 gene inhibited angiogenesis and neovascularization of transplanted tumors. This study also showed that after S1PR1 gene knockout, the maturation and establishment of blood vessels in mice were impaired, suggesting that S1PR1 is an important receptor for stimulating tumor angiogenesis and vascular maturation. Priceman et al. [86] found that S1PR1 can promote the growth of tumors by regulating the enrichment of Treg cells, inhibiting the penetration of $CD8^+$ T cells and its function in the B16 mouse model and E0771 medullary breast cancer model, which is related to the work of Arikawa et al. [87]. In addition, Chae et al. [88] found that S1PR1 is up-regulated in tumor blood vessels. Downregulation of its expression can inhibit tumor angiogenesis and tumor growth, indicating that S1PR1 is an important regulator of tumor

angiogenesis. Further, it was also found that S1PR1 overexpressed in murine melanoma cells promoted migration and invasion of cancer cells [87].

There is still disagreement about the precise impact of S1PR1 in the pathogenesis and progression of GBM. Immunohistochemical analyses from Quint et al. [89] showed that S1PR1 is overexpressed in GBM of human patients. However, Watts et al. [90] observed that a low expression of S1PR1 in tumor tissue is significantly associated with the worse survival rate of patients with malignant glioblastoma. The downregulation of S1PR1 expression promoted the proliferation of tumor cells which reduced the survival rate of patients. Our team's experimental results also demonstrate that downregulation of S1PR1 expression enhances the malignancy of glioblastoma leading to poor survival rates of patients suffering from GBM [62] which is in agreement with a study from Yoshida and colleagues [91]. This is unexpected since S1P is known to stimulate tumor cell proliferation and migration through binding to $S1P_1$. Nevertheless, siRNA-mediated silencing of $S1P_1$ in T98G and G112 glioma cells results in increased cell proliferation [91]. Depending on the individual expression of $S1P_1$ and the other S1P receptor subtypes as well as the connection to differentially activated intracellular signaling pathways, S1P may mediate both pro- and anti-tumorigenic effects. Our group could not show an extraordinary role of $S1P_1$ in proliferation of LN18 glioma cells since the $S1P_1$ inhibitor W146 only slightly decreased cell viability whereas a potent function of $S1P_1$ in S1P-mediated GBM cell migration was observed [62]. In general, stimulation of cultured GBM cells with S1P either results in unchanged or enhanced cell proliferation mediated by $S1P_1$, $S1P_2$ and $S1P_3$ whereas $S1P_5$ inhibits S1P-stimulated cell proliferation [92,93]. It has been further shown that motility of GBM cells is stimulated by S1P and involves both $S1P_1$ and $S1P_3$ [94]. Our group demonstrated a role of $S1P_1$ and $S1P_2$ but not of $S1P_3$ in migration of GBM cells [62]. At present, most of the research results support the idea that S1PR1 promotes tumor development. Nevertheless, the relationship between S1PR1 and GBM needs to be further studied to draw a final conclusion. Interestingly, a sphingosine analogue named fingolimod (FTY720), that down regulates expression of sphingosine-1-phosphate receptors, causes apoptosis of multiple tumor cell types, including glioma cells. This immunosuppressant modulator of S1P signaling, which is proved for treatment of multiple sclerosis, also induces apoptosis in brain tumor stem cells representing thus a potential therapeutic agent for glioblastoma patients. Further S1PR1

modulators has been developed by Actelion Pharmaceutics (Basel, Schweiz) such as ponesimod (ACT128800) and ACT-209905 [95,96]. The latter one is composed of an amino pyridine group, an oxadiazole spacer, a 2-ethyl-5-methylphenol moiety and a chiral 1-amino-2-propanol side chain (Figure 1).

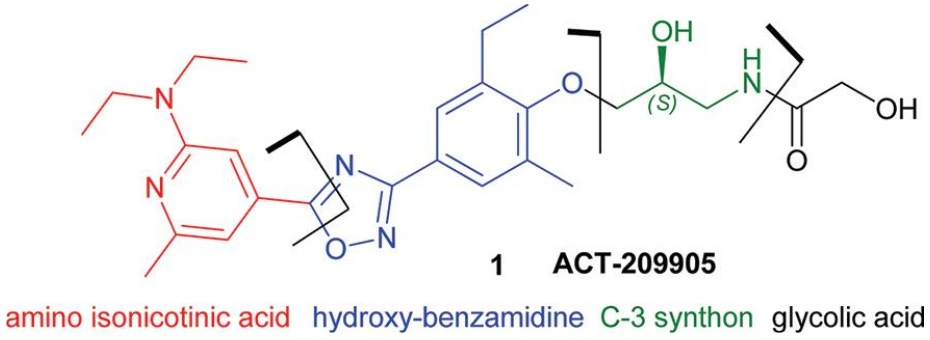

Figure 1. Chemical structure of the S1PR1 modulator ACT-209905 (from [95]).

As FTY720 and ponesimod, ACT-209905 is a S1PR1 receptor modulator with immunomodulating properties that could be of use in autoimmune diseases [97,98]. So far, there are no reports investigating the potential anti-glioma effects of ponesimod or ACT-209905.

Although the signaling mechanisms of S1P receptor subtypes have been comparatively easy to recognize, due to their heterogeneity, the S1P signaling pathways involved in the pathogenesis of GBM might be quite different. To unravel the complex pathogenic mechanisms of GBM, a more in-depth study is required to clarify the role of the S1P signaling in the development of GBM.

2.4 Objective

Glioblastoma (GBM) is the most common malignant tumor of the CNS in the adults. After maximal safe surgical resection, the conventional standard of care is radiotherapy with concomitant temozolomide followed by maintenance temozolomide [99]. Despite aggressive multimodal therapy, the prognosis of patients with GBM is poor [100]. S1P is one of the metabolite products of membrane sphingomyelin, and it plays an important role in formation, transformation and progression of many malignant tumors as well as the regulation of cell proliferation, apoptosis and angiogenesis. A targeted modulation of S1P

receptor subtypes may thus represent a promising therapeutic strategy against the progression of GBM.

Therefore, expression of all five S1P receptor subtypes was also analyzed in different GBM cell lines and stem-like GBM cells. Afterwards, the influence of S1P receptor 1 (S1PR1) inhibition by ACT-209905 on proliferation, apoptosis and migration were studied in two human (LN18, U87MG) and one murine (GL261) GBM cell line. Also, a combined blockade of S1PR1 and S1PR2 was investigated in the GBM cells. Further, expression of GBM stem cell marker proteins (Nestin and CD133) was analyzed after inhibition of S1PR1 by ACT-209905. To gain an insight in the underlying post-receptor signaling pathways, we determined the activation status of AKT1 and ERK1/2 as two potential down-stream kinases of the S1PR1. Overall, the purpose of this study was to understand the molecular role of S1PR1 in the pathognesis of GBM, to pre-clinically evaluate ACT-209905 as possible therapeutic agent in GBM cells, and clarify whether ACT-209905 has similar effects as fingolimod on growth behaviour of GBM cells *in vitro*.

3 Material

3.1 Laboratory equipment and aids

Cell culture incubator	BBD 6220, Heraeus Instruments, Hanau
Blot Apparatur	Biometra®, Göttingen
Casy® 1 Modell TT	Schärfe-System GmbH, Reutlingen
ChemiDoc™ XRS	Bio-Rad Molecular Imager® Bio-Rad, München
Compact Line OV 4	Biometra®, Göttingen
Filter paper	VWR International GmbH, Hannover
QBT Dry Block Heating Systems	Bioblock Scientific, Thermolyne Corp., Dubuque, Iowa, USA
Shaker	Rocking Platform, Biometra®, Göttingen
Infinite M200 Microplate reader	TECAN, Crailsheim
MULTIWELL™ 6/12/96-well-Platten	BD Falcon™, Heidelberg
Nanodrop ND-1000	peqLab Biotechnology GmbH, Erlangen
Nitrocellulose membran	Whatman GmbH, Protan®, Dassel
PIKO Real 96	Thermo Scientific, Waltham, Massachusetts, USA
Pipetboy acu	Integra Biosciences GmbH, Fernwald
SDS-Page Elektrophoresekammer	Biometra®, Göttingen
Software	i-Control Infinite M200, TECAN, Crailsheim
	Nanodrop, v3.5.2, Thermo Scientific, Waltham, Massachusetts, USA
	Office 2010, Microsoft, USA
	Prism 6 for Windows, v6.01, GraphPad Software, Inc., USA
	QuantityOne®, v4.6.9, Bio-Rad, München

Standard Power Pack P25	Biometra®, Göttingen
Laminar flow bench	HERASafe, Heraeus Instruments, Hanau
T100™ Thermal Cycler	Bio-Rad Laboratories GmbH, München
Vacuum pump	Vacuubrand, Wertheim
Vortexer	Reaxtop, Heidolph, Schwabach
	VWR International GmbH, Hannover
Weighing machine	Explorer, Ohaus, Schweiz
Water bath	Julabo, Seelbach GFL, Burgwedel
Tissue Culture Flask 25 cm^3, 75 cm^3	BD Falcon™, Heidelberg
Centrifuge	Centrifuge 5430 R Eppendorf AG Hamburg
	Centrifuge 5804 R Eppendorf AG Hamburg
	Heraeus Fresco 21, Thermo Scientific,
M-Pact AX822 Balance	Waltham, Massachusetts, USA
MR 3001 Magnetic Stirring Hotplate	Sartorius, USA
	Heidolph, Schwabach, Germany

3.2 Chemicals

Acrylamide	Carl Roth GmbH, Karlsruhe
Amersham™ ECL Select™ Western Blotting Detection Reagent	GE Healthcare, Buckinghamshire, UK
Ammonium persulphate (APS)	Sigma-Aldrich Co, Deisenhofen
Aprotinin	Sigma-Aldrich Co, Deisenhofen
Aqua dest.	B. Braun, Melsungen
Bicinchoninic Acid Solution (BCA)	Sigma-Aldrich Co, Deisenhofen
Bovine serum albumin (BSA)	Paa Laboratories GmbH, Pasching, Österreich
Casy®ton	Schärfe-System GmbH, Reutlingen

CAY10444	CAYMAN Chemicals, Michigan, USA
Desoxyribonucleotidtriphosphate (dNTP) (10 mM)	Applied Biosystems™, Weiterstadt
DMEM Medium	PAN-Biotech GmbH, Germany
DPBS Medium	PAN-Biotech GmbH, Germany
Ethanol 70 %	Carl Roth GmbH, Karlsruhe
Fetale calve serum (FCS)	GIBCO®, Invitrogen, Karlsruhe
Glutamine	GIBCO®, Invitrogen, Karlsruhe
Glycerol	Carl Roth GmbH, Karlsruhe
Isopropanol	Carl Roth GmbH, Karlsruhe
Potassium chloridechlorid (KCl)	Sigma-Aldrich Co, Deisenhofen
Leupeptin	Sigma-Aldrich Co, Deisenhofen
Lipofectamine 2000	Invitrogen, life technologies™, Darmstadt
Skimmed milk powder	Krüger GmbH & Co. KG, Bergisch-Gladbach
Magnesium chloride ($MgCl_2$) (25 mM)	Promega Corporation, Mannheim
Methanol	Merck, Darmstadt
Sodium chloride (NaCl)	Sigma-Aldrich Co, Deisenhofen
Sodiumdodecylsulfat (SDS)	Carl Roth GmbH, Karlsruhe
Non-essential Amino acids (NEAS)	Paa Laboratories GmbH, Pasching, Österreich
Penicillin/Streptomycin	Paa Laboratories GmbH, Pasching, Österreich
Phenylmethylsulfonylfluoride (PMSF)	Carl Roth GmbH, Karlsruhe
Phosphate-buffered saline solution (PBS)	Seromed Biochrom KG, Berlin
Pierce® BCA Protein Assay	Thermo Scientific, Lumigen Inc., Southfield, USA
Sphingosine-1-Phosphate (S1P)	Sigma-Aldrich Co, Deisenhofen

ACT-209905	Actelion Pharmaceuticals, Basel,Switzerland
Fluorometric Cell Viability Kit I(Resazurin)	PromoCell GmbH, Heidelberg, Germany
Puromycin dihydrochloride (CAS 58-58-2)	Santa Cruz Biotechnology, Inc., USA
Tetramethylethylendiamine (TEMED)	Carl Roth GmbH, Karlsruhe
Tris-hydrochloride (Tris-HCl)	Carl Roth GmbH, Karlsruhe
Triton-x-100	SERVA, Heidelberg
Trypsin / EDTA	PAN-Biotech GmbH, Aidenbach
W146	Tocris Bioscience, UK
Caspase-3 Colorimetric Assay	R&D Systems, USA
NeuroCult™ NS-A Basal Medium	Stemcell Technologies Inc., Canada
NeuroCult™ NS-A Proliferation Kit (Human)	Stemcell Technologies Inc., Canada

3.3 Buffers and solutions

Blocking Solution 10 %	Skimmed milk powder	3 g
	TBST (1 x)	ad 30 ml
DMEM- Culture Medium	FCS	50 ml
	Glutamine	5,5 ml
	NEAS	5,5 ml
	DMEM	500 ml
Laemmli-buffer (4 x)	0,25 mM Tris-HCl (pH 6,8)	3.125 ml
	SDS	1 g
	Glycerol (100 %)	5.8 ml
	Bromophenol blue	5 mg
	β-Mercaptoethanol	2.5 ml

	Aqua dest.	ad 12.5 ml
Lysis-buffer pH 7.4	50 mM Tris-HCl	0.606 g
	100 mM NaCl	0.584 g
	0.1 % Triton-x-100	100 µl
	5 mM EDTA	2.5 ml
Phosphate-buffered	NaCl	80.0 g
saline solution (10 x PBS)	KCl	2.0 g
	$(NH_4)2HPO_4$	14.4 g
	KH_2PO_4	2.4 g
	Aqua dest.	ad 1000 ml
Stacking gel buffer pH 6.8	Tris-HCl	6 g
	with NaOH	auf pH 6.8
	Aqua dest.	ad 100 ml
Stripping buffer	Tris-Ultra	7.57 g
	SDS	20 g
	Aqua dest.	ad 1000 ml
Tank buffer (10 x)	Tris-Ultra	60 g
	Glycine	288 g
	SDS	20 g
	Aqua dest.	ad 2000 ml
Tank buffer (1 x)	Tank buffer (10 x)	100 ml
	Aqua dest.	ad 1000 ml
Towbin buffer (10 x)	Tris-Ultra	60.6 g
	Glycine	288 g
	Aqua dest.	ad 2000 ml

Towbin buffer (1 x)	Towbin buffer (10 x)	100 ml
	Methanol	200 ml
	Aqua dest.	ad 1000 ml
Separating gel buffer pH 8.8	Tris-HCl	59.1 g
	Aqua dest.	ad 250 ml
Washing buffer TBS (10 x)	NaCl	80 g
	KCl	2 g
	Tris-Ultra	30 g
	Aqua dest.	ad 1000 ml
		pH with HCl to 7.4
Washing buffer TBST (1 x)	TBS (10 x)	200 ml
	Tween 20	800 µl
	Aqua dest.	ad 2000 ml

3.4 Cell Lines

In this research, we used three cell lines: two human GBM cell lines (LN18, U87MG) and a murine GBM cell line (GL261). The details are as following:

Name	Supplier
LN18	ATCC, Manassas, VA, USA
U87MG	ATCC, Manassas, VA, USA
GL261	ATCC, Manassas, VA, USA (kindly provided by M. Synowitz, Kiel, Germany)

3.5 Primary and secondary antibodies

3.5.1 Primary antibodies

Name	Species	Molecular Weight	Supplier
Phospho-Akt 1	Rabbit	60 kDa	Cell Signaling Technology, Inc.,

			Massachusetts
Total-Akt1	Rabbit	60 kDa	Cell Signaling Technology, Inc., Massachusetts
Phospho-ERK 1/2	Mouse	42/44 kDa	Cell Signaling Technology, Inc., Massachusetts
Total-ERK 1/2	Mouse	42/44 kDa	Cell Signaling Technology, Inc., Massachusetts
CD133	Mouse	97-120 kDa	Cell Signaling Technology, Inc., Massachusetts
Nestin	Mouse	200-250 kDa	STEMCELL Technologies Inc., Canada
GAPDH	Mouse	36 kDa	Meridian Life Science, Inc., USA
S1PR1	Rabbit	43 kDa	Abcam, Oregon, USA
S1PR2	Mouse	39/48 kDa	Santa Cruz Biotechnology, Inc., USA
S1PR3	Rabbit	42 kDa	Abcam, Oregon, USA
S1PR4	Rabbit	40 kDa	Abcam, Oregon, USA
S1PR5	Rabbit	42 kDa	Abcam, Oregon, USA

3.5.2 Secondary antibodies

Name	Species	Linked to	Supplier
Anti-mouse	goat	HRP	Bio-Rad Laboratories GmbH, München
Anti-rabbit	goat	HRP	Bio-Rad Laboratories GmbH, München

4 Methods

4.1 Cell culture

The cultivation of the cells was carried out at 37 °C, 95% relative humidity and 5% carbon dioxide fumigation in the incubator BBD 6220 (Heraeus Instruments, Hanau).

Once the GBM cells (LN18, GL261, U87MG) were confluent, they were passaged into a new cell culture flask. DPBS, trypsin/EDTA, DMEM (10% FCS, 2mM glutamine and 2mM non-essential amino acids) were placed in a water bath and preheated to 37 °C before usage.

For the passage, the medium was aspirated and the cells were washed with 10 ml of pre-warmed PBS (phosphate buffered saline) twice. The washing process removed serum residues and divalent cations (Ca^{2+}, Mg^{2+}). Subsequently, the cells were incubated with 3 ml of trypsin/EDTA for three to five minutes in the incubator. Trypsin is a serine protease which leads to the detachment of adherently growing cells from the surface of the cell culture flask. This process is accelerated by ethylenediaminetetraacetic acid (EDTA), as it complexes calcium and magnesium ions and causes the release of cell-cell compounds. The cells were detached from the cell culture bottom by gentle tapping, and trypsinization was stopped by adding 7 ml of DMEM medium (Dulbecco's Modified Eagle's Medium) with 10% FCS (Fetal Calf Serum). 20 ml of DMEM medium containing 10% FCS, 334 µl penicillin/streptomycin and 0.3 ml of the cell suspension were then pipetted into a new cell culture flask. The combination of the antibiotics penicillin and streptomycin prevented contamination with Gram-positive and Gram-negative bacteria.

4.2 Determination of the cell number

The cell number was determined in the CASY TT (Schärfe-System GmbH, Reutlingen). For this purpose, 50 µl of the cell suspension was added to 10 ml of isotonic electrolyte solution (Casy®ton solution) in a measuring cuvette. The measurement was based on the resistance measurement principle. The cell suspension flowed at a constant rate through a capillary bearing against a voltage source. When a cell passes the capillary, it displaces some of the electrolyte solution and increases the electrical resistance as a function of its volume. The

increase in resistance produces electrical signals whose number is proportional to the cell count.

4.3 Cell viability analysis (Resazurine assay and Crystal-violet test)

GBM cells were inoculated in 96-well plates with 10,000 cells in each well. After 24 hours, the medium was removed and the cells were cultured to different time points using fresh medium containing S1P or the respective S1P receptor agonist/inhibitor. Then the medium was removed and replaced with fresh medium containing 10% resazurine (PromoCell, Heidelberg, Germany), and the 96-well plates was returned to the 37 °C cell incubator for 1.5 to 2 hours, during which the culture medium changed from pure blue to pale pink depending on the viability of the cells. The fluorescence readings were recorded using a multi-plate reader (Tecan Infinite M200, Crailsheim, Germany, excitation wavelength 530 nm; emission wavelength 590 nm). The data was calculated as the percentage of cell viability of solvent (MeOH for S1P, DMSO for inhibitors) treated cells.

Afterwards, the supernatant was aspirated and cells were rinsed once with PBS. Then, cells were fixed for 10 minutes with 4 % paraformaldehyde followed by gently rinsing 3 times with PBS. 50 µL of 0.5% crystal violet staining solution were added to each well and the plates were incubated for 10 min at roomtemperature. Afterwards, the cells were washed with A. dest. several times until the dye stops coming off. After washing, the plate was gently tapped on filter paper to remove any remaining liquid. Finally, the stained cells were treated with 100ul SDS solution (1%) for 5 min while shaking gently on a rocking shaker. The optical density of each well was measured at 560 nm (OD_{560}) with a multiplate reader.

4.4 Scratch wound healing assay

GBM cells were inoculated into a 24-well plate with a total of 150,000 cells per well and a volume of 1 ml per well. When the cells have built a complete confluent monolayer, a scratch (“wound”) was made with a yellow 100 µl pipette tip in the cell layer. Afterwards, the culture media was removed and cells were washed twice 1 ml of DPBS to remove the isolated cells away to prevent that these cells reattach. DPBS was removed and the pre-warmed cell culture medium containing 0.05% FCS and 5 mM hydroxyurea as a proliferation

inhibitor. The wounds were imaged using the PALM Robo software of the AxioVision HXP 120C microscope (Carl Zeiss Microscopy, Jena, Germany), and the exact location of the images was saved to analyze the same area after the corresponding incubation time. After pre-incubation with hydroxyurea for one hour, the cells were treated with AC-209905 and/or S1P at different doses for 16 hours in hydroxyurea containing medium, then the images were taken again and the wound width was calculated (Software AxioVision SE64 Rel. 4.9, Carl Zeiss Microscopy).

4.5 Boyden chamber migration assay

4.5.1 Membrane preparation

Membranes with a pore diameter of 8 µm were used and coated with collagen (1918 µl A. dest., 12 µl 96% Acidic Acid, 70 µl Collagen solution) for 24 hours at room temperature. After incubation, the membranes were washed in PBS and hang up to dry. The upper right corner (glossy page face up) was cut. Until use, the membrane was covered with a cloth, placed in a 50 ml tube and put in the fridge (4 °C).

4.5.2 Experimental procedure

Firstly, GBM cells were seeded cells at a density of 300.000 cells/well in a 6-well-plate as usual.

The migration stimuli for the lower chamber of the Boyden plate were prepared and in each well of the lower chamber28 µl were filled in, the membrane (with the glossy page facing up) was set on lower chamber and the silicone mat was applied upon the membrane. The upper chamber was fixed on it. Then, the cell solution for the upper chamber was prepared: the medium was removed from the 6-well-plates and cells were detached by incubation with 500 µl Trypsin/EDTA for 5 min at 37°C. Next, cells were transferred in 2 mL-Eppis, 500 µL medium was added per tube and centrifuged at 1000 rpm for 5 min at 25°C. Now the medium was carefully aspirated and cells were resuspended in 1.5 ml medium (with 0.05% FCS). Carefully, 50 µl of the cell suspension were filled into each well of the upper chamber. The boyden chambers were incubated at 37°C, 95% relative humidity and 5% carbon dioxide fumigation in the incubator BBD 6220 (Heraeus Instruments, Hanau) for three hours.

Afterwards, the membranes were washed in PBS and the cells on the upper side of the membrane were scraped. The membranes were washed in PBS again and the cells were fixed on the lower side of the membrane in 4% PFA (paraformaldehyde) for 5 minutes. Then, the membrane was stained in crystal violet solution for 1 min (crystal violet solution: 5.4 ml ethanol [99.8%], 1.5 ml crystal violet). The membrane was washed twice in A. dest. and hang up to dry. The following day, the membrane was sticked between a microscopy slide and a cover glass with "Entellan®" drying period at least 24 hours). Images of the membrane were made using the PalmRobo microscope, and the cells were counted using the software "ImageJ".

4.6 Western blot analysis

4.6.1 Protein sample preparation

GBM cells were removed from the incubator, the culture medium was aspirated and 10 ml of cold DPBS was added to each flask of cells three times for washing. Then, the cells were scraped with cell spatula, transferred to a 1.5 ml centrifuge tube and lysis buffer was added (see 3.3 Buffers and Solution). The samples were put on ice for 30 minutes.

After the completion of the lysis, centrifugation was carried out at 12,000 rpm for 5 min at 4 °C, and the supernatant resulting from centrifugation was transferred to a new 1.5 ml centrifuge tube, and stored at -20 °C.

4.6.2 Preparation of SDS-PAGE gel

The separation gel (lower layer gel) and the stacking gel (upper layer gel) were prepared according to the Table 1 below.

Component	Stacking gel	Separating gel (8%)	Separating gel (10%)	Separating gel (12.5%)
Aqua dest.	2.1 ml	3.6 ml	3.0 ml	2.4 ml
Acrylamide	455 µl	1.9 ml	2.5 ml	3.1 ml
Stacking gel buffer	861 µl	-	-	-

Separating gel buffer	-	1.9 ml	1.9 ml	1.9 ml
10% SDS	35 µl	75 µl	75 µl	75 µl
10% APS	35 µl	75 µl	75 µl	75 µl
TEMED	3.5 µl	7.5 µl	7.5 µl	7.5 µl

***Table 1*. Compositin of the separating gel and the stacking gel (5%).**

When all elements of the running chamber are put together, the separation gel is filled in and gel is covered with 1-2 ml of isopropyl alcohol to flatten. Gelation is finished after about 30 min. The ethanol was removed and the stacking gel was overlayed. After 30 to 45 min of gelation, the electrophoresis tank solution was filled in the chamber.

4.6.3 Sample Processing

Before electrophoresis is started, an appropriate amount of 4x SDS-PAGE protein loading buffer (4x Laemmli buffer) was added to the protein samples: 30 µl sample and 10 µl loading buffer. The samples were heated at 95°C for 5 min before loading

4.6.4 Sample Loading

The samples were filled into the gel slots with a micropipette. Before adding the next sample, the injector should be washed three times in the outer tank running buffer to prevent cross-contamination.

4.6.5 Electrophoresis

In this work the Bio-Rad's standard electrophoresis device was used. The sample was electrophoresed with low voltage of 80 V (about 15 minutes) in the stacking gel, and high voltage (120 V) was used for electrophoresis in the separating gel. The electrophoresis was terminated when the bromophenol blue (from the loading buffer) reaches the bottom end of the gel.

4.6.6 Transfer

The transfer buffer was freshly prepared (see 3.3 Buffers and Solution) and stored at 4°C until used. Six sheets of Whatman® filter paper and one nitrocellulose membrane are needed for the assembly of the blotting conditions.

Using Bio-Rad's standard transfer unit, we set the transfer current to 370 mA, transfer time to 90 minutes, and ensured the ice box does not overheat. After the transfer was completed, Ponceau's stain liquid was used for five minutes (on a shaker) to check the transfer effect.

4.6.7 Blocking

The membrane was rinsed three times with TBST washing solution for five minutes each time to wash away the Ponceau's stain solution. Then, 10% skimmed milk blocking solution was added, and the membrane was incubated room temperature for 60 minutes on a horizontal shaker.

4.6.8 Primary antibody incubation

After blocking, the membrane was rinsed three times with TBST for five minutes each time. The primary antibody diluted to the appropriate concentration (see Table 2 below) with TBST was added and incubated overnight under rotating conditions at 4°C.

Target protein	Molecular weight	Antibody Dilution
pAkt 1	60 kDa	1 : 1000
tAkt 1	60 kDa	1 : 1000
pERK 1/2	42/ 44 kDa	1 : 800
tERK 1/2	42/ 44 kDa	1 : 800
CD133	97-120 kDa	1 : 500
GAPDH	36 kDa	1 : 2000
Nestin	200-250 kDa	1 : 500
S1PR1	43 kDa	1 : 1000
S1PR2	39/48 kDa	1 : 500
S1PR3	42 kDa	1 : 800
S1PR4	40 kDa	1 : 1000
S1PR5	42 kDa	1 : 1000

***Table 2*: Summary of Western Blot-Detected Proteins and Primary Antibody Dilutions.**

4.6.9 Secondary antibody incubation

After incubation overnight, the primary antibody solution was removed and the membrane was rinsed three times with TBST for five minutes each time. Then, the secondary horseradish peroxidase-conjugated antibody (see chapter 3.5.2) was added at a dilution of 1:1000 and incubated for one hour at room temperature on a horizontal shaker with gentle shaking. After incubation, the membrane was rinsed with TBST at room temperature on a horizontal shaker three times for five minutes each time.

4.6.10 Detection of proteins

Chemiluminescence signals were detected with ChemiDoc™ XRS Imaging System (Bio-Rad, Hempstead, UK) using ECL Plus Western Blotting Substrate (Thermo Scientific, Rockford, USA) followed by densitometric analysis (Quantity One, Bio-Rad). The relative optical densities of the specific bands were calculated and normalized to GAPDH as a loading control.

4.7 Neurosphere culture

LN18 neurospheres, which are thought to be enriched in cancer stem cells [101], are cultured with the NeuroCult™ NS-A Proliferation Kit (Human, STEMCELL Technologies, Cologne, Germany) added with 20 ng/ml rh EGF, 10 ng/ml rh bFGF, and 0.0002% heparin according to the manufacturer's protocol.

Briefly, LN18 GBM cells were trypsinized with 3 ml of trypsin/EDTA for 3–5 minutes at 37°CThen, 7 ml of FCS containing DMEM was added to the flask.

The cell suspension was transferred to a sterile 15 ml tube and centrifuged at 1000 rpm for three minutes. After aspirating the supernatant, the cells were washed with 10 ml of DPBS, and the cell suspension was again centrifuged at 1000 rpm for three minutes. This washing step with DPBS was repeated twice. Afterwards, the cells were resuspendend into the complete NeuroCult™ NS-A Proliferation medium (see above).

4.8 Caspase 3 activity assay

Caspase 3 activity assay was performed using the commercially available kit *Caspase 3 fluorometric assay* (from R&D systems). Cells were seeded in a 96-well plate and incubated with respective test substance for appropriate time. After treatment, the medium with cells that have been detached due to apoptosis were collected in a conical tube, adherent cells were scraped and collected in the same tube. Afterwards, cells were rinsed with ice-cold PBS three times and centrifuged at 250 x g for 10 minutes. The supernate was gently removed and discarded while the cell pellet was lysed by the addition of the Lysis Buffer. The amount of Lysis Buffer to be added to the pellet is determined by the number of cells present. 25 µL of cold Lysis Buffer were added per 1 x 10^6 cells. The cell lysate was incubated on ice for 10 minutes and then centrifuged at 10,000 x g for 1 minute. The supernatant was tranferred to a new tube and kept on ice. After the protein determination assay (BCA Protein Assay), 50 µL of cell lysate and 50 µL of 2X Reaction Buffer 3 were mixed. Prior to using the 2X Reaction Buffer 3, 10 µL of fresh DTT stock per 1 mL of 2X Reaction Buffer 3 were added. To each reaction well (96-well plate) 5 µL of Caspase-3 colorimetric substrate (DEVD-pNA) were added and the plate was incubated at 37 °C for 1-2 hours. Then the plates were read on a microplate reader using a wavelength of 405 nm.

5 Results

5.1 Expression of S1P receptors in various GBM cell lines

First, we checked whether S1P receptors are indeed expressed in GBM cells to make sure that S1P as well as the S1PR1 modulator ACT-209905 and the S1PR2 inhibitors Compound 16/16-ME can act on these cells. To study the expression of S1P receptors in GBM cells, five different GBM cell lines derived from humans (A172, GaMG, HF66, LN18 and U87MG) and one murine GBM cell line (GL261) were selected. As seen in Figure 2 all S1P receptors (1-5) were found on protein level in the investigated human and murine GBM cell lines. In the murine GL261 cell line, the S1PR1, S1PR4 and S1PR5 showed a considerably lower expression than all human GBM cell lines whereas S1PR2 and S1PR3 seem to have a more comparable expression in all tested GBM cells.

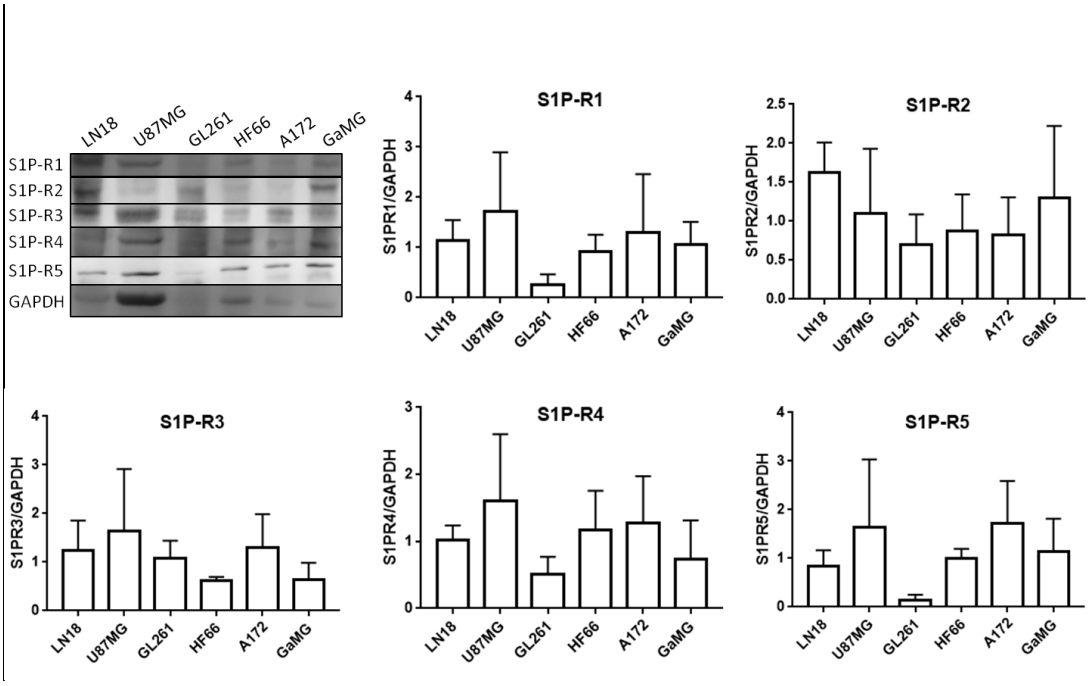

Figure 2: Expression of S1P receptors in various GBM cell lines. Five different human GBM cell lines (A172, GaMG, HF66, LN18 and U87MG) and one murine GBM cell line (GL261) were analyzed for expression of S1P receptors by immunoblotting. Mean values and SD, *n* = 4.

5.2 Influence of ACT-209905 on the viability of GBM cells *in vitro*

Treatment of GBM cells with different ACT-209905 concentrations (0.5 to 50 µM) for 24 h, 48 h and 72 h resulted in significant changes of cell viability (Resazurine assay) and cell vitality (Crystal violet staining).

As shown in Figure 2A-C, in LN18 GBM cells, 10, 20, 30 and 50 µM ACT-209905 significantly attenuated the viability after 24 h to 69.2%, 40.3%, 32.1% and 7.3%, respectively (Figure 3A). After 48 hours, viability of LN18 cells further decreased to 36.2%, 18.5%, 2.7% and nearly 0% (Figure 3B). LN18 cell viability rate decreased to 38.9%, 15.7%, 8.0% and 0.4% after 72 hours treatment with 10, 20, 30 or 50 µM ACT-209905 (Figure 3C). Crystal-violet Assay's results (Figure 3D-F) showed that cell vitality decreased to 84.0%, 39.5%, 49.1% and 29.6% after 24 hours of treatment with 10, 20, 30 and 50 µM ACT-209905 (Figure 3D). The LN18 cell vitality after application of 10, 20, 30 or 50 µM ACT-209905 further decreased to 60.7%, 43.7%, 52.3% and 31.0% after 48 hours (Figure 3E), and to 41.9%, 33.0%, 39.0% and 24.6% after 72 hours treatment, respectively (Figure 3F). Interestingly, for 0.5 and 5 µM ACT-209905 a significantly increased cell viability was observed to about 120%.

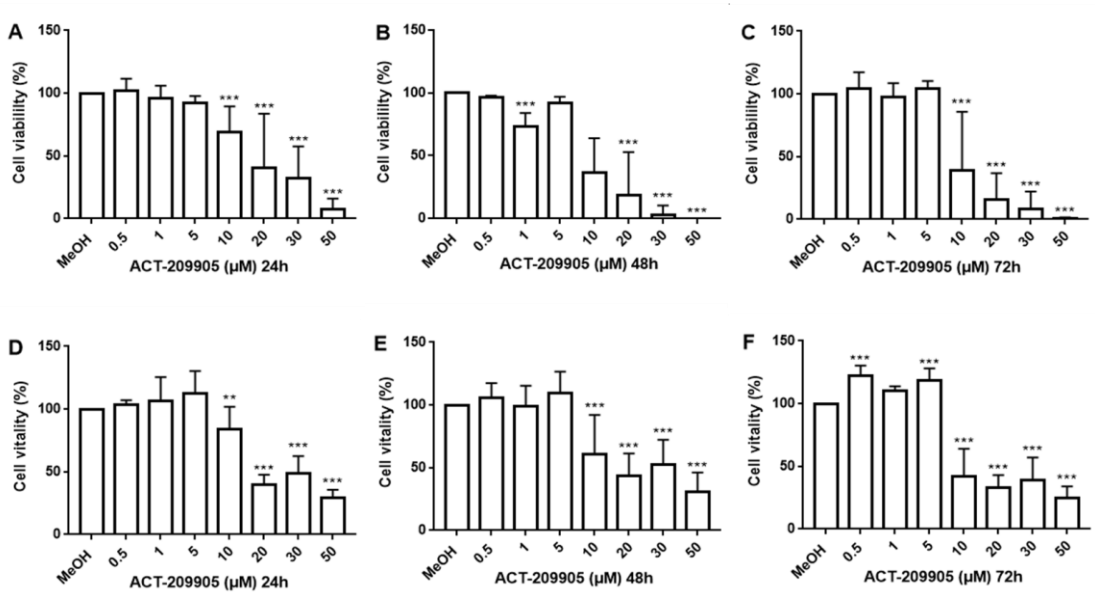

Figure 3: Treatment of LN18 GBM cells with ACT-209905. The cell viability and vitality of human LN18 GBM cells was determined using the resazurine and crystal-violet assay after treatment with ACT-209905 (0.5, 1, 5, 10, 20, 30 and 50 µM) for 24, 48 and 72 hours. Control cells were treated with MeOH as solvent for ACT-209905. (A-C) Determination of LN18 cell viability by using the resazurine assay after treatment with ACT-209905, (D-F) analysis of LN18 cell vitality by using the Crystal-violet assay after treatment with ACT-209905 for the respective time points. Cell viability is shown in relation to the MeOH control (100%), mean values and SD, $n = 5$, one-way analysis of variance with Dunnett´s multiple comparison test, $*p < 0.05$, $**p < 0.005$ and $***p < 0.001$ vs. MeOH control.

In U87MG cells, treated with 10 to 50 µM ACT-209905, cell viability decreased to 90.7%, 36.5%, 36.9% and 11.9% after 24 hours (Figure 4A). U87MG cell viability further decreased to 82.7%, 2.8%, 1.0% and 0.1% after 48 hours of treatment with ACT-209905 (Figure 4B). Cell survival rate of ACT-209905 treated U87MG (10, 20, 30 and 50 µM) was diminished to 58.3%, 13.2%, 1.2% and 0 after 72 hours (Figure 4C). Crystal-violet Assay's results showed that cell vitality of ACT-209905 treated U87MG cells (10, 20, 30 and 50 µM) decreased to 77.4%, 32.4%, 37.0% and 22.7% after 24 hours (Figure 4D). U87MG cell vitality was further significantly reduced to 33.1%, 29.2% and 26.5% 48 hours after application of 20, 30 or 50 µM ACT-209905, and to 70.7%, 30.3%, 23.0% and 21.2% after 72 hours treatment with 10, 20, 30 or 50 µM ACT-209905, respectively (Figure 4F).

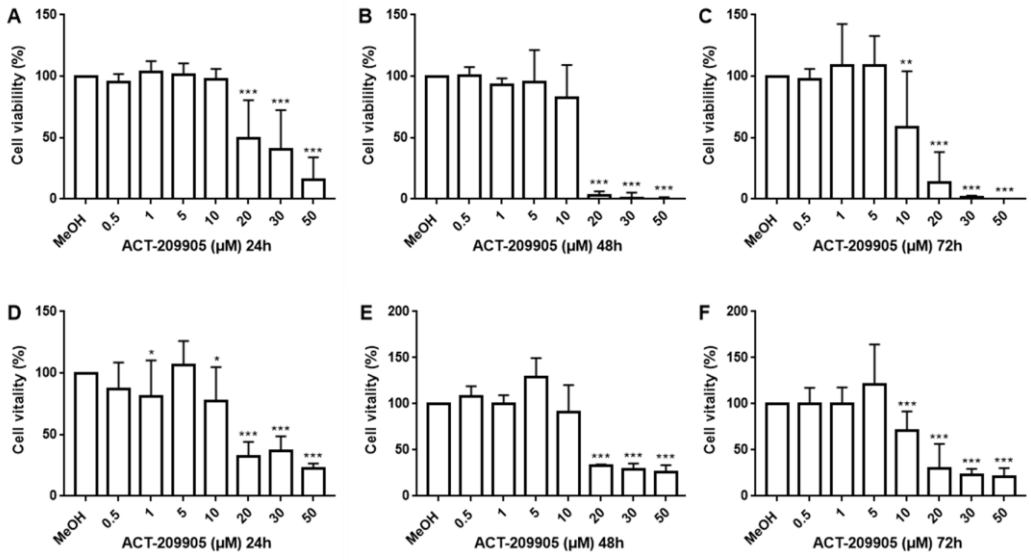

Figure 4: Treatment of U87MG GBM cells with ACT-209905. The cell viability and vitality of human U87MG GBM cells was determined using the resazurine and crystal-violet assay after treatment with ACT-209905 (0.5, 1, 5, 10, 20, 30 and 50 µM) for 24, 48 and 72 hours. Control cells were treated with MeOH as solvent for ACT-209905. (A-C) Determination of LN18 cell viability by using the resazurine assay after treatment with ACT-209905, (D-F) analysis of LN18 cell vitality by using the Crystal-violet assay after treatment with ACT-209905 for the respective time points. Cell viability is shown in relation to the MeOH control (100%), mean values and SD, $n = 5$, one-way analysis of variance with Dunnett´s multiple comparison test, $*p < 0.05$, $**p < 0.005$ and $***p < 0.001$ vs. MeOH control.

In the murine GL261 GBM cells, 20 to 50 µM ACT-209905, viability also decreased to 61.7%, 42.7% and 18.4% after 24 hours (Figure 5A). Cell viability decreased to 8.9%, 23.6% and 0% after 48 hours of treatment of GL261 cells with 20, 30 or 50 µM ACT-209905 (Figure 5B). And, cell survival rate was significantly reduced to 7.6%, 6.5% and 0% after 72 hours of treatment

with 20, 30 and 50 µM ACT-209905 (Figure 5C). The results of crystal-violet Assay showed that cell vitality was siginificantly decreased to 51.4%, 51.9% and 27.0% after 24 hours of treatment of GL261 cells with 20, 30 or 50 µM ACT-209905 (Figure 5D). 48 hours after application of 20, 30 and 50 µM ACT-209905, cell vitality was significantly reduced to 59.2%, 38.6% and 21.1% (Figure 5E). Cell vitality was significantly diminished to 36.9%, 34.2% and 31.2% after 72 hours of treatment with 20, 30 or 30 µM ACT-209905, respectively (Figure 5F).

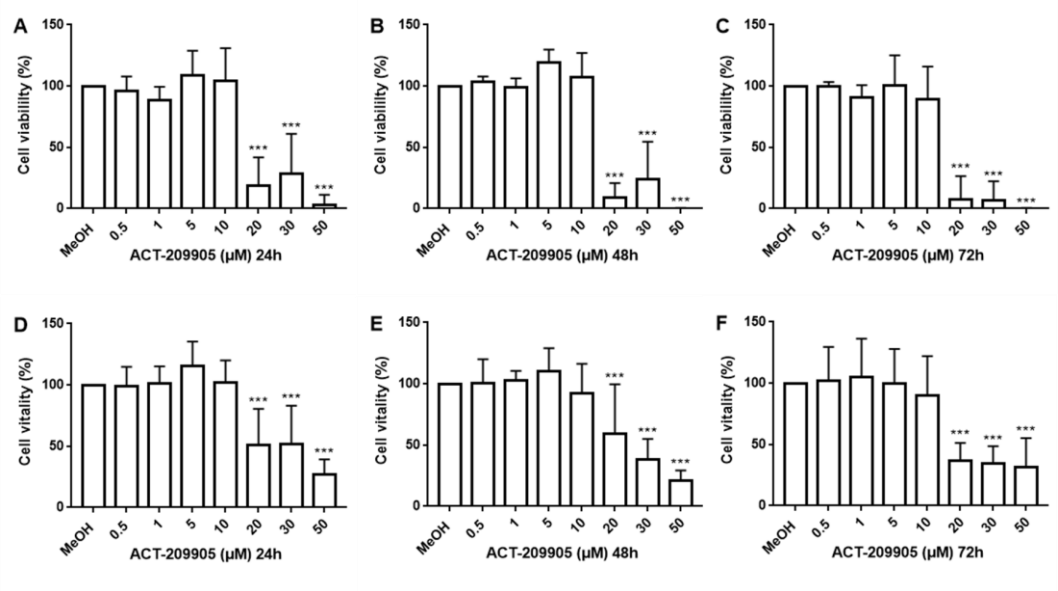

Figure 5: Treatment of GL261 GBM cells with ACT-209905. The cell viability and vitality of murine GL261 GBM cells was determined using the resazurine and crystal-violet assay after treatment with ACT-209905 (0.5, 1, 5, 10, 20, 30 and 50 µM) for 24, 48 and 72 hours. Control cells were treated with MeOH as solvent for ACT-209905. (A-C) Determination of LN18 cell viability by using the resazurine assay after treatment with ACT-209905, (D-F) analysis of LN18 cell vitality by using the Crystal-violet assay after treatment with ACT-209905 for the respective time points. Cell viability is shown in relation to the MeOH control (100%), mean values and SD, $n = 5$, one-way analysis of variance with Dunnett´s multiple comparison test, $*p < 0.05$, $**p < 0.005$ and $***p < 0.001$ vs. MeOH control.

5.3 Influence of ACT-209905 and S1P on the migration of LN18 and GL261 GBM cells

Further, the influence of ACT-209905 on GBM cell migration was investigated. Migration of LN18 and GL261 cells was analysed with the scratch wound healing assay (after 16 h) and the Boyden chamber assay (after 3 h). Selected examples of both assays are illustrated in Figure 6A and 7A, whereas the statistical analyses are shown in Figure 6B and 7B. In LN18 GBM cells, 10 µM and 30 µM ACT-209905 treatment reduced the migration significantly to 82.4% and 59.7% (Figure 6). The motility of GL261 cells treated with 10 µM and 30 µM ACT-209905 was significantly decreased to 88.3% and 83.2% respectively, compared to control cells (Figure 7).

The additional application of S1P reversed the inhibitory effect of ACT-209905 on migration of GBM cells (Figure 6 and 7).

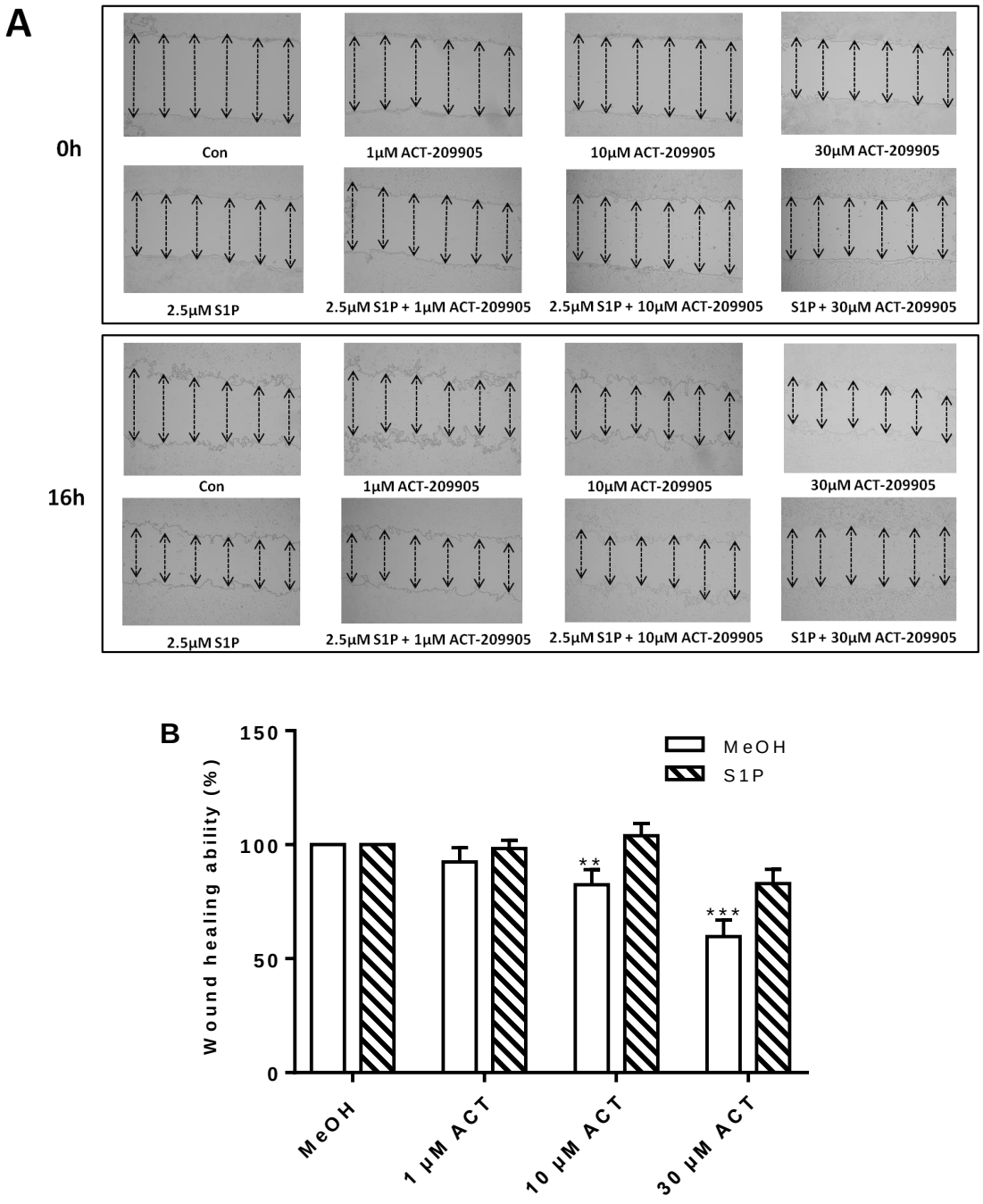

Figure 6: Influence of ACT-209905 on migration of LN18 GBM cells. LN18 cell migration was analyzed using the wound closure assay by scratching the cell layer and adding the ACT-209905 (ACT, 1 µM, 10 µM, 30 µM), then measuring the wound width at the beginning of the experiment (0 h) and again after 16 hours with S1P (2.5µM). Cell proliferation was inhibited by co-application of hydroxyurea (5 mM). (A) Illustration of representative images of LN18 cells at 0 and 16 hours, (B) statistical analysis of LN18 GBM cell migration behaviour. Wound closure ability is shown in relation to the MeOH control (Con, 100%), mean values and SD, n = 3, one-way analysis of variance with Dunnett´s multiple comparison test, $^{**}p < 0.005$ and $^{***}p < 0.0001$ vs. control.

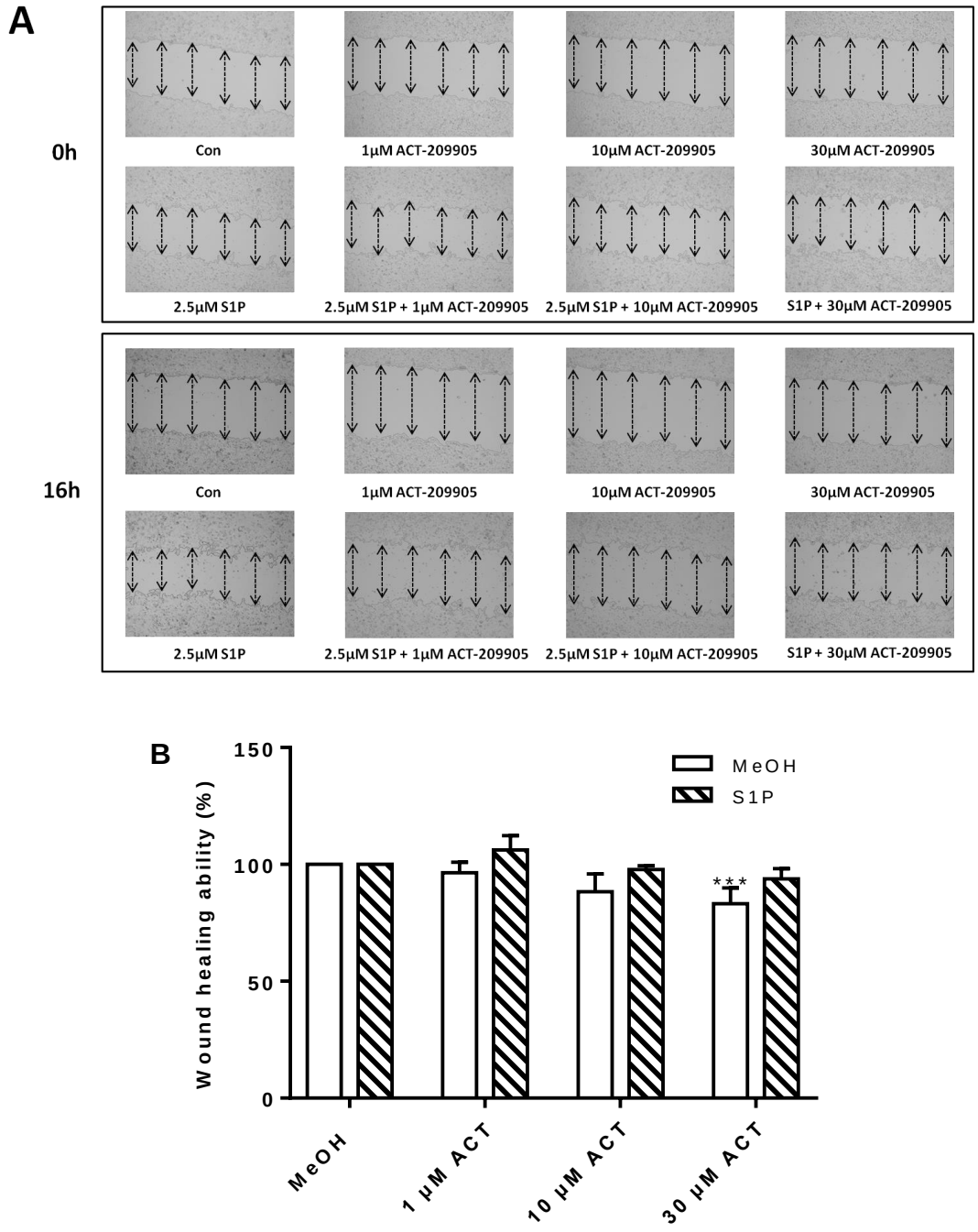

Figure 7: Influence of ACT-209905 on migration of GL261 GBM cells. GL261 cell migration was analyzed using the wound closure assay by scratching the cell layer and adding the ACT-209905 (ACT, 1 µM, 10 µM, 30 µM), then measuring the wound width at the beginning of the experiment (0 h) and again after 16 hours with S1P (2.5µM). Cell proliferation was inhibited by co-application of hydroxyurea (5 mM). (A) Illustration of representative images of LN18 cells at 0 and 16 hours, (B) statistical analysis of LN18 GBM cell migration behaviour. Wound closure ability is shown in relation to the MeOH control (Con, 100%), mean values and SD, *n* = 3, one-way analysis of variance with Dunnett´s multiple comparison test, ** $p < 0.005$ and *** $p < 0.0001$ vs. control.

To further analyze the effect of ACT-209905 on GBM cell migration, we used the Boyden chamber assay to determine the influence of ACT-209905 on LN18 GBM cell motility. The

results are shown in Figure 8. The migration of LN18 GBM cells was significantly lesser in the 10 µM and 30 µM ACT-209905 treatment groups. In comparison to the MeOH treated control cells, which were set to 100% migratory potential, the relative number of migrated cells was significantly reduced to 88.8% and 84.2% 6 hours after application of 10 and 30 µM ACT-209905, while the relative number of migrated cells in the S1P co-treated group was 98.9% and 90.6%. The single application of LN18 cells with 2.5 µM S1P resulted in enhanced migratory potential of 112% membrane invasion.

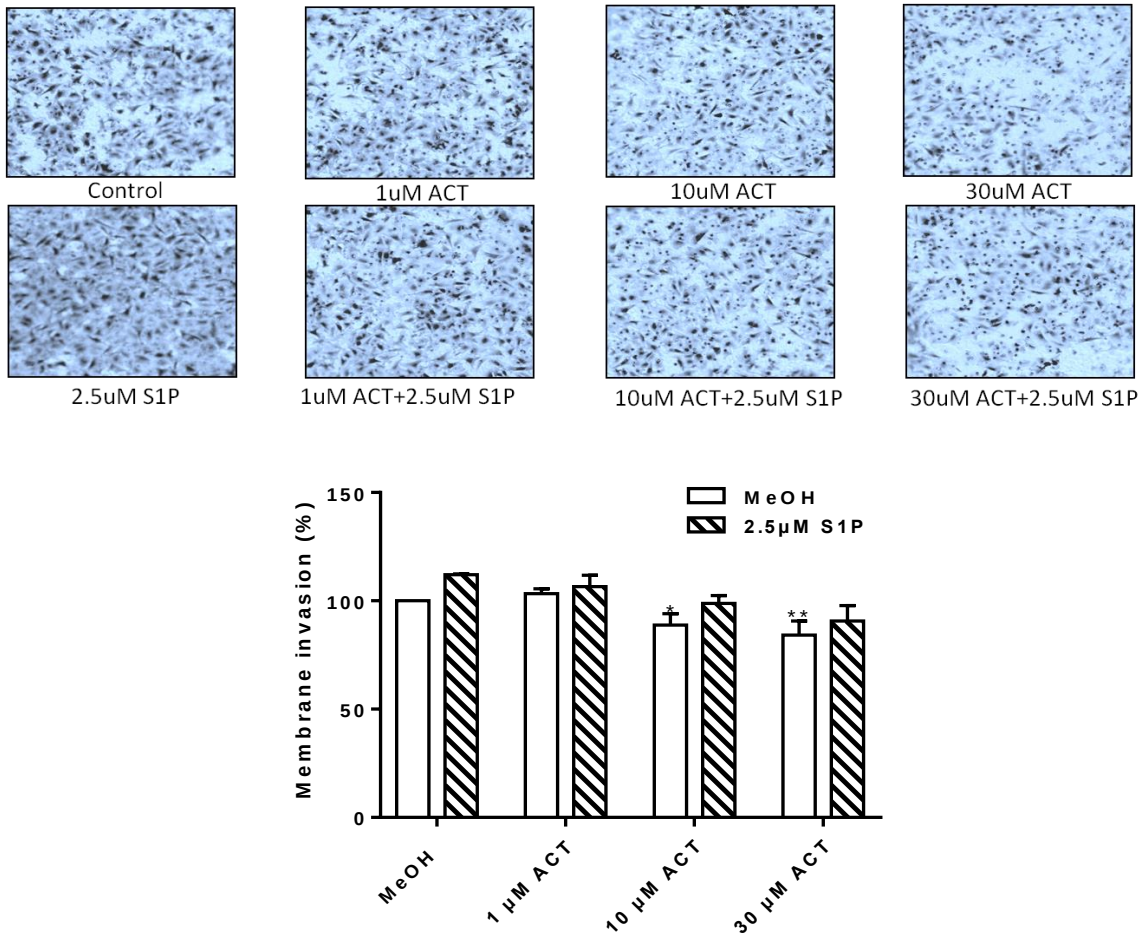

Figure 8: Analysis of LN18 cell migration using the Boyden chamber assay. Cells were allowed to migrate for three hours after application of S1P (2.5 µM) alone or together with ACT-209905 (ACT, 10 µM), fixed on the lower side of the membrane, stained with crystal violet, and then counted. Representative images of the migrated and stained cells are shown in the upper panel of the figure. Counted cells (lower panel) are shown in relation to the control (con, 100%), mean values and SD, n = 3, one-way analysis of variance with Dunnett´s multiple comparison test, *$p < 0.05$ and **$p < 0.005$ vs. control.

5.4 Influence of ACT-209905 on AKT1 and ERK1/2 activation

Immunoblotting was used to analyze the influence of ACT-209905 on the phosphorylation and activation status of AKT1 and ERK1/2 (normalized to the total kinase) to determine whether these kinases might be involved in the inhibitory effect of ACT-209905 on GBM cell viability and migration. Firstly, the phosphorylation of AKT1 (pAKT1) and ERK1/2 (pERK1/2) was investigated 5, 10 and 30 minutes after stimulation of LN18 cells with 2.5 µM S1P. Results of the LN18 GBM cells are illustrated in Figure 9. In the S1P-treated group, the phosphorylation state was significantly increased by a factor of 2.5 after 5 minutes (Figure 9C and 9D). The elevated pAKT1 status was also seen after 10 and 30 minutes of S1P treatment but this was not so pronounced. In contrast, in LN18 cells pre-treated for 24 hours with 10 µM ACT-209905, a significant increase in pAKT1 was not observed in the S1P-treated group. The phosphorylation of ERK1/2 (pERK1/2) was also significantly elevated after 5, 10 and 30 min of S1P stimulation in LN18 GBM cells.

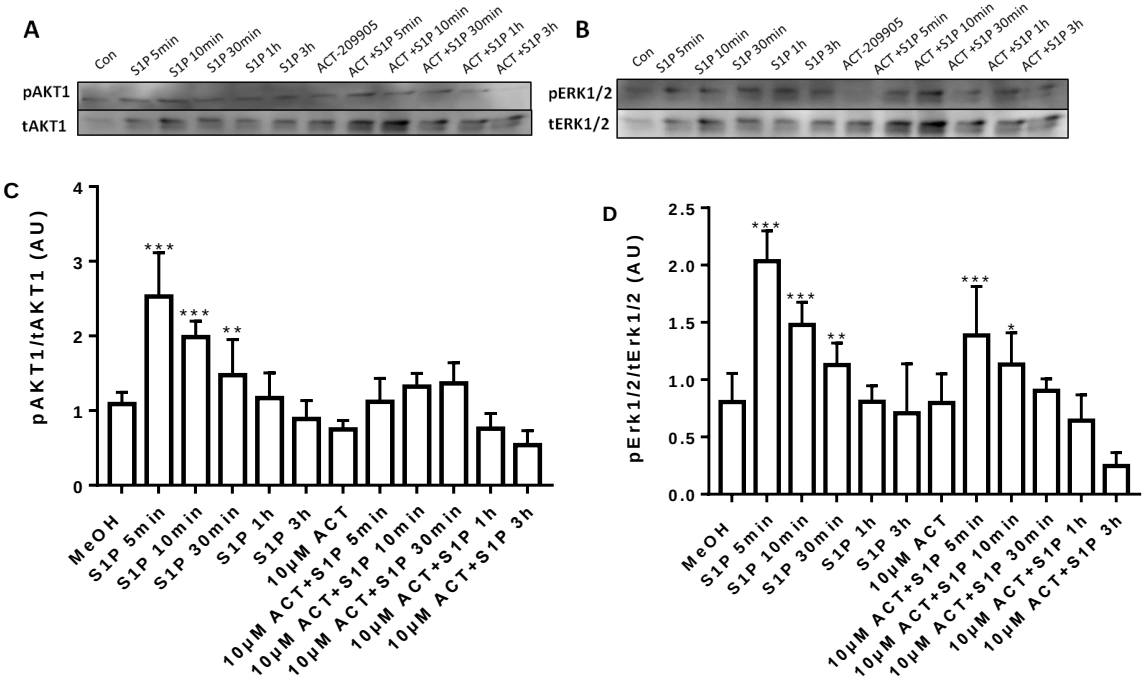

Figure 9: Immunoblot analysis of phosphorylated (p) and total (t) AKT1 and ERK1/2 in LN18 GBM cells. LN18 cells were treated with 2.5 µM S1P for 5, 10 and 30 min as well as 1 h and 3 h. Further, in the combined treatment group, firstly 10 µM ACT-209905 (ACT) was added for 24 h and afterwards the cells were treated with 2.5 µM S1P for 5 min, 10 min, 30 min, 1 h and 3 h. (A and C) Immunoblot analysis of AKT1 and (B and D) immunoblot analysis of ERK1/2. Representative blots are shown in the panels (A) for AKT1 and (B) for ERK1/2. The corresponding densitometric analyses are shown in the panels (C) for AKT1 and (D) for ERK1/2, the phosphorylated protein level (p) was normalized to the total protein level (t), mean values and SD, $n = 5$, One-way analysis of variance with Dunnett´s multiple comparison test, $*p < 0.05$, $**p < 0.005$ and $**p < 0.0001$ vs. control.

This S1P-induced increase in pERK1/2 was slightly reduced by pre-treatment of LN18 cells with ACT-209905 for 24 hours but there was still a significant pERK1/2 increase in the S1P-group, too (Figure 9B and D).

In the murine GL261 GBM cells (Figure 10), the single application of S1P did not result in an elevated pAKT1 status. But interestingly, the combined stimulation of GL261 cells with 10 µM ACT-209905 (pre-treated for 24 hours) and 2.5 µM S1P caused a significant elevation in pAKT1 after 5 and 30 minutes and after 1 and 3 hours. ACT-209905 alone was not able to increase the pAKT1 status (Figure 10A and C). In contrast, the phosphorylation status of ERK1/2 (pERK1/2) was significantly enhanced after 5, 10 and 30 minutes of S1P treatment. Interestingly, the combined application of ACT-209905 (pre-treated for 24 hours) and S1P resulted in a three times stronger up-regulation of pERK1/2 after 5 minutes than the single S1P treatment (Figure 10B and 10D).

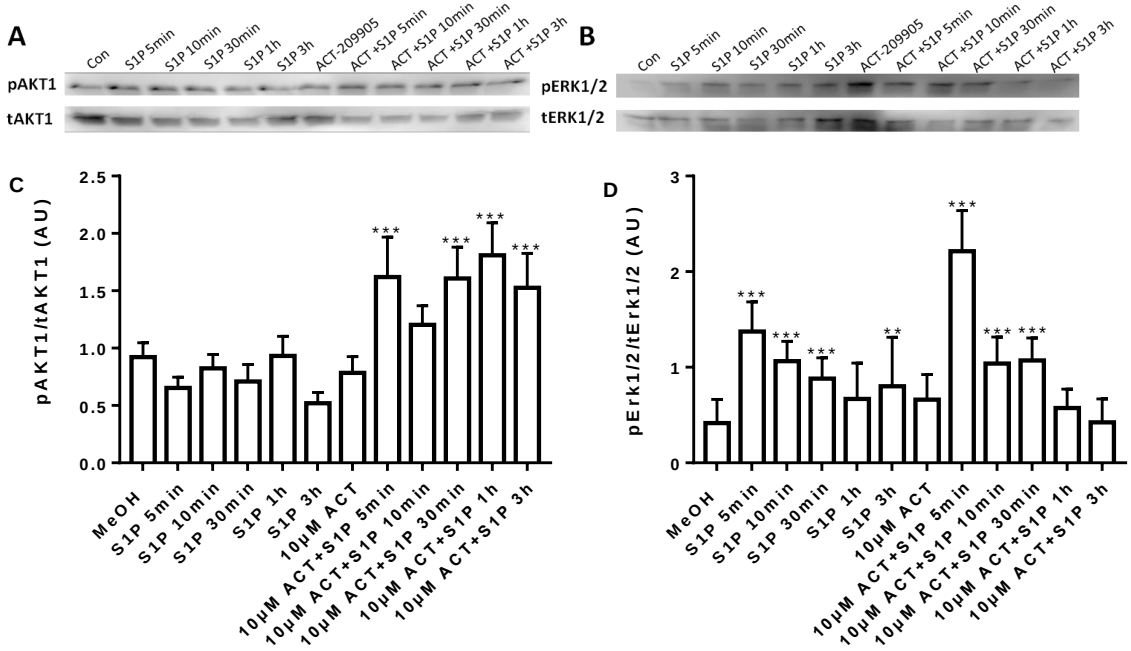

Figure 10: Immunoblot analysis of phosphorylated (p) and total (t) AKT1 and ERK1/2 in GL261 GBM cells. GL261 cells were treated with 2.5 µM S1P for 5, 10 and 30 min as well as 1 h and 3 h. Further, in the combined treatment group, firstly 10 µM ACT-209905 (ACT) was added for 24 h and afterwards the cells were treated with 2.5 µM S1P for 5 min, 10 min, 30 min, 1 h and 3 h. (A and C) Immunoblot analysis of AKT1 and (B and D) immunoblot analysis of ERK1/2. Representative blots are shown in the panels (A) for AKT1 and (B) for ERK1/2. The corresponding densitometric analyses are shown in the panels (C) for AKT1 and (D) for ERK1/2, the phosphorylated protein level (p) was normalized to the total protein level (t), mean values and SD, $n = 5$, One-way analysis of variance with Dunnett´s multiple comparison test, $*p < 0.05$, $**p < 0.005$ and $**p < 0.0001$ vs. control.

5.5Influence of ACT-209905, Compound 16 and Compound 16-ME on CD133 and Nestin protein expression

It is postulated that a tumor contains a subpopulation of tumor cells that exhibit key defining characteristics of somatic stem cells, including the ability to exhibit self-renewal, multipotent differentiation and the expression of stem cell markers such as CD133 and Nestin [102-105].

To investigate whether inhibition of S1PR1 or S1PR2 signaling is involved in regulation of stem cell behavior, LN18 and GL261 GBM cells were treated with S1P, ACT-209905 (S1PR1 antagonist), Compound 16 (antagonist of S1PR2), Compound 16-ME (antagonist of S1PR2) and analyzed the protein expression of CD133 and Nestin by immunoblotting. The respective immunoblot results for LN18 cells are shown in Figure 11).

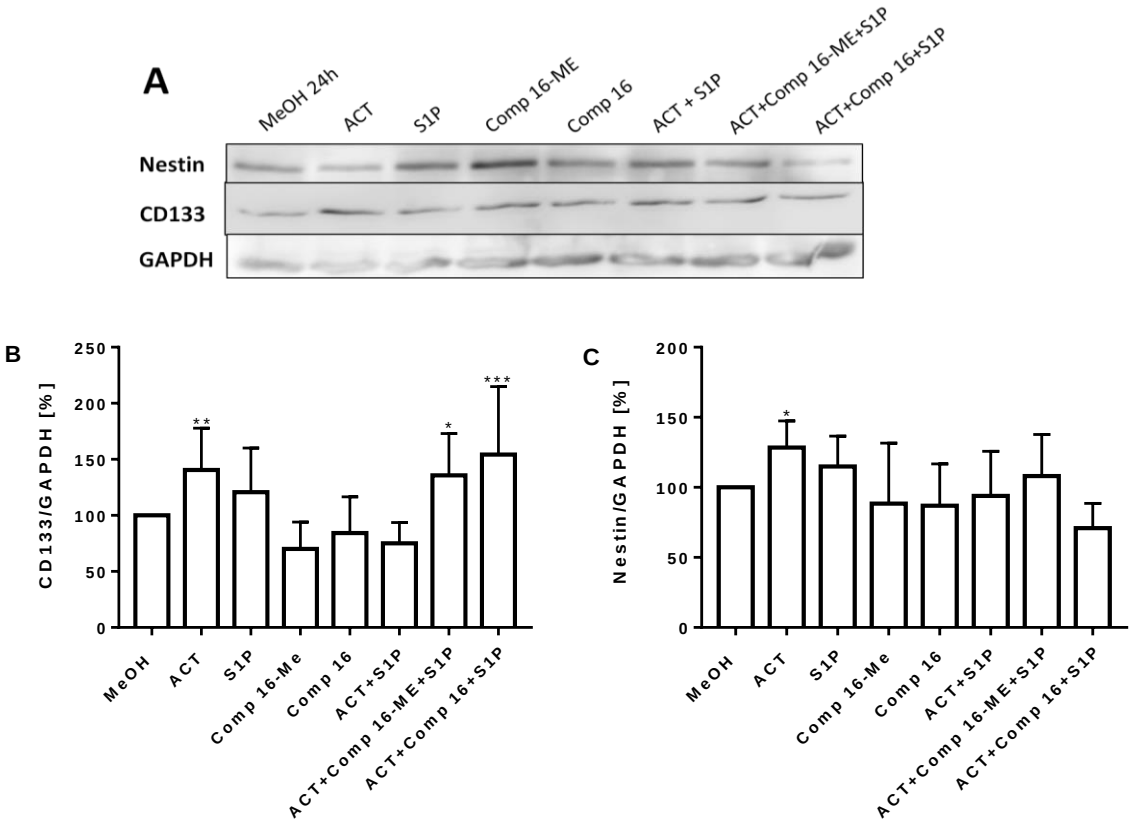

Figure 11: Immunoblot analysis of the stem cell marker CD133 and Nestin. LN18 GBM cells were treated with 10 µM ACT-209905 (ACT), 2.5 µM S1P, 10 µM Compound 16 (Comp 16) or Compound 16-ME (Comp 16-ME) for 6 h. For the combined treatment of the substances, LN18 cells were pre-treated with 10 µM ACT-209905 for 24 h and 10 µM Comp 16/Comp 16-ME for 6 h followed by application of 2.5 µM S1P for 6 h. Control cells were treated with MeOH. Treated cells are shown in relation to the MeOH control (100%), mean values and SD, $n = 3$, one-way analysis of variance with Dunnett´s multiple comparison test, *$p < 0.05$, **$p < 0.005$ and ***$p < 0.001$ vs. control.

In LN18 cells, treatment ACT-209905 alone and in combination with Compound 16, Compound 16-ME and S1P resulted in a significantly elevated CD133 protein expression of about 150% compared to the MeOH control cells. In contrast, Nestin protein expression was only significantly enhanced by single application of ACT-209905 (Figure 11A and C).

In murine GL261 cells, the results for CD133 and Nestin protein expression differ from those of human LN18 GBM cells as illustrated in Figure 12. Treatment of GL261 cells with ACT-209905 did not result in a change of CD133 or Nestin protein expression. In contrast, single application of S1P and Compound 16-ME caused a significant up-regulation of both CD133 and Nestin protein expression after 24 hours.

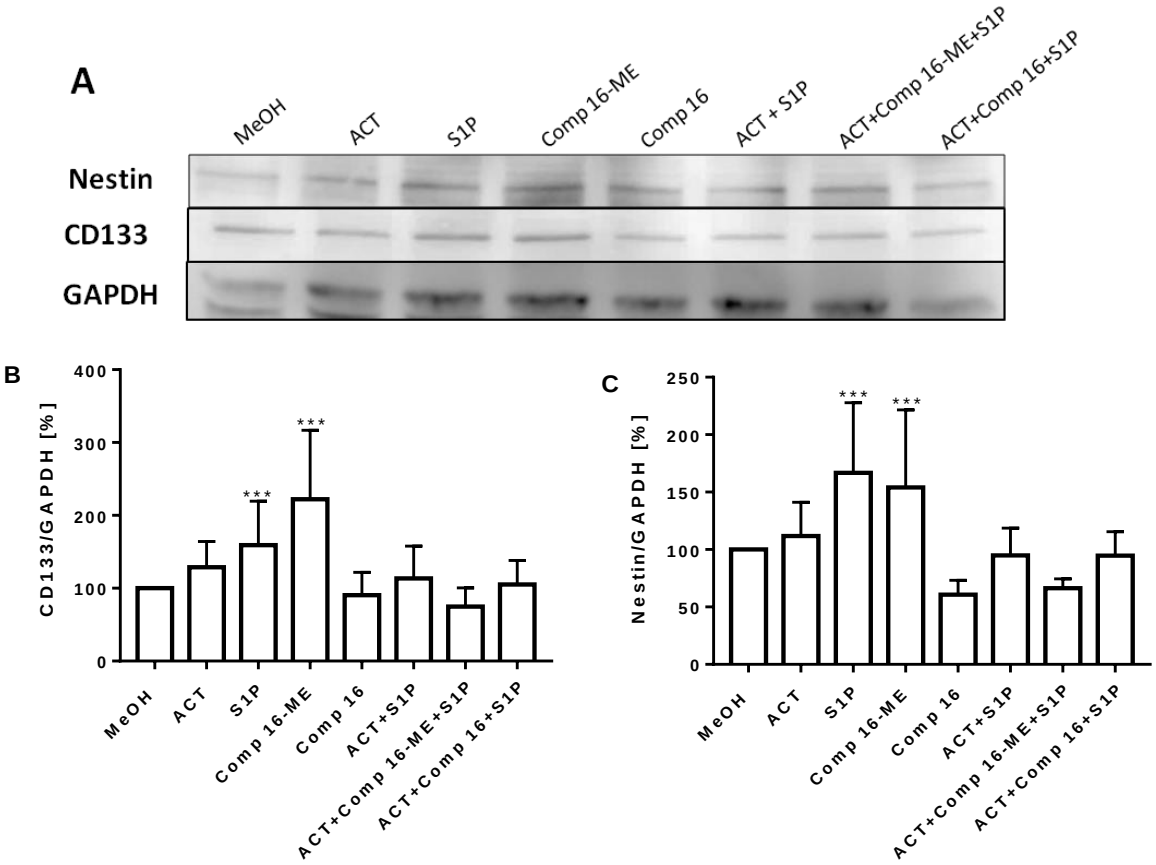

Figure 12: Immunoblot analysis of the stem cell marker CD133 and Nestin. GL261 GBM cells were treated with 10 µM ACT-209905 (ACT), 2.5 µM S1P, 10 µM Compound 16 (Comp 16) or Compound 16-ME (Comp 16-ME) for 6 h. For the combined treatment of the substances, LN18 cells were pre-treated with 10 µM ACT-209905 for 24 h and 10 µM Comp 16/Comp 16-ME for 6 h followed by application of 2.5 µM S1P for 6 h. Control cells were treated with MeOH. Treated cells are shown in relation to the MeOH control (100%), mean values and SD, $n = 3$, one-way analysis of variance with Dunnett´s multiple comparison test, $*p < 0.05$, $**p < 0.005$ and $***p < 0.001$ vs. control.

To further validate the molecular mechanisms of ACT-209905 and Compound 16/16-ME regarding GBM stem cell behavior, we pre-treated human LN18 and murine GL261 GBM cells with ACT-209905, Compound 16 or Compound 16-ME for 24 hours followed by application of S1P for 6 or 24 hours. Afterwards, the expression of the stem cell marker CD133 and Nestin was analyzed by immunoblotting. As seen in Figure 12 in the LN18 GBM cell line, there was a significant increase in the expression of CD133 after treatment with all tested drugs for 6 hours (Figure 13A). The strongest effect was observed for treatment with ACT-209905 alone (399.2%) which was similar to the combined application of ACT-209905 and S1P (369.3%). Compound 16 and Compound 16-ME increased the expression of CD133 to 344.8% and 258.5%, respectively, and this effect was somewhat smaller when the compounds were combined with S1P (293.0% and 185.3%). The single application of S1P caused an increase of CD133 protein expression to 294.4% in LN18 cells after 6 hours (Figure 13A). After 24 hours, the rise in CD133 expression was not so pronounced as seen for the 6 hours incubation time. Here, the single application of ACT-209905 and Compound 16 did not result in an elevated CD133 protein expression whereas Compound 16-ME caused an increase to 237.9%. The application of S1P alone as well as the combination with ACT-209905 or Compound 16-ME, but not with Compound 16, also enhanced the CD133 protein expression to 216.4%, 241.6% and 364.2%, respectively.

Nestin protein expression was significantly elevated in LN18 cells after 6 hours by single application of S1P, ACT-209905 and Compound 16 to 226.3%, 261.4% and 197.8%, respectively (Figure 13B). Also, the combination of S1P with ACT-209905 increased the Nestin expression (255.3%) in similar way as for the single ACT-209905 treatment. These inducing effects were strongly mitigated after 24 hours of treatment.

In contrast, in GL261 GBM cells, only the combined application of ACT-209905 and S1P caused a significant increase in CD133 expression to 170.6% and 136.6% after 6 and 24 hours (Figure 13C). An enhanced Nestin protein expression in GL261 cells was seen for all tested substances after 6 hours whereby the strongest induction was caused by the combined application of ACT-209905 and S1P to 285.6% (Figure 13D) which was much higher than for single treatment with S1P (217.0%) or ACT-209905 (176.3%) (Figure 13D). The changes in Nestin protein expression in GL261 cells after 24 hours were consistent with the results from the 6 hours treatment. Interestingly, as also seen for CD133, the strongest induction of

Nestin protein expression in GL261 cells was found for combined treatment with ACT-209905 and S1P.

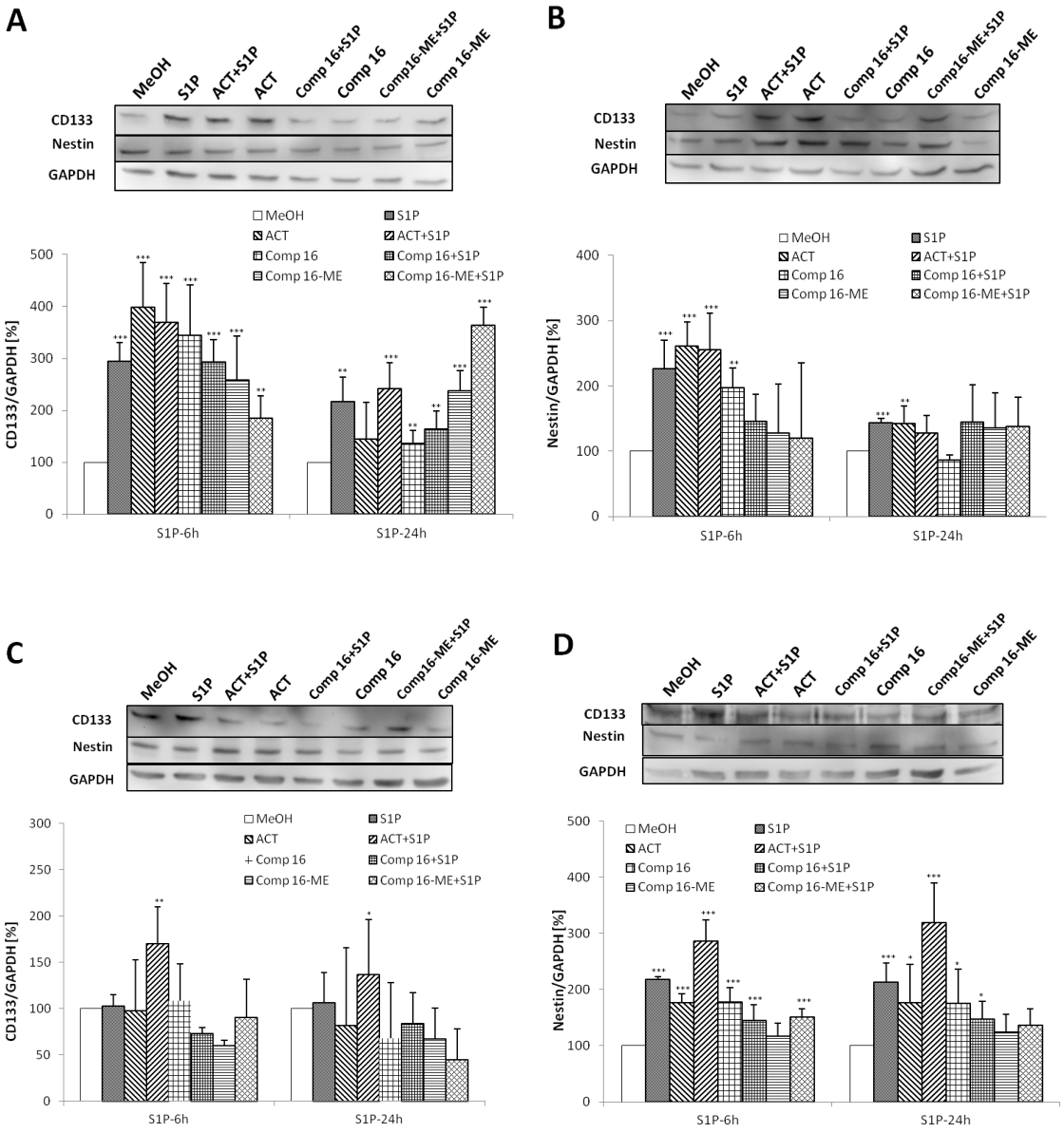

Figure 13: Immunoblot analysis of CD133 and Nestin protein expression in the LN18 and GL261 GBM cell lines. After 24 hours of pre-treatment with ACT-209905 (ACT, 10 µM), Compound 16 (Comp 16, 10 µM) and Compound 16-ME (Comp 16-ME, 10 µM), 2.5 µM S1P was given for 6 hours and 24 hours. Afterwards, the extracted proteins were subjected to immunoblot analysis. Control cells were treated with MeOH (0.1%). (A+B) Expression of CD133 and Nestin in human LN18 GBM cells, (C+D) expression of CD133 and Nestin in murine GL261 GBM cells. Treated cells are shown in relation to the MeOH control (set to 100%), mean values and SD, $n = 3$, one-way analysis of variance with Dunnett´s multiple comparison test, $*p < 0.05$, $**p < 0.005$ and $***p < 0.001$ vs. control.

5.6 Effect of a dual inhibition of S1PR1 and S1PR2 signaling by different compounds on viability of GBM cells *in vitro*

To understand the role of the S1P signaling pathways on GBM cell growth, different inhibitors of S1PR1 and S1PR2 were used: ACT-209905 (S1PR1 modulator/antagonist), Compound 16/16-ME (S1PR2 antagonists), JTE-013 (S1PR2 antagonist) and W146 (S1PR1 antagonist). Figures 13-15 show the results of single treatment or a combination of the respective substances on viability of the human LN18 and U87MG GBM cells as well as the murine GL261 GBM cells.

In LN18 GBM cells (Figure 14A-D), Compound 16, W146 and JTE-013 treatment as well as the combined application of Compound 16 and W146 decreased the cell viability to 65.7%, 71.2%, 64.9%, 76.0% and 70.6% after 6 hours. After 24 hours, the single application of Compound 16 and JTE-013 resulted in a significantly reduced viability of LN18 cells. Additionally, all combined treatment regimens decreased the viability of LN18 cells significantly with the exception of the dual application of Compound 16-ME and W146. The cell viability further decreased significantly after 48 and 72 hours of treatment as seen in Figure 12C and D. The strongest effects were observed after 72 hours for the combined application of the Comp 16-ME/ACT-209905 and JTE-013/ACT-209905 and JTE-013 (7.6% and 13.7%). Similar results were found for the determination of LN18 cell vitality using crystal violet staining (Figure 14E-H).

In human U87MG GBM cells (Figure 15B), after 24 hours of treatment with JTE-013 alone as well as all dual S1PR1/2 blocking regimens caused a significantly reduced cell viability whereas after 6 hours only the single application of JTE-013 was associated with a decreased U87MG viability (Figure 15A). After 48 hours, the single application of ACT-209905, Compound 16 and JTE-013 decreased the viability of U87MG cells significantly. Except for the combined application of Compound 16-ME and W146, the cell viability upon all other dual S1PR1/S1PR2 blocking regimens was significantly reduced. After 72 hours, with the exception of the single application of W146, all other single and dual blocking regimens using ACT-209905, Compound 16, Compound 16-ME, JTE-013 and W146 resulted in a significant reduction of the cell viability of U87MG cells (Figure 15D). Again, the results of the cell vitality analyses with crystal violet staining showed similar results as the cell viability experiments (Figure 15E-H).

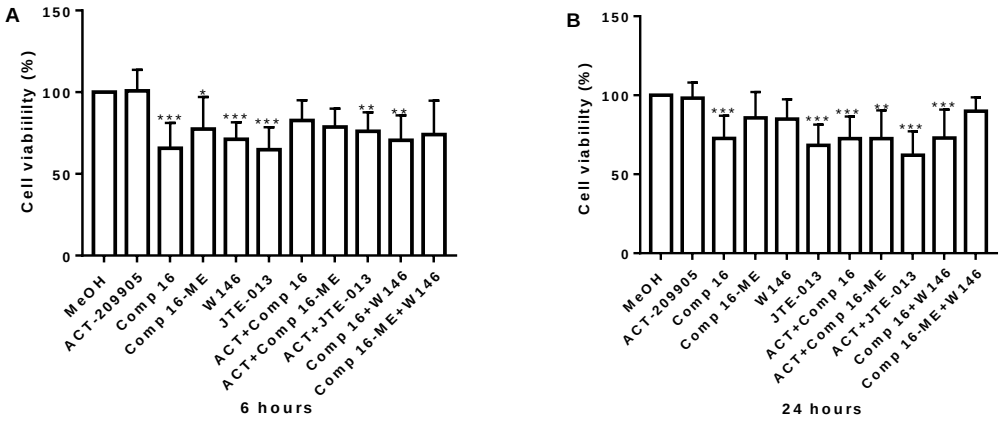
A
Cell viabiilility (%)
150
100
50
0
MeOH
ACT-209905
Comp 16
Comp 16-ME
W146
JTE-013
ACT+Comp 16
ACT+Comp 16-ME
ACT+JTE-013
Comp 16+W146
Comp 16-ME+W146
6 hours
B
Cell viabilility (%)
150
100
50
0
MeOH
ACT-209905
Comp 16
Comp 16-ME
W146
JTE-013
ACT+Comp 16
ACT+Comp 16-ME
ACT+JTE-013
Comp 16+W146
Comp 16-ME+W146
24 hours

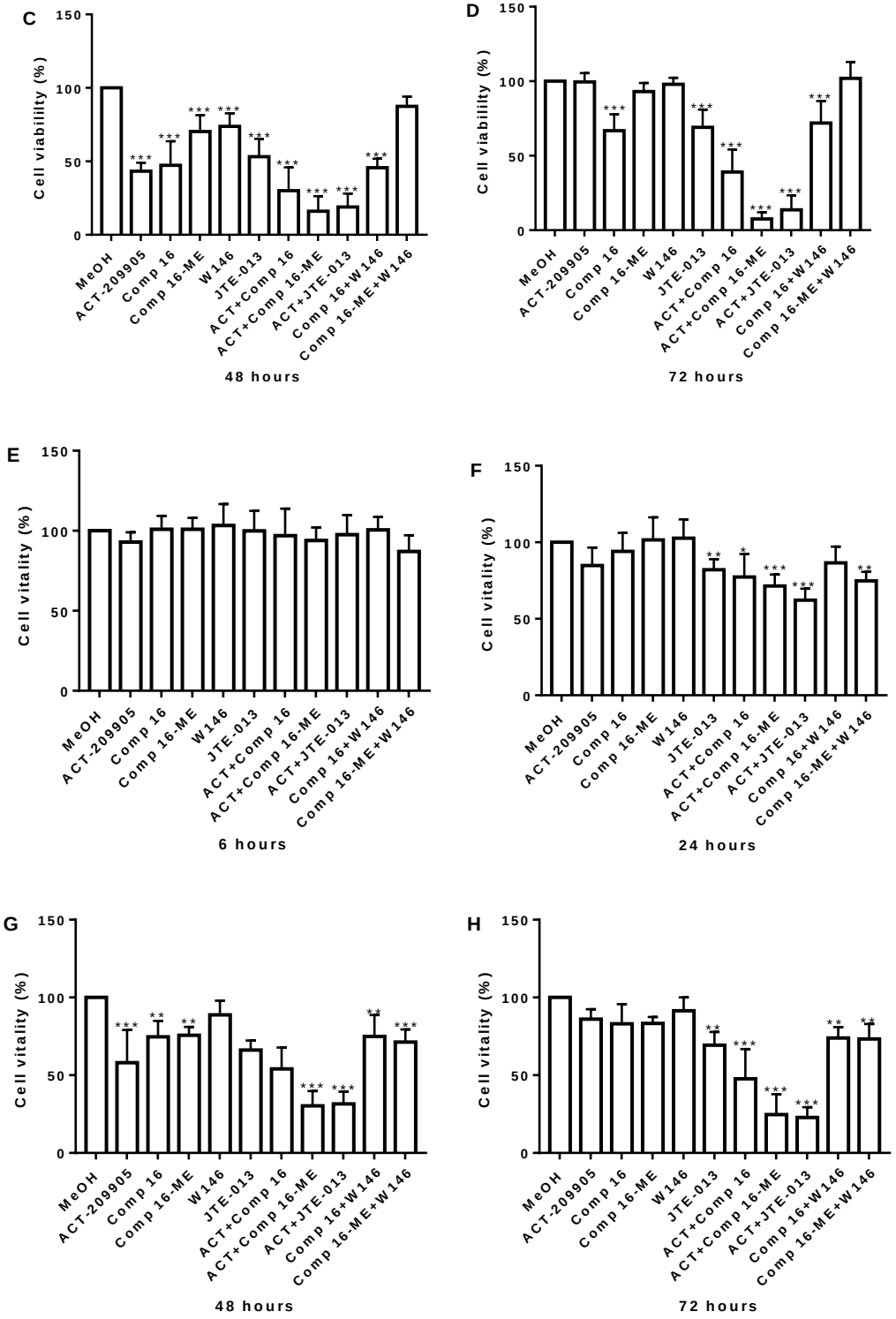

Figure 14: Treatment of LN18 GBM cells with ACT-209905, Compound 16, Compound 16-ME, JTE-013 and W146. Resazurine assay (A-D) and Crystal-violet assay (E-H) after treatment with ACT-209905 (ACT, 10 µM), Compound 16 (Comp 16, 10 µM), Compound 16-ME (Comp 16-ME, 10 µM), JTE-013 (10 µM) and W146 (10 µM) for 6, 24, 48 and 72 h, administered alone and in combination. Control cells were treated with MeOH (0.1%). Cell viability (Resazurine assay) and cell vitality (Crystal-violet assay) are shown in relation to the MeOH control (set to 100%), mean values and SD, $n = 4$, one-way analysis of variance with Dunnett´s multiple comparison test, $*p < 0.05$, $**p < 0.005$ and $***p < 0.001$ vs. control.

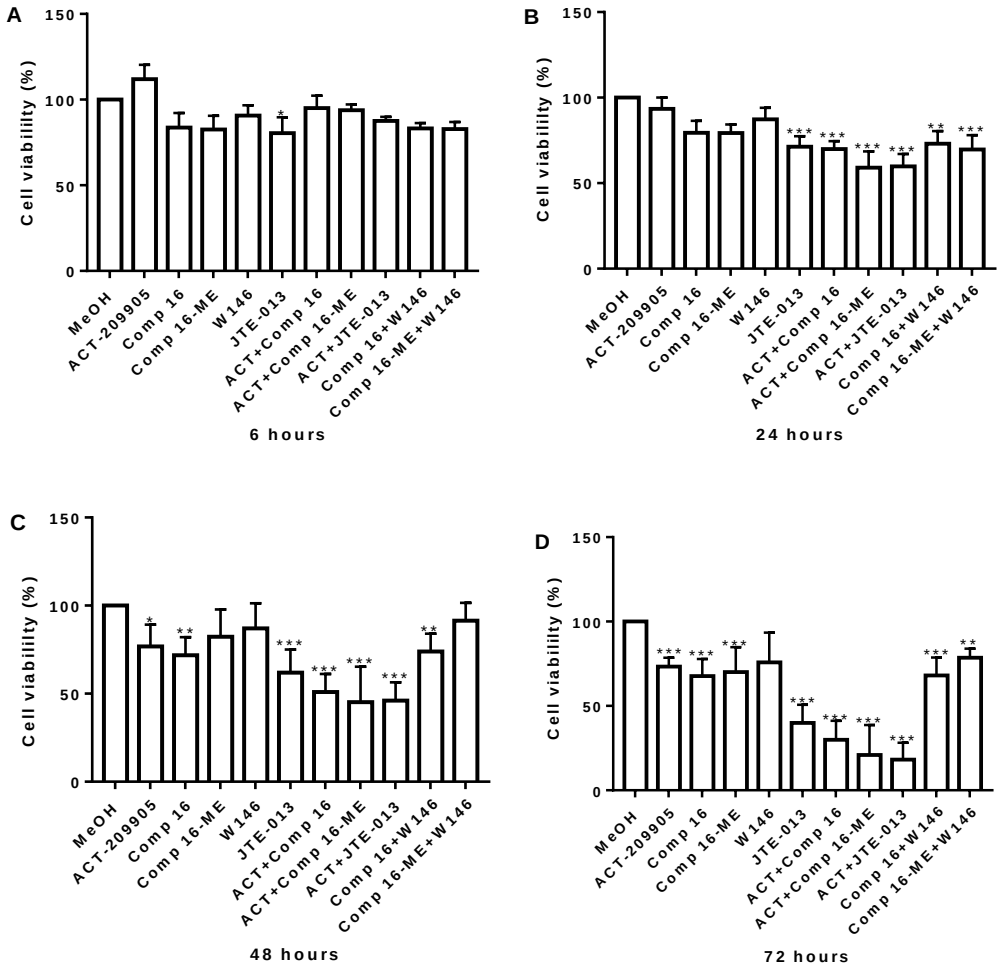
A
Cell viability (%)
150
100
50
0
MeOH
ACT-209905
Comp 16
Comp 16-ME
W146
JTE-013
ACT+Comp 16
ACT+Comp 16-ME
ACT+JTE-013
Comp 16+W146
Comp 16-ME+W146
6 hours
B
Cell viability (%)
24 hours
C
Cell viability (%)
48 hours
D
Cell viability (%)
72 hours

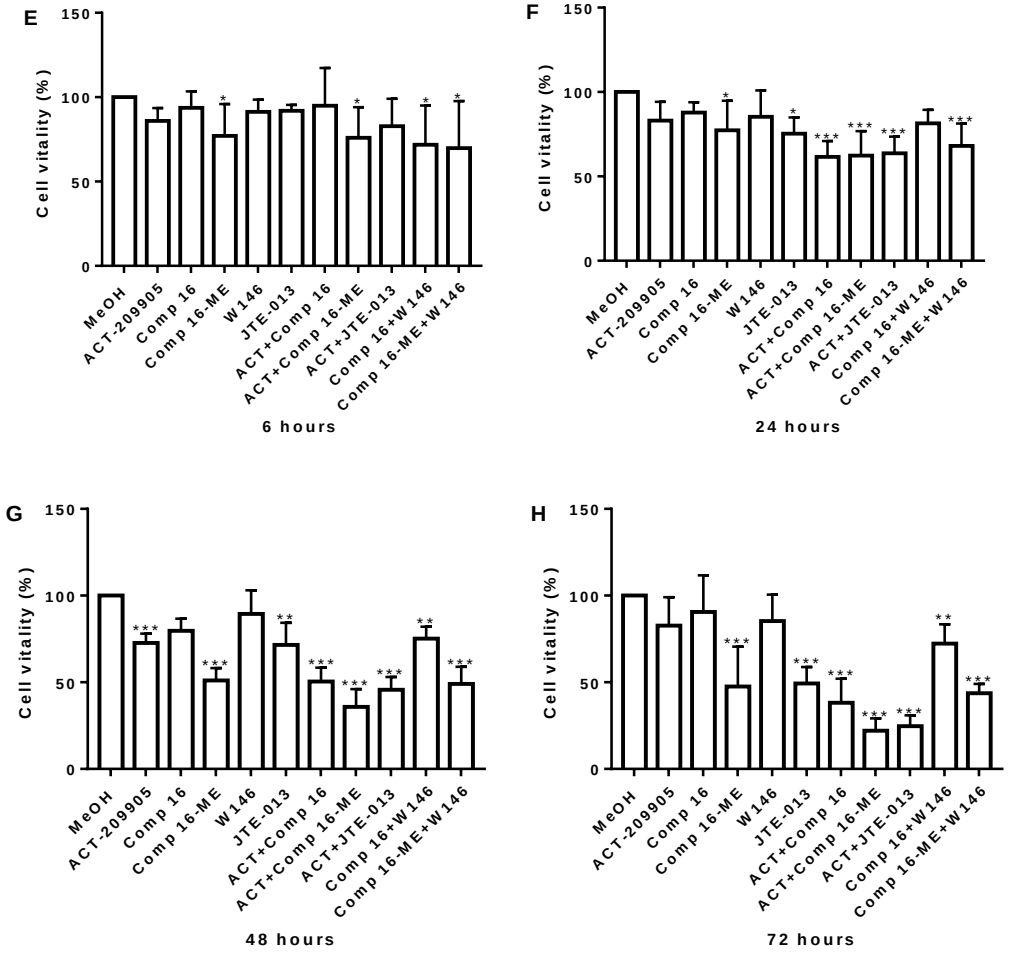

Figure 15: Treatment of U87MG GBM cells with ACT-209905, Compound 16, Compound 16-ME, JTE-013 and W146. Resazurine assay (A-D) and Crystal-violet assay (E-H) after treatment with ACT-209905 (ACT, 10 µM), Compound 16 (Comp 16, 10 µM), Compound 16-ME (Comp 16-ME, 10 µM), JTE-013 (10 µM) and W146 (10 µM) for 6, 24, 48 and 72 h, administered alone and in combination. Control cells were treated with MeOH (0.1%). Cell viability (Resazurine assay) and cell vitality (Crystal-violet assay) are shown in relation to the MeOH control (set to 100%), mean values and SD, $n = 4$, one-way analysis of variance with Dunnett´s multiple comparison test, $*p < 0.05$, $**p < 0.005$ and $***p < 0.001$ vs. control.

In murine GL261 GBM cells (Figure 16A), after 6 hours, with the exception of the dual application of Compound 16-ME and W146, all other single and dual S1PR1/S1PR2 blocking regimens decreased the viability of GL261 cells significantly. After 24 hours of treatment, the GL261 cell viability was significantly reduced in all single and dual application protocols except for the single application of Compound 16 and the combined treatment with Compound 16-ME and W146. After 48 hours, Compound 16, Compound 16-ME and JET-013 treatment caused a significant reduction of GL261 cell viability. Additionally, the combination of ACT-209905 with Compound 16 or JTE-013 also resulted in significantly diminished viability of GL261 cells. After 72 hours, the GL261 cell viability of all treatment

groups was significantly reduced with the strongest effects seen for dual application of ACT-209905 together with Compound 16-ME or JTE-013. For GL261 cell vitality using crystal violet staining similar results as for the cell viability analyses was observed (Figure 16E-H).

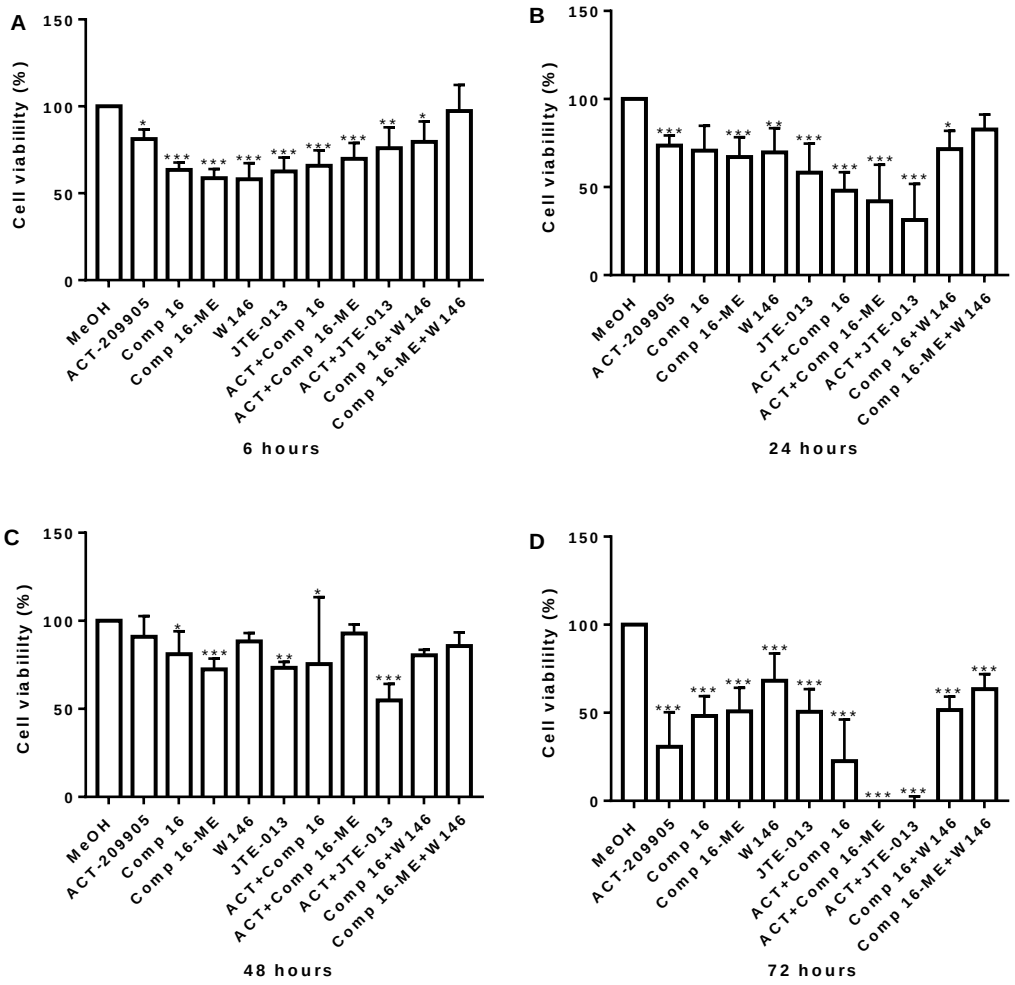

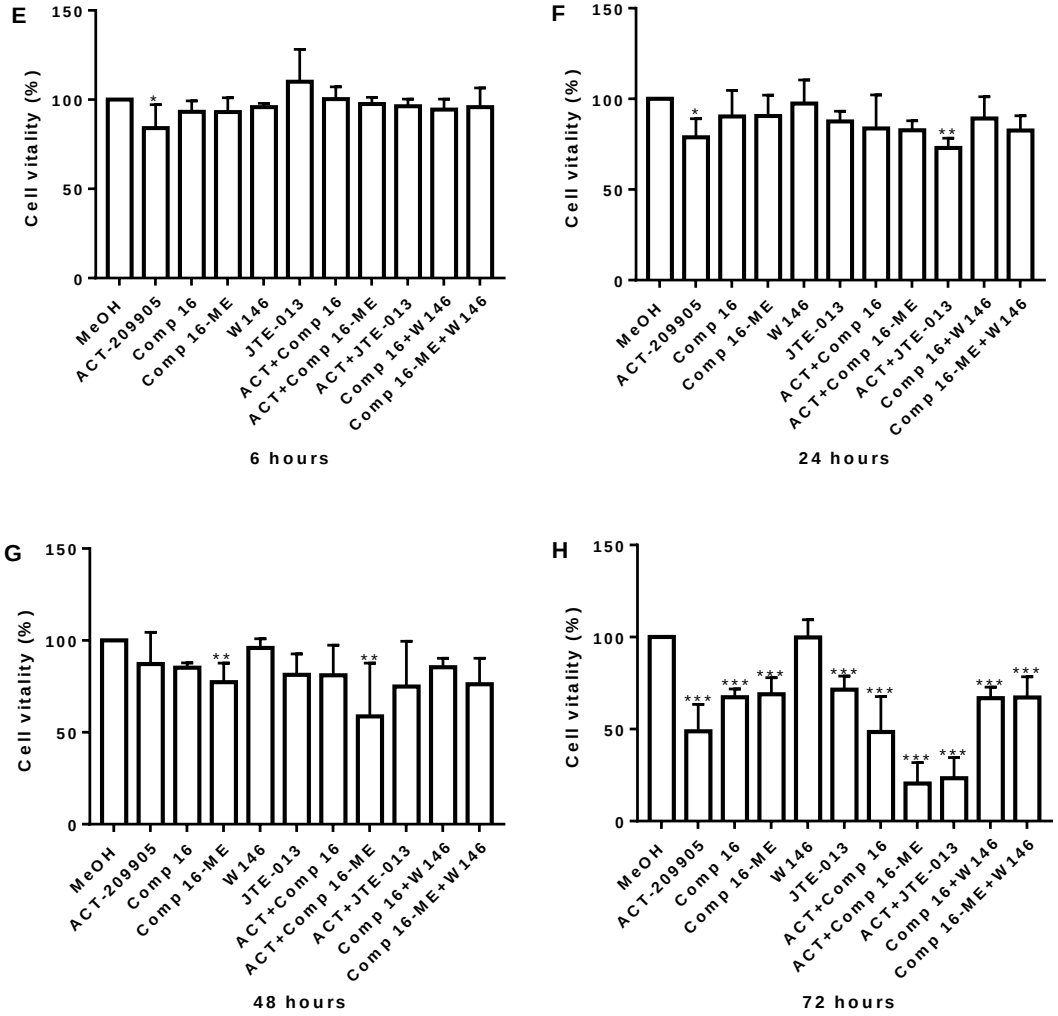

Figure 16: Treatment of GL261 GBM cells with ACT-209905, Compound 16, Compound 16-ME, JTE-013 and W146. Resazurine assay (A-D) and Crystal-violet assay (E-H) after treatment with ACT-209905 (ACT, 10 µM), Compound 16 (Comp 16, 10 µM), Compound 16-ME (Comp 16-ME, 10 µM), JTE-013 (10 µM) and W146 (10 µM) for 6, 24, 48 and 72 h, administered alone and in combination. Control cells were treated with MeOH (0.1%). Cell viability (Resazurine assay) and cell vitality (Crystal-violet assay) are shown in relation to the MeOH control (set to 100%), mean values and SD, $n = 4$, one-way analysis of variance with Dunnett´s multiple comparison test, $*p < 0.05$, $**p < 0.005$ and $***p < 0.001$ vs. control.

5.7 Expression of S1P receptors in LN18 GBM stem-like neurospheres

Immunoblotting was used to compare and evaluate the expression of S1P receptors in adherent LN18 cells and stem-like LN18 neurospheres. For this purpose, LN18 cells were cultured in serum-free medium in the presence of growth factors (EGF, bFGF, heparin) with formation of neurospheres bearing stem cell features [106-108]. As control, LN18 cells are maintained in parallel as adherent cells under standard conditions in serum containing medium (10% FCS). The results of the immunoblot analysis are shown in Figure 17 demonstrating that the expression of S1PR1, 2, 3 and 5 is slightly higher in stem-like LN18 neurospheres than in adherent LN18 GBM cells. This increase was only statistically significant for the expression of S1PR2.

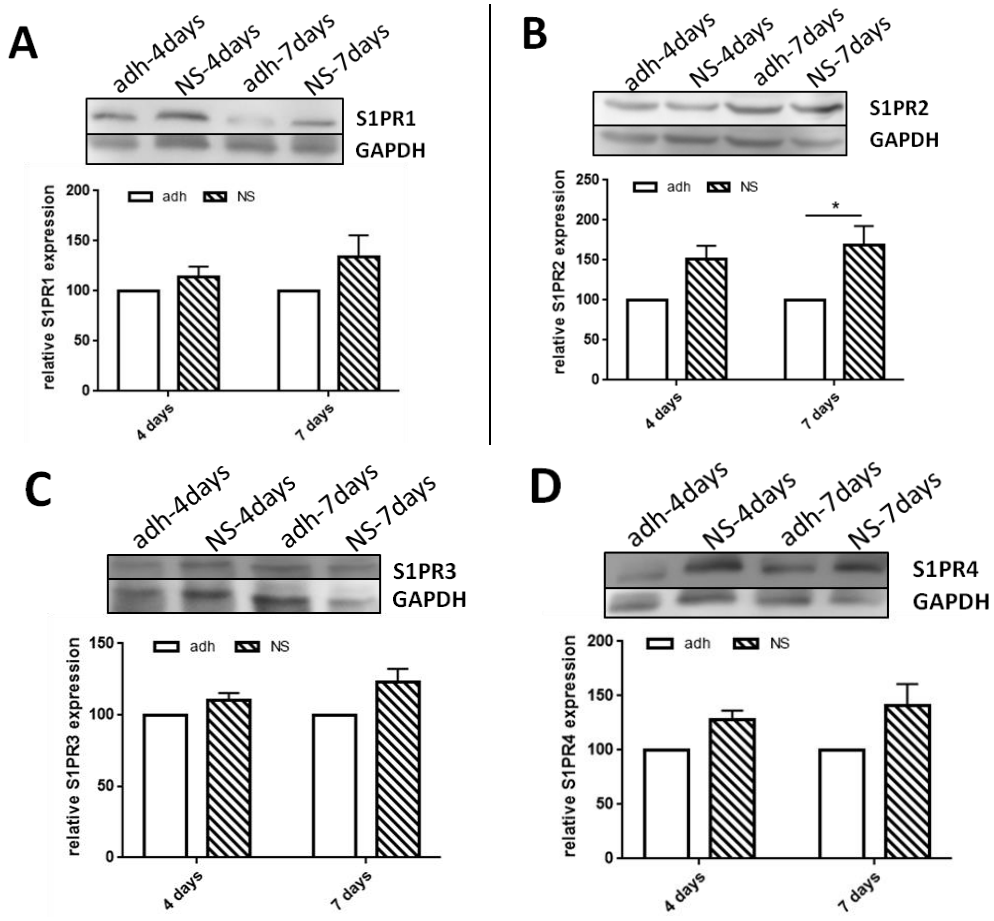

Figure 17: Expression of S1P receptors in LN18 GBM stem-like neurospheres. LN18 GBM cells were cultured for 4 and 7 days either as adherent cells in serum-containing standard medium (10% FCS) and as stem-like neurospheres in serum-free medium in the presence of EGF, bFGF and heparin. Afterwards, proteins were separately extracted for subsequent Western blotting experiments. (A) S1PR1 expression, (B) S1PR2 expression, (C) S1PR3 expression and (D) S1PR5 expression. S1P receptor expression of LN18 neurospheres is shown in relation to the adherent LN18 cells (set to 100%), mean values and SD, $n = 3$, one-way analysis of variance with Dunnett´s multiple comparison test, $*p < 0.05$.

5.8 Viability of GBM cells after treatment with ACT-209905, Compound 16 and Compound 16-ME together with temozolomide (TMZ) *in vitro*

The current standard chemotherapeutic drug for clinical treatment of GBM is temozolomide (TMZ). In this set of experiments, we investigated whether an inhibition of S1PR1 (by ACT-209905) or S1PR2 (by Compound 16 and Compound 16-ME) sensitizes GBM cells against TMZ. As seen in Figure 16, we did not find a significant synergistic or additive effect between ACT-209905 and TMZ in GBM cells. We unexpectedly found that that in some cases TMZ appeared to reverse the cytotoxic effects of ACT-209905 in the murine GL261 GBM cell line (Figure 18E and 18F), but this was obeserved in the human GBM cells (LN18, U-87MG) (Figure 18A-D).

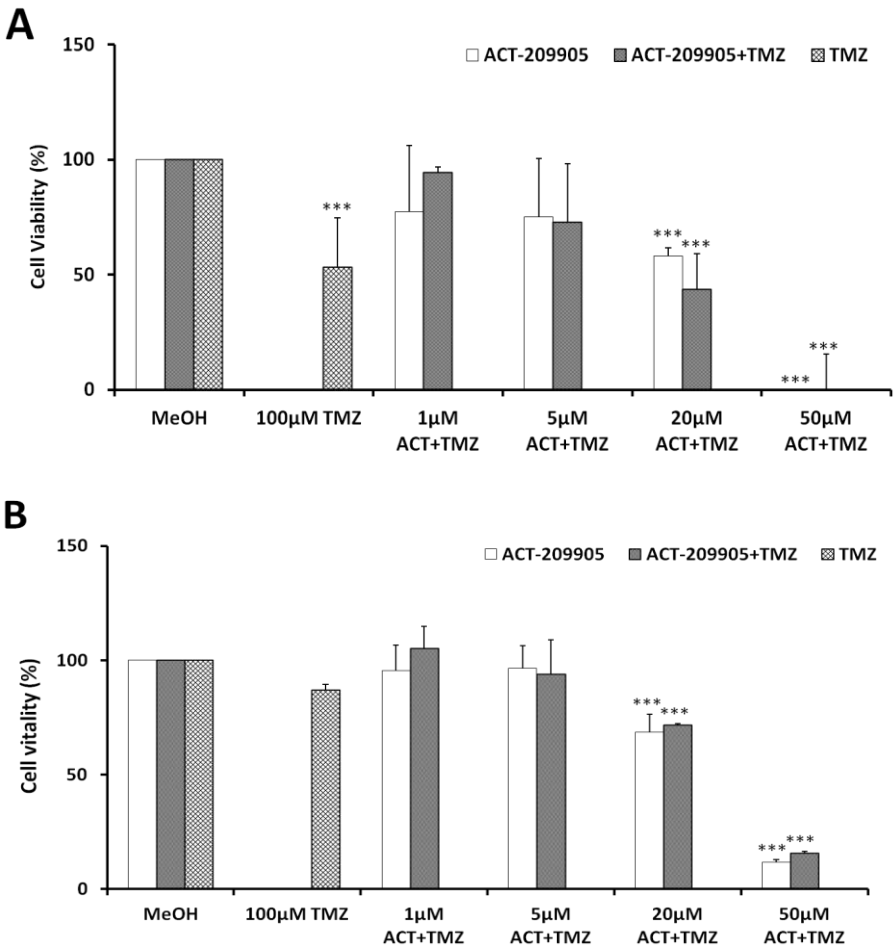

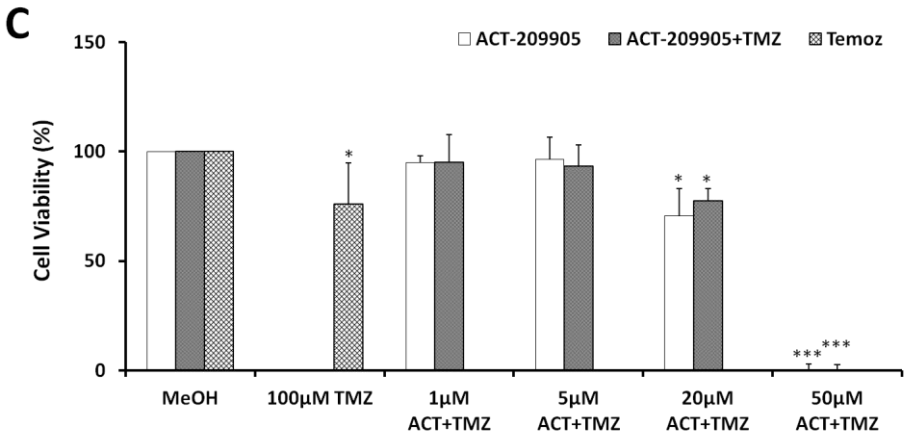
C
ACT-209905
ACT-209905+TMZ
Temoz
Cell Viability (%)
150
100
50
0
MeOH
100µM TMZ
1µM ACT+TMZ
5µM ACT+TMZ
20µM ACT+TMZ
50µM ACT+TMZ

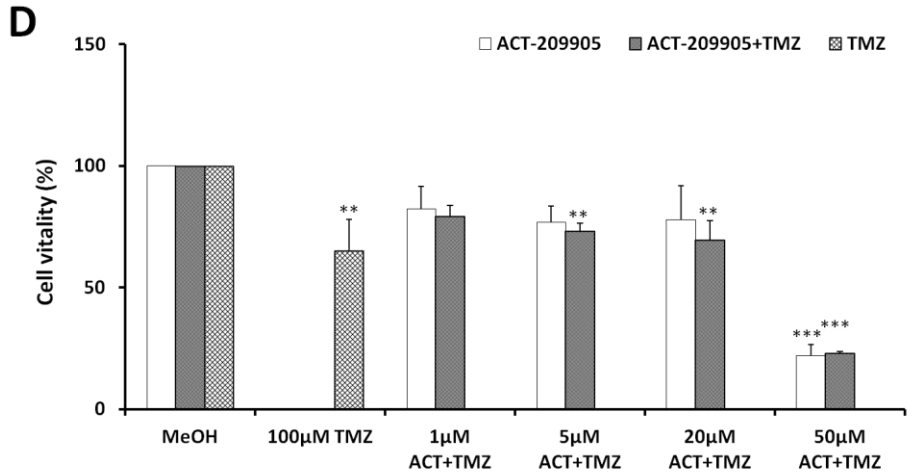
D
ACT-209905
ACT-209905+TMZ
TMZ
Cell vitality (%)
150
100
50
0
MeOH
100µM TMZ
1µM ACT+TMZ
5µM ACT+TMZ
20µM ACT+TMZ
50µM ACT+TMZ

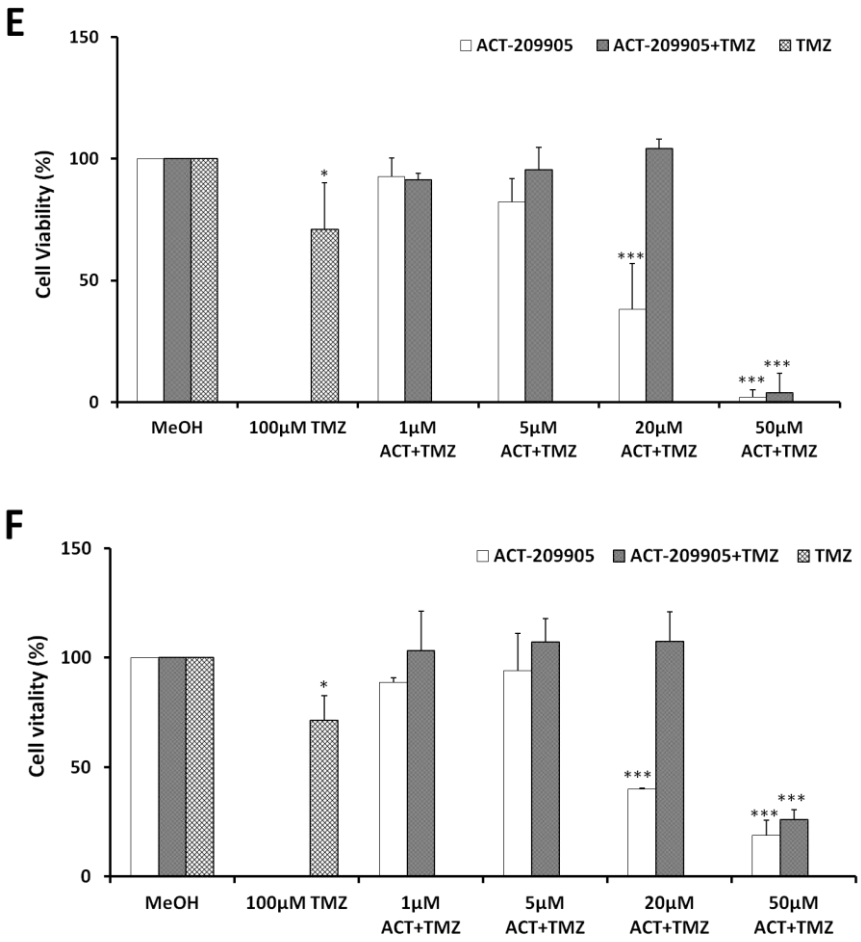

Figure 18: Influence of ACT-209905 and TMZ on cell viability of GBM cells. Resazurine assay (A, C, E) and Crystal-violet assay (B, D, F) after treatment of GBM cells with ACT-209905 (ACT, 1 µM, 5 µM, 20 µM, 50 µM), Temozolomide (TMZ, 100 µM) for 24 hours, administered alone and in combination. Control cells (CON) were treated with MeOH. (A) LN18 cell viability using the resazurine assay. (B) LN18 cell vitality using the Crystal-violet assay. (C) U-87MG cell viability using the resazurine assay. (D) U-87MG cell vitality using the Crystal-violet assay. (E) GL261 cell viability using the resazurine assay. (F) GL261 cell vitality using the Crystal-violet assay. Cell viability and cell vitality are shown in relation to the control (set to 100%), mean values and SD, $n = 3$, one-way analysis of variance with Dunnett´s multiple comparison test, $*p < 0.05$, $**p < 0.005$ and $***p < 0.001$ vs. control.

Furthermore, we treated the GBM cells with Compound 16 and Compound 16-ME together with TMZ in comparison to the single application of ACT-209905, Copmpound 16 and Compound 16-ME. The results of the respective cell viability/vitality analyses are shown in the Figure 18-20 below.

In the human GBM cell lines LN18 (Figure 19) and U87MG (Figure 20), the viability of all cells treated for 48 and 72 hours with ACT-209905 alone or in combination with Compound 16, Compound 16-ME and TMZ was strongly reduced which was more pronounced in the combination treatment groups. Again, we unexpectedly found that temozolomide appeared

to reverse the cytotoxic effects of ACT-209905 in GL261 cells (Figure 20), but this was not observed in the human GBM cells.

In LN18 cells, ACT-209905 alone reduced the viability to 73.9%, this effect was more pronounced in the ACT-209905/Compound 16 treatment group (21.2%), in the ACT-209905/Compound 16-ME treatment group (nearly 0%), ACT-209905 and together with TMZ (17.8%) after 48 hours (Figure 18A). The combination of Compound 16 or Compound 16-ME as inhibitors of S1PR2 with TMZ did not result in a signifcantly decreased cell viability. Interestingly, the combination of ACT-209905 with TMZ showed nearly similar effects as the combination of ACT-209905 with Compound 16. Very similar effects were seen after 72 hours of treatment (Figure 19B). The results of the LN18 cell vitality analyses are seen in Figure 18C+D showing the same as the cell viability data.

In the U87MG cells, the application of 10 µM ACT-209905 alone caused no significant decrease of the cell viability after 48 and 72 hours. The dual application of ACT-209905 with Compound 16 or Compound 16-ME showed the strongest cytotoxic effects both after 48 hours (45.8% and 39.2% cell viability, Figure 20A) and 72 hours (24.0% and 23.0% cell viability, Figure 20B), too. The combination of Compound 16 or Compound 16-ME, as inhibitors of S1PR2, with TMZ also significantly reduced the U87MG to 71.2% and 62.2% after 48 hours, and to 52.2% and 44.8% after 72 hours, respectively (Figure 20A+B). This effect was just as strongly as for the combination of ACT-209905 with TMZ whereas the single application of 10 µM ACT-209905 caused no significant decrease of U87MG cell viability. The Crystal-violet analyses revealed similar results (Figure 20C+D).

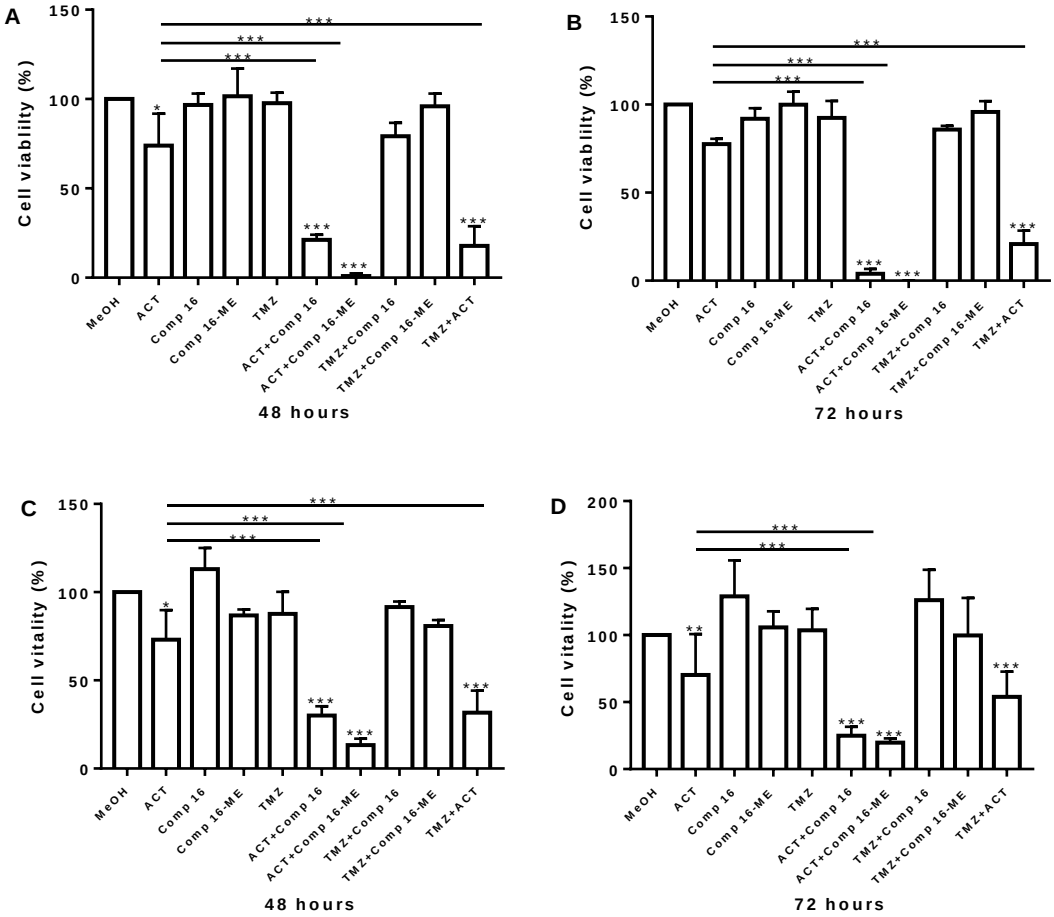

Figure 19: LN18 GBM cell viability and vitality after dual treatment with ACT-209905, Compound 16, Compound 16-ME and temozolomide. Resazurine assay (A+B) and Crystal-violet assay (C+D) after treatment with ACT-209905 (ACT, 10 µM), Compound 16 (Comp 16, 10 µM), Compound 16-ME (Comp 16-ME, 10 µM) and temozolomide (TMZ, 100 µM) for 48 and 72 h, administered alone and in combination. Control cells (CON) were treated with MeOH. (A+B) LN18 cell viability using the resazurine assay. (C+D) LN18 cell vitality using the Crystal-violet assay. Cell viability and vitality are shown in relation to the control (set to 100%), mean values and SD, $n = 3$, one-way analysis of variance with Dunnett´s multiple comparison test, $*p < 0.05$, $**p < 0.005$ and $***p < 0.001$ vs. control.

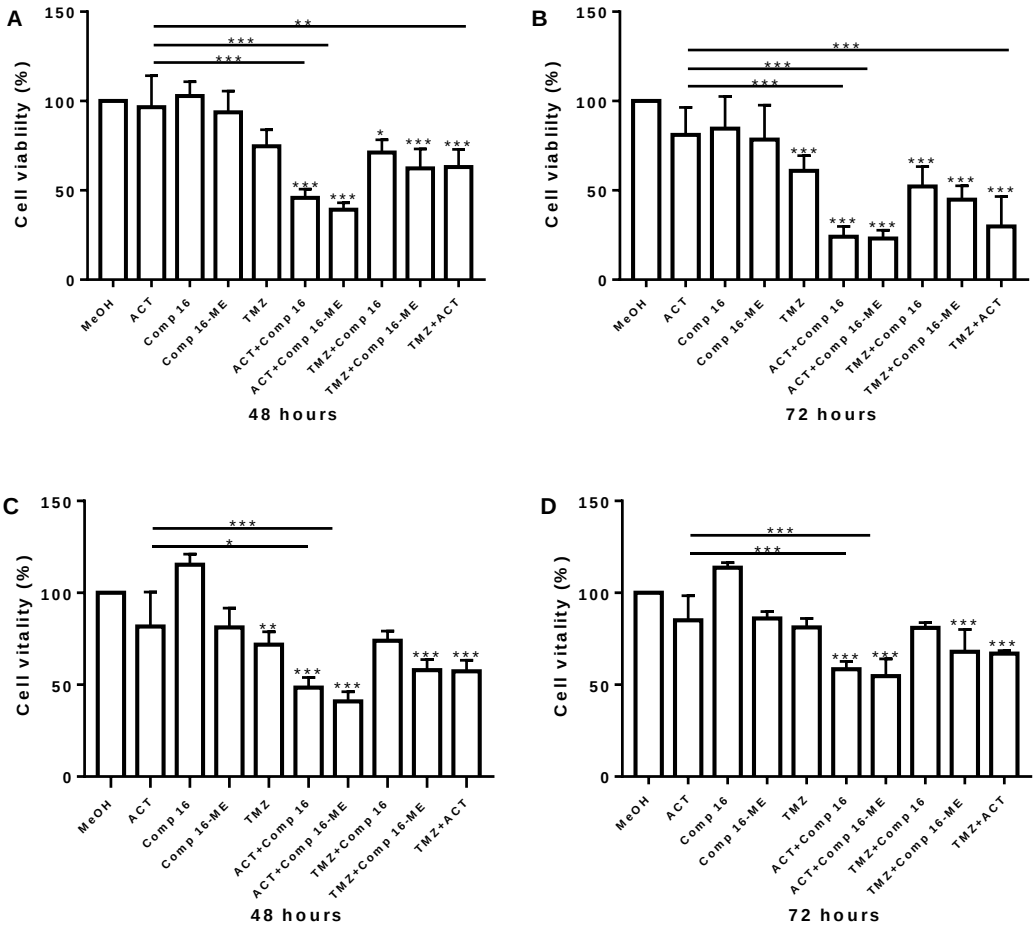

Figure 20: U87MG GBM cell viability and vitality after dual treatment with ACT-209905, Compound 16, Compound 16-ME and temozolomide. Resazurine assay (A+B) and Crystal-violet assay (C+D) after treatment with ACT-209905 (ACT, 10 µM), Compound 16 (Comp 16, 10 µM), Compound 16-ME (Comp 16-ME, 10 µM) and temozolomide (TMZ, 100 µM) for 48 and 72 h, administered alone and in combination. Control cells (CON) were treated with MeOH. (A+B) LN18 cell viability using the resazurine assay. (C+D) LN18 cell vitality using the Crystal-violet assay. Cell viability and vitality are shown in relation to the control (set to 100%), mean values and SD, *n* = 3, one-way analysis of variance with Dunnett´s multiple comparison test, **p* < 0.05, ***p* < 0.005 and ****p* < 0.001 vs. control.

In the GL261 cells (Figure 21A-D), the strongest cytotoxic effect was observed for the combined application of ACT-209905 and Compound 16-ME with a remaining viability level of only 12.0% after 48 hours (Figure 20A). Nearly all GL261 had died after 72 hours of treatment with ACT-209905 and Compound 16-ME together (Figure 21B). The application of 10 µM ACT-209905 alone or together with TMZ did not reduce cell viability. The dual treatment of GL261 cells with Compound 16 or Compound 16-ME together with TMZ decreased the cell viability significantly to 56.4% and 72.4% after 48 hours, and to 63.5% and 72.9% after 72 hours (Figure 20B), respectively. In contrast, incubation of GL261 cells with ACT-209905 and TMZ together did not significantly affect the cell viability (Figure 21). The

results of the cell vitality analyses (Crystal-violet staining, Figure 21C+D) showed similar data as for the cell viability experiments (Resazurine assay).

In all GBM cell lines, single application of 100 µM TMZ or 10 µM Compound 16/16-ME did not or only slightly reduced the cell viability and cell vitality.

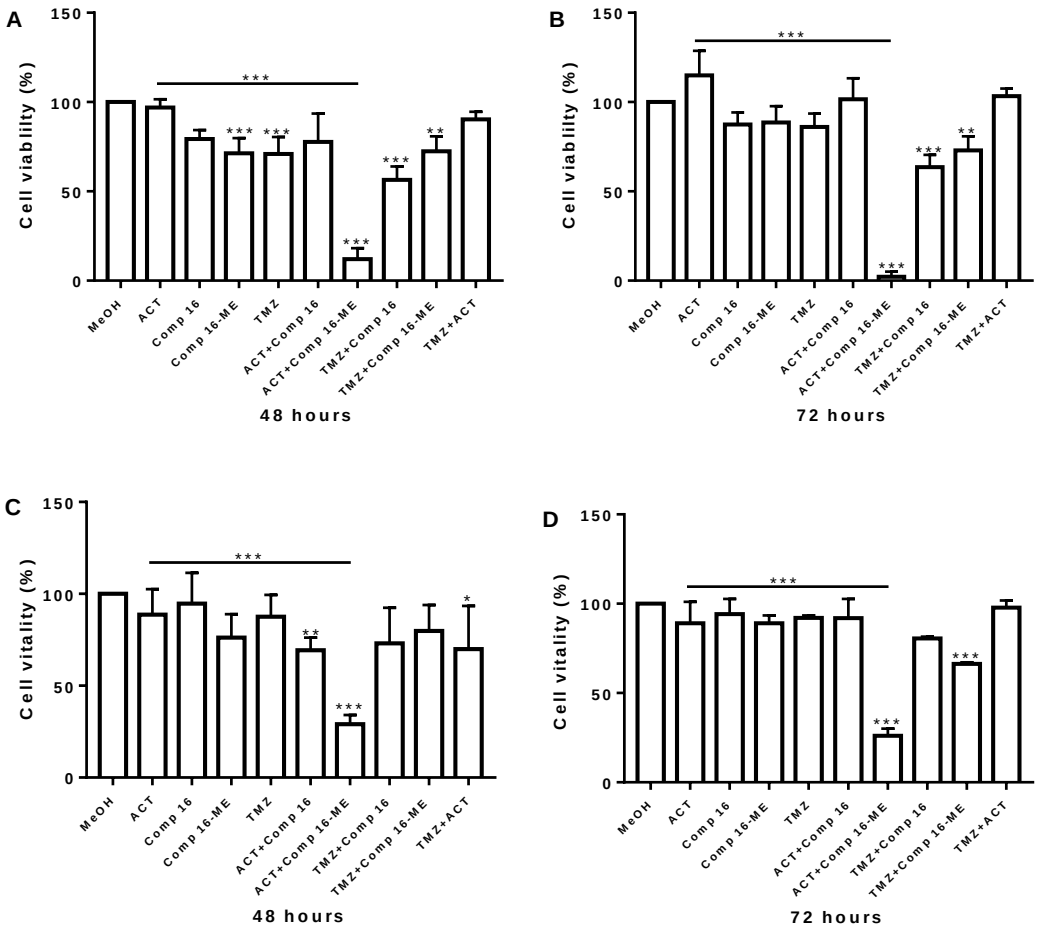

Figure 21: GL261 GBM cell viability and vitality after dual treatment with ACT-209905, Compound 16, Compound 16-ME and temozolomide. Resazurine assay (A+B) and Crystal-violet assay (C+D) after treatment with ACT-209905 (ACT, 10 µM), Compound 16 (Comp 16, 10 µM), Compound 16-ME (Comp 16-ME, 10 µM) and temozolomide (TMZ, 100 µM) for 48 and 72 h, administered alone and in combination. Control cells (CON) were treated with MeOH. (A+B) LN18 cell viability using the resazurine assay. (C+D) LN18 cell vitality using the Crystal-violet assay. Cell viability and vitality are shown in relation to the control (set to 100%), mean values and SD, $n = 3$, one-way analysis of variance with Dunnett´s multiple comparison test, $*p < 0.05$, $**p < 0.005$ and $***p < 0.001$ vs. control.

5.9 Influence of ACT-209905 on caspase 3 activity in GBM cells *in vitro*

Caspase 3 is a cysteine protease that plays an important role in the process of apoptotic cell death [109-111]. To investigate whether the cytotoxic effect of ACT-209905 in GBM cells

involves the induction of apoptosis, the activity of caspase 3 was determined. The results of caspase 3 measurement are shown in Figure 22.

Treatment of all GBM cells (LN18, U87MG and GL261) with 5 µM ACT-209905 for 48 hours did not result in significant changes of caspase 3 activity. The GBM cells treated with 20 µM ACT-209905 for 48 hours showed an increased activity of caspase 3 but this was not statistically significant. Only application of 50 µM ACT-209905 caused an elevated activity of caspase 3 with relative values of 0.067 AU, 0.031 AU and 0.024 AU in LN18, GL261 and U87MG cells, respectively, compared to XX AU, XX AU and XX AU in MeOH treated control cells.

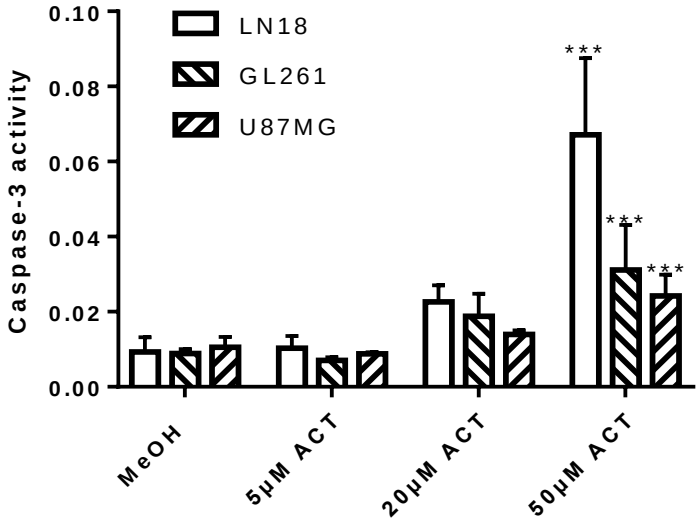

Figure 22. Activity of caspase 3 in GBM cells after treatment with ACT-209905. LN18, U87MG (both human GBM cell lines) and GL261 (a murine GBM cell line) were treated with ACT-209905 (ACT; 5, 20 and 50 µM) for 48 hours. Control cells were treated with the respective solvent (MeOH, 0.1%). Afterwards, caspase 3 activity was determined with a commercially available kit according to the manufactureers instruction. Mean values and SD, $n = 3$, One-way analysis of variance with Dunnett´s multiple comparison test, ***$p < 0.001$ vs. MeOH control.

5.10 Effects of ACT-209905 on viability of LN18 GBM stem-like cells *in vitro*

Glioma stem cells have emerged as a crucial player in the pathogenesis of GBM and are thought to be responsible for resistance to conventional therapy resulting in the rapid occurrence of relapses [112,113]. The cultivation of GBM neurospheres, which represent stem cell features, is a well-accepted method for investigation of GBM stem cell characteristics and behavior [114,115]. In this work, the human GBM cell line LN18 was used to further validate the potential therapeutic effects of ACT-209905 on GBM stem-like cells.

The adherent and neurosphere cells were cultured for 4 (Figure 23A) or 7 days (Figure 23B) followed by application of 10 µM ACT-209905 and subsequent cell viability and vitality analyses. 24 hours after application of 10 µM ACT-209905, the viability of LN18 adherent cells was not significantly diminished whereas the LN18 neurosphere cells showed a reduced viability of 75.2% in the 4 day-culture group (Figure 23A). Such a difference in the response to ACT-209905 was also found after 48 hours: the viability of adherent LN18 cells was diminished to 59.0% and of LN18 neurospheres to 39.2%, respectively. In contrast, 72 hours after application of ACT-209905 the decrease in cell viability was nearly similar for the adherent and neurosphere cells (4 days culture group). In sum, after treatment of LN18 stem-like neurospheres cells (4 days in culture) with ACT-209905 for 24 h, 48 h and 72 h, the cell viability decreased to 75.2%, 39.2% and 6.2%, respectively. And after treatment of LN18 stem-like neurospheres cells (7 days in culture) with ACT-209905 for 24 h, 48 h and 72 h, the cell viability was much more reduced to 36.6%, 4.1% and 1.1%, respectively. In the adherent LN18 group (serum containing media), after treatment with ACT-209905 for 24 h, 48 h and 72 h, the cell viability decreased to 94.0%, 63.2% and 2.6% in the 4 day culture group (Figure 23A), and to 84.1%, 59.0% and 26.7% in the 7 day culture group (Figure 23B), respectively.

Interestingly, ACT-209905 seems to have cytotoxic effects not only in adherent glioma cells but also in stem-like neurosphere cells, and the cytotoxicity of ACT-209905 is even more pronounced in neurospheres.

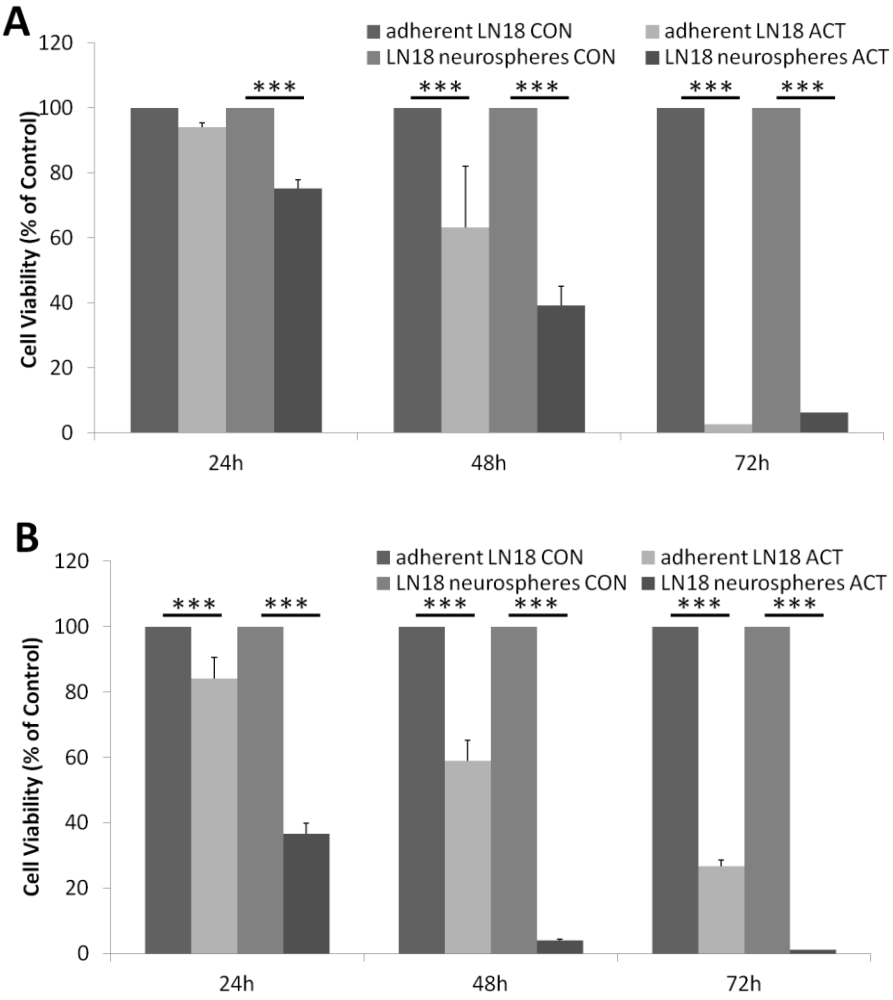

Figure 23: Treatment of LN18 adherent cells and stem-like neurospheres with ACT-209905. LN18 cells were cultured for 4 (A) or 7 days (B) either as adherent cells or as stem-like neurospheres followed by treatment with ACT-209905 (10 µM) for 24 h, 48 h and 72 h. Control cells (CON) were treated with MeOH (0.1%). Cell viability was determined with the Resazurine assay and is shown in relation to the MeOH control (set to 100%), mean values and SD, n = 3, one-way analysis of variance with Dunnett´s multiple comparison test, *$p < 0.05$, **$p < 0.005$ and ***$p < 0.001$ vs. control.

6 Discussion

Glioblastoma multiforme (GBM), the most common and aggressive primary malignant brain tumor of adults, is notoriously fatal. Despite surgical resection and post-operative radiochemotherapy as the standard treatment for GBM, affected patients have a poor median survival of around 15 months. Therefore, an improvement of the therapeutic strategies is urgently needed and targeted therapies might be an alternative to the standard chemotherapy regimen. The bioactive lipid sphingosine-1-phosphate (S1P) has been implicated in various disorders such as cancer and inflammatory diseases. It is involved in proliferation, migration and invasion of a broad range of healthy and malignant cells [26], and is widely present in body fluids and cells such as red blood cells, neutrophils, and platelets [26]. S1P participates in various physiological functions such as immune regulation, hematopoietic regulation, allograft response, glucose metabolism regulation and inflammation [116]. S1P can act intracellularly as a second messenger or it can be moved outside the cell via a transporter to bind to the corresponding receptors (S1P receptors 1-5, S1PR1-5), and activates a series of downstream signaling pathways to produce important physiological functions [31]. These include cell proliferation, migration, survival, apoptosis and cell communication. Previous studies have shown that S1P receptors are involved in the regulation of proliferation, invasion, metastasis, vascular maturation and angiogenesis of various tumor cells, and are closely related to the occurrence and development of tumors [33]. Furthermore, recent studies argue for a potential role of S1P signaling in GBM growth and progress, too [62,69,93,117,118]. DifferentS1PR modulators have been developed such as fingolimod (FTY720) which is approved for treatment of multiple sclerosis. Interestingly, fingolimod as an S1PR1 modulator is also effective against GBM cells *in vitro* and in an *in vivo* mouse model, and sensitizes GBM cells to the chemotherapeutic temozolomide [119,120]. Whether other S1PR modulators are also active against GBM cells and whether they can be used clinically to provide new and effective cancer treatments is currently not known.

Therefore, the purpose of this study was to investigate the influence of the S1PR1 modulator ACT-209905 (a chemical S1PR1 agonist but a functional S1PR1 antagonist) and the S1PR2 blocker Compound 16 and Compound 16-ME on growth and migration of GBM cells *in vitro*. Thereby, the focus lay on the analysis of ACT-209905 mediated effects. In sum, the results of this study indicate that ACT-209905 and Compound 16/16-ME can induce a growth arrest in

GBM cells by inhibiting the proliferation, viability and migration of GBM cells. In the following chapters, the results of the present work will be discussed and compared to other already published studies regarding the impact of S1P signaling in the pathogenesis of GBM.

6.1 ACT-209905 reduces the viability of GBM cells and promote their apoptosis

In our *in vitro* cell viability analyses, we found that ACT-209905 significantly reduced viability of the human LN18 and U87MG GBM cells as well as of the murine GL261 GBM cells. Studies have shown that the expression of S1PR1, S1PR2 and S1PR3 is increased in GBM tissue specimens compared with healthy brain tissue, but only S1PR1 and S1PR2 are significantly associated with patient survival [62,69]. Our previous laboratory studies showed that S1PR1 and 2 play an important role in cell migration and invasion of LN18 GBM cells which were also used as an in vitro GBM cell model in the present work [62]. To understand the role of the S1PR1 and S1PR2 in migration and proliferation of GBM cells, we used ACT-209905 (S1PR1 modulator, see above), Compound 16/16-ME (S1PR2 antagonists), W146 (S1PR1 antagonist) and JTE-013 (S1PR2 antagonist) alone or in combination to treat different GBM cell lines *in vitro*. The results showed that the combined administration of the S1PR1 and S1PR2 antagonists has a more pronounced cytotoxic effect than single administration arguing for a role of both S1P receptor 1 and 2 in the growth of GBM cells. Considering the cell viability analyses, a direct comparison of the cytotoxic effect of ACT-209905, Compound 16 and Compound 16-ME showed that all three substances are similar active 48 and 72 hours after application. This also supports the assumption that both S1PR1 and S1PR2 are involved in the growth of GBM cells. Furthermore, we found a synergistic/additive effect of dual treatment of GBM cells with ACT-209905 together with the current standard chemotherapeutic drug temozolomide (TMZ) for 48 and 72 hours in the human LN18 and U87MG GBM cells but not in the murine GL261 GBM cell line. This discrepancy between human and murine GBM cells could be based on a different expression level of the S1P receptor subtype 1 (S1PR1). Our own immunoblotting results showed that the human LN18 and U87MG cells have a 5- to 7-fold higher S1PR1 protein expression than the murine GL261 cell line. Thus, the molecular target of ACT-209905 might be present in higher amounts in human GBM cell than in murine GBM cells. Unfortunately, this can´t be examined in more detail since there is no other murine GBM cell line available to date. The synergistic/additive

effect, observed for co-application of ACT-209905 and temozolomide, was not seen (LN18, GL261) or at least not so pronounced (U87MG) for the dual application of Compound 16/Compound 16-ME and temozolomide. Thus, inhibition of S1PR1 but not of S1PR2 activates pathways which sensitize the GBM cells against temozolomide.

To further analyze which pathway might be involved in the cytotoxic effect of ACT-209905 in GBM cells, we investigated the activation status of kinases which were previously identified as a part of the S1P signaling. Immunoblot analyses showed a significant 2.5-fold increase in the phosphorylation/activation status for both AKT1 (pAKT1) and ERK1/2 (pERK1/2) 5 and 10 min after stimulation of LN18 cells with 2.5 µM S1P. In contrast, this increase in AKT1 and ERK1/2 activation by S1P was significantly diminished by application of ACT-209905. Thus, in LN18 cells S1PR1 seems to be responsible for the activation of AKT1 and ERK1/2 by S1P, and an inhibition of these kinases could be one mechanism of the cytotoxic effect of ACT-209905. Consistent with our results, S1P-induced G_i-coupled receptors require ERK1/2 activation to stimulate glioma cell proliferation and survival, and an overexpression of S1PR1 leads to ERK1/2 activation, which correspondingly regulates the survival and proliferation of GBM cells [121]. In addition, it is reported in the literature that S1PR1 and S1PR3 are responsible for promoting migration and survival of GBM cells, while S1PR2 attenuates cell migration [122]. Our previous studies have shown that S1P-stimulated LN18 cell migration can be completely inhibited only by blocking PI3K/AKT1 but not by inhibition of the ERK1/2 signaling [62]. In the present study, an increase in phosphorylation of AKT1 was seen in LN18 cells stimulated with S1P but not in the murine GL261 cells. Again, a various expression status of S1P receptor subtypes or downstream signaling molecules might be responsible for the different response to S1P. It is known that the PI3K/AKT1 pathway is activated by S1PR1, S1PR2 and S1PR3 by G_i coupling of these receptors, of which AKT1 is considered to be the major downstream signaling molecule of S1PR1 [124]. Thus, it seems possible that ACT-209905 is capable of inducing autophagy, apoptosis and necrosis in GBM cells because these cell death processes may be reliant on the phosphatidylinositol 3-kinase/protein Kinase B (PI3K/AKT1) signaling pathway. Consistent with this, ACT-209905 caused the activation of caspase 3 as the main effector caspase of apoptosis in both LN18, U87MG and GL261 GBM cells.

6.2 ACT-209905 inhibits the migration of GBM cells

Using two different approaches (wound healing scratch assay, Boyden chamber invasion assay), the data of the present work demonstrate that ACT-209905 inhibits the migration of GBM cells., This might be primarily caused through the inhibition of S1PR1 by ACT-209905, since it is known that the activation of S1PR1 leads to the activation of ERK1/2, which in turn results in the migration of GBM cells [125,126]. ERK1/2 and AKT1 activation was inhibited by ACT-209905 in LN18 GBM cells which can both be activated by stimulation of S1PR1 by S1P [127]. Thus, inhibition of both the PI3K/AKT1 and the ERK1/2 signaling pathway by ACT-209905 may be responsible for the decreased migration of GBM cells after application of ACT-209905.

The PI3K/AKT1 signaling pathway is important for intracellular regulation of cell survival or death. Moreover, the PI3K/AKT1 is pathway is closely related to cell invasion and metastasis. A recent study of our group has shown that inhibition of PI3K/AKT1 signaling by LY294002 completely inhibited S1P stimulated LN18 cell migration but not inhibition of ERK1/2 by PD98059 [62]. The PI3K/AKT1 pathway is known to be activated by S1PR1, S1PR2 and S1PR3 via G_i-coupling of these receptors [118]. For S1PR1 and S1PR3 a PI3K/AKT1-dependent stimulation of cell migration is described whereas S1PR2 uses this signaling cascade only as a side trail while Rho signaling as the main pathway may negatively regulate cell migration [118]. Thus, at least in LN18 GBM cells, the PI3K/AKT1 pathway may be primarily responsible for migration after stimulation with S1P which is in turn reduced through the inhibition of the S1PR1-PI3K/AKT1 signaling cascade by ACT-209905. Studies have found that in mouse glioma cells, the use of PI3K inhibitors cause concentration- and time-dependent inhibition of tumor cell invasion, and this invasion inhibition is closely related to the phosphorylation level of AKT1 [62,124]. After application of the inhibitors, the expression levels of MMP-2 and MMP-9 in the tumor cells was significantly decreased. This suggests that the PI3K/AKT1 signaling pathway is also involved in the regulation of MMPs which in turn modifies the invasive capacity of tumor cells [128]. It was also found that FTY720 (fingolimod), another S1PR1 modulator, significantly inhibited the phosphorylation levels of AKT1, mTOR and p70S6K in the human U251MG and U87MG cell lines without significant effects on total AKT, mTOR and p70S6K [120]. In addition, PI3K kinase inhibitor LY294002 down-regulated the expression of MMP-2 and MMP-9, and up-regulated the expression of TIMP-1 and TIMP-2,

indicating that the PI3K/AKT1 signaling pathway and FTY720-mediated inhibition of GBM cell invasion are closely related to each other [120]. Overall, our data argue for a participation of S1PR1 signaling in proliferation and migration of GBM cells, at least in the human GBM cell lines LN18 and U87MG and the mouse GBM cell line GL261. Whether this is also true for primary GBM cells, freshly isolated from tumor tissue, has to be analyzed in further studies.

6.3 ACT-209905 reduces the viability of GBM stem cells, and modifies their CD133 and Nestin expression

The theory of cancer stem cells makes us realize that malignant tumors are formed by the ability of stem cells to undergo abnormal self-renewal after multiple mutations, and further proliferate and differentiate [129]. According to the theory of cancer stem cells, only a very small number of cells in the tumor have the potential of unlimited proliferation, self-renewal and multi-directional differentiation. They are the root cause of tumorigenesis, metastasis and recurrence, and are the main targets of tumor treatment in the future [130]. Unfortunately, the current medical treatment strategies based on chemotherapy and radiotherapy only kills the tumor cells after the differentiation of cancer stem cells, so that the number of tumor cells is reduced, and the tumor shrinkage can be observed, but the tumor stem cells have no obvious effect [131-140], so the patient is difficult to get long-term survival. Studies have shown that brain tumor stem cells (BTSCs) are insensitive to chemotherapy and radiotherapy. BTSCs can proliferate to form new tumors due to their ability to self-renew, which is why there is recurrence after the surgical removal of tumors. Therefore, targeted treatment of BTSCs holds the key to prevent tumor recurrence after surgery and (radio)chemotherapy [130]. GBM stem cells are a popular field of research for studying the efficiency and molecular pathways of anti-GBM drugs because they are generally not sensitive to the clinical application of modern drugs, and radiotherapy is almost ineffective. CD133 is a transmembrane protein with a molecular weight of 120 kDa, which initially thought to be a marker of hematopoietic stem cells, but it was later found that CD133 mRNA transcripts were also detected in normal non-lymphoid hematopoietic tissues [141]. Since Singh et al. [102] isolated CD133-positive cells with tumor stem cell characteristics from the tumor tissues in 2003, CD133 has been used for the identification of various tumor stem cells. Moreover, a large number of studies have also confirmed that in

gliomas the proportion of CD133-positive cells is increased with the grade of tumor, and tumors with a high amount of CD133-positive cells have a high malignancy, short patients survival time after surgery, and a high recurrence rate [103]. A further stem cell marker is the type VI intermediate filament protein Nestin which was discovered in 1985 to be expressed in the spinal canal neural stem cells of embryonic rat. Since Nestin expression is high in neural precursor cells, it was always considered to be a marker of neural precursor cell [105]. With the development of glioma stem cell theory and the studies of related markers, Nestin has also been used in the identification of cancer stem cells in recent years, and has been recognized by many scholars as a marker of brain cancer stem cells [142-144].

Our immunoblot data showed that Nestin and CD133 were more highly expressed in the ACT-209905 treated LN18 cells than the S1P treated cells (Figure 10). In contrast, in the murine GL261 GBM cells, ACT-209905 did not cause a significant increase in CD133 and Nestin expression whereas S1P significantly enhanced the protein level of CD133 and Nestin in these cells (Figure 11). Of note, a various S1PR1 expression may be responsible for such cell type dependent differences. Such a cell type dependent effect was also seen for Compound 16: whereas the S1PR2 inhibitor did not cause an increase of CD133 or Nestin in the human LN18 cells, a significant up-regulation of both stem cell marker was observed in the mouse GL261 cells. Nevertheless, it does not mean that ACT-209905 or Compound 16 have no therapeutic effect on GBM stem cells while ACT-209905 acts as an structural activator of S1PR1 but is an functional S1PR1 antagonist. The reason may be that CD133 has limitations as a glioma stem cell marker. Comparing the tumorigenic ability of CD133 positive and negative cells, it was found that CD133 positive cells have strong tumorigenic ability, while negative cells have no tumorigenic ability [141,145]. For this reason, CD133 was considered to be the most important marker for brain tumor stem cells. Since then, CD133 has been widely used as a molecular marker for the isolation and purification of brain tumor stem cells, and plays an important role in the research of brain tumor stem cells. CD133 expression is not detected in most glioma cell lines and in some fresh malignant glioma tissues [146,147]. Notably, in the present study, CD133 protein was detected by immunoblotting in the human LN18 GBM cell line as well as in the murine GL251 GBM cell line which is accordance with our previous work and the studies from Hossain and colleagues [148,149]. A close correlation has been observed between CD133 expression and

chemoresistance as well as GBM survival [101,134,150]. Interestingly, recent studies depict that also CD133-negative glioma stem-like cells exist [147,151], and that the expression of CD133 may reflect the environmental conditions and stress responses. Further, several models have shown the stem cell capacity of CD133-negative GBM cells [152-155]. It is assumed that the presence of various CD133 phenotypes in glioma stem cells may be due to the differences in their originally differentiated cells [156,157]. Of note, it is believed that a phenotypic shift from CD133 negative to CD133 positive cells under hypoxic conditions exist, while CD133 postive cells return to CD133 negative cells under normal oxygen conditions [153]. Joo et al. [146] found that four of six resected GBM tissues had CD133 positive cells, and two of them contained CD133 negative cells. After inoculation into NOD-SCID (non-obese diabetes in severe combined immunodeficiency) mice, both CD133 positive and CD133 negative cells caused a glioblastoma, and the CD133 negative cells showed greater invasiveness and angiogenic ability. Thus, an up-regulation of CD133, as seen in our study, by both S1P and the functional S1PR1 receptor antagonist ACT-209905 does not necessarily result in a higher aggressivenes of the tumor cells. Interestingly, the S1PR2 blocker Compound 16/16-ME did not cause an increase in CD133 or Nestin expression in human LN18 GBM cells arguing for a S1PR1 subtype dependent effect. And in conclusion, the results suggest the complexity of CD133 as a marker for glioma tumor stem cells. From the functional aspect, the physiological function of the CD133 protein has not yet been elucidated.

Besides CD133, the intermediate filament protein Nestin was increased after application of ACT-209905 in human LN18 GBM cells. Nestin is a molecular marker that is specifically expressed on neuroepithelial stem cells, and it is also one of the most commonly recognized markers of BTSC in addition to CD133. Nestin expression is closely related to the "stem cell" phenotype and is a skeleton protein expressed in progenitor cells and neural stem cells. Cattaneo et al. [158] found that the expression of differentiation markers such as GFAP (Glial fibrillary acidic protein) in neural stem cells increased while the expression of Nestin decreased. Tohyama and colleagues [159] showed that Nestin expression was positive in multiple types of brain tumors. Studies from Rutka et al. [143] demonstrate that Nestin positive brain glioma cells have some features in common with neural stem cells. Compared with Nestin-negative tumor cells, they have stronger invasion and migration ability.

Kleeberger et al. [160] found that Nestin expression can promote tumor migration and metastasis. In line with these observations, a prognostic influence of Nestin expression in GBM was shown [148,150,161]. But Nestin expression is not sufficient to indicate that Nestin-expressing cells are indeed cancer stem cells. It is one typical marker of tumor stem cell but not the only one. To clarify the meaning of the up-regulation of both Nestin and CD133 by ACT-209905 in human LN18 GBM cells further detailed studies are urgently needed. At this point of work, a conclusion cannot be drawn, but although ACT-209905 induced a higher expression of Nestin and CD133 in GBM cells, ACT-209905 still had the capacity to inhibit the proliferation, migration and invasion of LN18, U87MG and GL261 GBM cells in the present study.

Of note, the cell viability analyses of the present work show that the application of ACT-209905 was effective against adherent GBM cells whereas the standard chemotherapeutic temozolomide (100 µM) had only minor cytotoxic effects. Studies have shown that the maximal temozolomide concentration in serum is about 75 µM [162], thus the temozolomide concentration chosen in the present work is comparable to the *in vivo* situation.

Interestingly, the cytotoxic effects of ACT-209905 were more pronounced in the LN18 neurosphere cells which are described to have stem cell features [101,163]. We hypothesize that ACT-209905 has a similar effect as the S1PR1 modulator FTY720 (fingolimod), because FTY720 also causes apoptosis of glioma cells and has cytotoxic effects against glioma stem cells, too [117,119]. FTY720 rapidly inactivates the ERK1/2 kinase activity of BTSCs and increases the expression of cleaved Caspase 9, Caspase 7 and Caspase 3, resulting in the death of brain tumor stem cells [117]. In the present work, the S1PR1 modulator ACT-209905 also diminished the activity of ERK1/2 induced by S1P in LN18 GBM cells but has no effect on the basal ERK1/2 activity as described for FTY720. In concordance with FTY720, caspase 3 activity was also increased by ACT-209905 leading to cell death of GBM cells in our study. Further, FTY720 is known to inhibit the activation of the PI3K/AKT1 pathway leading to a reduced migration of GBM cells [120]. A related effect was observed in the present work for ACT-209905 which caused a decrease in the S1P-induced activation of AKT1 combined with a diminished migration of LN18 cells but had only a slight influence on the basal AKT1 activity.Stem cells have been shown to be self-renewing and to form new tumors in nude

mice, similar to the original tumors [140], and are therefore considered to be important cells for the targeted treatment of GBM. When human GBM-derived stem cells, which formed neurosphere-like cells, are injected into the brain of nude mice, new tumors develop representing an accurate and reliable pathological model of GBM [164]. Therefore, we also used the neurosphere model to investigate the cytotoxic efficiency of ACT-209905 in GBM cells. As described above, the viability of LN18 neurosphere cells was stronger affected than their adherent counterparts arguing for a potential therapeutic effect of ACT-209905 against glioma stem cells. In a next step to preclinically evaluate ACT-209905 as treatment option, GL261 GBM cells and GL261-derived GBM stem cells should be injected into the brain of mice followed by ACT-209905 treatment as performed for FTY720 by Estrada-Bernal and colleagues [117]. If the results show that ACT-209905 is effective in treating GBM *in vivo*, and can significantly prolong the survival period and reduce tumor growth (consistent with our *in vitro* studies) this would validate the anti-GBM effect of ACT-209905 much more. Although TMZ is still the current mainstream anti-tumor drug for therapy of GBM, a combination of ACT-209905 and TMZ may then show better therapeutic effects. This question should therefore be urgently addressed.

6.4 ACT-209905 might have various effects in different source GBM cells

Our *in vitro* results show some differences in the effects of ACT-209905 in the human LN18 and the mouse GL261 cell line. Despite a similar cytotoxicity of ACT-209905 in both cell lines, the migration was somewhat more inhibited in GL261 cells and the induction of caspase 3 activity as apoptosis marker was more pronounced in LN18 GBM cells. A strong difference was found for the AKT1 and ERK1/2 activity influenced by ACT-209905. Whereas in LN18 cells, ACT-209905 caused a decrease in S1P-induced activation of both kinases, in GL261 cells S1P-induced activation of ERK1/2 was not diminished by ACT-209905. Additionally, in murine GL261 GBM cells no activation of AKT1 was observed by S1P alone but curiously by co-application S1P and ACT-209905 together. Compared with the S1PR1 modulator FTY720, which also inhibits activation of both AKT1 and ERK1/2 in human GBM cells, ACT-209905 has similar effects in the human LN18 GBM cells [117,120]. A further interesting difference was observed for expression of the stem cell marker CD133 and Nestin. In the human LN18 GBM cells, ACT209905 caused a significant up-regulation of CD133 and Nestin but this wasn´t seen

in the mouse GL261 cells (Figure 10 and 11). The potential consequences were already discussed in chapter 6.3.

This difference in the response of GBM cells to ACT-209905 could be based on different genetic backgrounds, pathological types, differentiation states, gene mutation profiles and transcriptomes, proteome expression profiles, etc., reflecting the high complexity and diversity of GBM cells [165-170]. Furthermore, an intra-tumoral heterogeneity of GBM is shown by how the cellular composition of each tumor is more heterogeneous than previously predicted, resulting in a diversification of cells within the tumor. This is due to the different cells in the tumor exhibiting various mutations and expressing genes in different ways. This diversity may lead to tumor resistance and recurrence. To map out these differences, Patel et al. [171] isolated glioblastoma tissue from five patients and made a single cell suspension for 430 isolated tumor single cells. Afterwards, RNA-sequencing (RNA-Seq) technology for transcriptome analysis successfully obtained a more detailed map of tumor cell composition. Their results showed that each glioblastoma contains cells from multiple cancer subtypes, and the distribution of these cells between tumors differs. Further clustering occurs according to their similarity, and although each patient's cell similarity was found to be higher (than the individual), there are still some differences. The cancer cells in these tumors survived in various states. Some of them have stem cell features with the ability to self-renew, which may play a role in tumor recurrence after treatment. More mature, differentiated cancer cells constitute the majority of the tumor cell population. It is this tumor heterogeneity that causes great difficulties in the treatment of GBM, and is one of the most important scientific issues in the research field of GBM development mechanics.

Matching with this, the GBM cell lines analyzed in the present work had different expression levels of the five S1P receptor subtypes (Figure 1). For example, the human LN18 cells, used in this study, showed a higher expression of the S1PR1, S1PR2, S1PR4 and S1PR5 than the murine GBM cells whereas the S1PR3 was very similar between both cell lines. GBM cells of different species may have different biological characteristics and this could be responsible for the inconsistency of some experimental results as described above. The opposite results obtained from human LN18 and murine GL261 GBM cells may be possibly caused of differences in biological characteristics due to their species. This suggests that when performing *in vitro* experiments with cell lines of different species and origin, we should

consider these potential differences in experimental results in light of their biological characteristics and with regard to a generalisation and transferring results from one cell line to another or even to primary cells. We have to keep in mind that there are multiple subtypes of GBM with heterogeneous genetic/genomic/epigenetic features leading to various methods to classify tumors according to the key molecular events that drive the most aggressive cellular components so that targeted therapies can be developed for individual subtypes [172]. Further, depending on the different GBM cell types within the same tumor, we may need to treat malignant tumors based on all the cell subtypes contained in each tumor rather than just the most common subtype [173-175].

6.5 Outlook

Taken together, our results indicate that ACT-209905, a modulator of S1PR1 function, inhibits GBM growth/proliferation, invasion and migration, and also induces apoptosis in GBM cells. In addition, ACT-209905 is effective against GBM stem-like cells demonstrated by the neurospheres assays performed in this study. Therefore, further systematic studies of the anti-tumoral mechanisms of S1PR1 modulators, such as ACT-209905 or FTY720, may help to develop new strategies to treat patients suffering from GBM. For example, it is necessary to evaluate the specific pathways involved in the cytotoxic effect of ACT-209905 for better understanding of both the tumor pathogenesis and the molecular mode of action of ACT-209905. Additionally, primary GBM cells freshly isolated from tumors should be treated with ACT-209905, too, to examine whether ACT-209905 is also effective in these cells. The use of astrocytic and neural cell models could further clarify if healthy astrocytes and neurons are also killed by ACT-209905 to assess potential adverse effects. Furthermore, it is particularly important to pre-clinically evaluate the efficiency of ACT-209905 in a suitable animal model to check whether blocking of S1PR1 indeed reduces the growth of GBM *in vivo* without causing major side effects.

7 Abbreviations

± SD	±Standard Deviation
Aqua dest.	(Aqua destillata) distilled water
APS	Ammonium Peroxodisulfate
DMEM	Dulbecco's Modified Eagle Medium
DPBS	Dulbecco’s Phosphate-Buffered Saline
DTT	Dithiothreitol
ECL	enhanced chemiluminescence
et al.	(et alii) and others
FCS	Fetal Calf Serum
HLA	Human Leukocyte Antigen
HRP	Horseradish Peroxidase
PAGE	Polyacrylamide Gel Electrophoresis
PFA	Paraformaldehyde
pH	pondus hydrogenii
PMSF	Phenylmethylsulfonyl Fluoride
SDS	Sodium Dodecyl Sulfate
TBST	Tris-buffered saline with Tween20
TEMED	Tetramethylethylendiamin
Tris	Tromethamol
DMEM	Dulbecco's Modified Eagle Medium
DNA	Desoxyribonucleic Acid
EDTA	Ethylenediaminetetraacetic Acid
FA	Fractional Anisotropy
NaCl	World Health Organization

Dimensions and units

%	Percent
°C	Degree Celsius
ml	Milliliter
µl	Microliter
m	Meter
cm	Centimeter
mm	Millimeter
µm	Micrometre
nm	Nanometer
cm^3	Square Centimeter
g	Gram
µg	Micrograms
h	Hour
min	Minute
s	Second
mmol	Millimol

8 References

1. Ji Zhang. Deepening the comprehensive treatment of glioma and its basic research. Chin J Neurosurg. 2003; 19(1):1-2.
2. Baan R, Grosse Y, Lauby-Secretan B, et al. Carcinogenicity of radiofrequency electromagnetic fields. Lancet Oncol. 2011; 12(7):624-626.
3. Coureau G, Bouvier G, Lebailly P, et al. Mobile phone use and brain tumours in the CERENAT case-control study. Occup Environ Med. 2014; 71(7):514-522.
4. Ohgaki H, Kleihues P. Population-based studies on incidence, survival rates, and genetic alterations in astrocytic and oligodendroglial gliomas. J Neuropathol Exp Neurol. 2005 Jun;64(6):479-89.
5. Michaelis M, Baumgarten P, Mittelbronn M, et al. Oncomodulation by human cytomegalovirus: novel clonical findings open new roads. Med Microbiol Immunol. 2011; 200(1):1-5.
6. Adel Fahmideh M, Schwartzbaum J, Frumento P, et al. Assocation between DNA repair gene polymorphisms and risk of glioma: a systematic review and meta-analysis. Neuro Oncol. 2014; 16(6):807-14.
7. Song Y, Luo Q, Long H, et al. Alpha-enolase as a potential cancer prognostic marker promotes cell growth, migration, and invasion in glioma. Mol Cancer. 2014; 13:65.
8. Zhang W, Zhang J, Hoadley K, et al. miR-181d: a predictive glioblastoma biomarker that downregulates MGMT expression. Neuro Oncol. 2012; 14(6):712-9.
9. Molenaar RJ, Radivoyevitch T, Maciejewski JP, et al. The driver and passenger effects of isocitrate dehydrogenase 1 and 2 mutations in oncogenesis and survival prolongation. Biochim Biophys Acta. 2014; 1846(2):326-41.
10. Wang P, Dong Q, Zhang C, et al. Mutations in isocitrate dehydrogenase 1 and 2 occur frequently in intrahepatic cholangiocarcinomas and share hyermethylation targets with glioblastomas. Oncogene. 2013; 32(25):3091-100.
11. Chen HI, Einbond A, Kwak SJ, et al. Characterization of the WW Domain of Human Yes-associated. J Biol Chem. 1997; 272(27):17070-7.
12. Gupta RK, Sharma MC, Suri V, et al. Study of chromosome 9q gain, Notch pathway regulators and Tenascin-C in ependymomas. J Neurooncol. 2014; 116(2): 267-274.
13. Mazza E, Belli C, Terreni M, et al. Breast metastases from oligodendroglioma: An

unusual extraneural spread in two young women and a review of the literature. Crit Rev Oncol Hematol. 2013; 88(3):564-572.

14. Pope WB. Genomics of brain tumor imaging. Neuroimaging Clin N Am. 2015; 25(1):105-119.
15. Franceschi E, Brandes AA. The role of bevacizumab in recurrent glioblastoma: New insights from randomized trials. CNS Oncol. 2015; 4(3):117-119.
16. Mann BS. Overall survival benefit from surgical resection in treatment of recurrent glioblastoma. Ann Oncol. 2014; 25(9):1866-1887.
17. Le Rhun E, Taillibert S, Chamberlain MC. Current management of adult diffuse infiltrative low grade gliomas. Curr Neurol Neurosci Rep. 2016;16(2): 15.
18. Buckner JC, Shaw EG, Pugh SL, et al. Radiation plus procarbazine, CCNU, andvincristine in low-grade glioma. N Engl J Med. 2016; 374(14):1344-1355.
19. Chandler KL, Prados MD, Malec M, et al. Long-term survival in patients with glioblastoma [discussion 720]. Neurosurgery. 1993; 32:716–20.
20. Lacroix M, Abi-Said D, Fourney DR, et al. A multivariate analysis of 416 patients with glioblastoma: prognosis, extent of resection, and survival. J Neurosurg 2001; 95:190-8.
21. Stummer W, Pichlmeier U, Meinel T, et al. Fluorescence-guided surgery with 5-aminolevulinic acid for resection of malignant glioma: a randomised controlled multicentre phase III trial. Lancet Oncol. 2006; 7:392–401.
22. Stupp R, Tonn JC, Brada M, et al. ESMO Guidelines Working Group. High-grade malignant glioma: ESMO Clinical Practice Guidelines for diagnosis, treatment and follow-up. Ann Oncol. 2010; 21(Suppl 5): v190-3.
23. US Food & Drug Administration. FDA approves expanded indication for medical device to treat a form of brain cancer. 2015.
24. Hottinger AF, Pacheco P, Stupp R. Tumor treating fields: a novel treatment modality and its use in brain tumors. Neuro Oncol. 2016; 18(10):1338-49.
25. Kesari S, Zvi Ram, et al.Tumor-treating fields plus chemotherapy versus chemotherapy alone forglioblastoma at firstrecurrence: a post hoc analysis of the EF-14 trial. CNSOncol. 2017; 6(3):185-193.
26. Strub GM, Maceyka M, Hait NC, et al. Extracellular and intracellular actions of sphingosine-1-phosphate. Adv.Exp.Med.Biol. 2010; 688:141-155.

27. Maceyka M, Milstien S, Spiegel S. Measurement of mammalian sphingosine-1-phosphate phosphohydrolase activity in vitro and in vivo. Methods Enzymol. 2007; 434:243-56.
28. Hait NC, Allegood J, Maceyka M, et al. Regulation of histone acetylation in the nucleus by sphingosine-1-phosphate. Science 2009; 325(5945):1254-1257.
29. Rivera J, Proia RL, Olivera A. The alliance of sphingosine-1-phosphate and its receptors in immunity. Nat Rev Immunol. 2008; 8(10):753-763.
30. Spiegel S, Milstien S. The outs and the ins of sphingosine-1-phosphate in immunity. Nat Rev Immunol 2011; 11(6):403-15.
31. Liu X, Zhang QH, Yi GH. Regulation of metabolism and transport of spingosine-1-phosphate in mammalian cells. Mol Cell Biochem. 2012; 363:21-33.
32. O'Sullivan C, Dev KK. The structure and function of the S1P1 receptor. Trends Pharmacol Sci. 2013; 34(7):401-412.
33. Rosen H, Stevens RC, Hanson M, et al. Sphingosine-1-phosphate and its receptors: structure, signaling, and influence. Annu Rev Biochem. 2013; 82:637-662.
34. Pyne NJ, Pyne S. Sphingosine 1-phosphate and cancer. Nat. Rev. Cancer. 2010; 10:489-503.
35. Ponnusamy S, Meyers-Needham M, Senkal CE, et al. Sphingolipids and cancer: Ceramide and sphingosine-1-phosphate in the regulation of cell death and drug resistance. Future Oncol. 2010; 6:1603-1624.
36. Pyne NJ, Ohotski J, Bittman R, et al. The role of sphingosine 1-phosphate in inflammation and cancer. Adv. Biol. Regul. 2014; 54:121-129.
37. Wang C, Mao J, et al. Systemic distribution, subcellular localization and differential expression of sphingosine-1-phosphate receptors in benign and malignant human tissues. Exp Mol Pathol. 2014; 97(2):259-65.
38. Siehler S, Manning DR. Pathways of transduction engaged by sphingosine 1-phosphate through G protein-coupled receptors. Biochim Biophys Acta. 2002; 1582(1-3):94-9.
39. Rosen H. Goetzl EJ Sphingosine 1-phosphate and its receptors: An autocrine and

paracrine network. Nat. Rev. Immunol. 2005; 5:560-570.

40. Kono M, Proia RL. Imaging S1P1 activation in vivo. Exp Cell Res. 2015; 333(2):178-182.
41. Bradaric MJ, Barua A, Penumatsa K, et al. Sphingosine-1 phosphate receptor (S1P1), a critical receptor controlling human lymphocyte trafficking, is expressed in hen and human ovaries and ovarian tumors. J Ovarian Res. 2011;4(1): 4.
42. You S, Piali L, Kuhn C, et al. Therapeutic use of a selective S1P1 receptor modulator ponesimod in autoimmune diabetes. PLoS One. 2013; 8(10): e77296.
43. Spiegel S, Milstien S. The outs and the ins of sphingosine-1-phosphate in immunity. Nat Rev Immunol. 2011; 11(6):403-415.
44. Wang C, Mao J, Redfield S, et al. Systemic distribution, subcellular localization and differential expression of sphingosine-1-phosphate receptors in benign and malignant human tissues. Exp Mol Pathol. 2014; 97(2):259-265.
45. Maceyka M, Spiegel S. Sphingolipid metabolites in inflammatory disease. Nature. 2014; 10(7503):58-67.
46. Kim RH, Takabe K, Allegood JC, et al. Estradiol induces export of sphingosine 1-phosphate from breast cancer cells via ABCC1 and ABCG2. The Journal of Biological Chemistry. 2010; 285(14):77-86.
47. Liang J, Nagahashi M, Kim EY, et al. Sphingosine-1-phosphate links persistent STAT3 activation, chronic intestinal inflammation, and development of colitis-associated cancer. Cancer Cell. 2013; 23(1) :107-120.
48. Theiss AL. Sphingosine-1-phosphate: Driver of NFκB and STAT3 persistent activation in chronic intestinal inflammation and colitis-associated cancer. JAKSTAT. 2013; 2(3):24150.
49. O'Brien N, Jones ST, Williams DG, et al. Production and characterization of monoclonal anti-sphingosine-1-phosphate antibodies. J Lipid Res. 2009; 50(11):2245-57.
50. Park KS, Kim MK, Lee HY, et al. S1P stimulates chemotactic migration and invasion in OVCAR3 cancer cells. Biochem Biophys Res Commun. 2007; 356(1):239-244.
51. Vadas M, Xia P, Mc Caughan, et al. The role of sphingosine kinase-1 in cancer: oncogene or non-oncogene addiction. Biochim Biophys Acta 2008; 1781(9):442-447.
52. Priceman SJ, Shen S, Wang L, et al. S1PR1 is crucial for accumulation of regulatory T cells in tumors via STAT3. Cell Rep. 2014; 6(6): 992-999.

53. Nagahashi M, Ramachandran S, Kim EY, et al. Sphingosine-1-phosphate produced by sphingosine kinase 1 promotes breast cancer progression by stimulating angiogenesis and lymphangiogenesis. Cancer Res. 2012; 72(3):726-735.
54. Patmanathan SN, Johnson SP, Lai SL, et al. Aberrant expression of the S1P regulating enzymes，SPHK1 and SGPL1, contributes to a migratory phenotype in OSCC mediated through S1PR2. Sci Rep. 2016; 6:25650.
55. Wang YC, Tsai CF, Chuang HL, et al. Benzyl butyl phthalate promotes breast cancer stem cell expansion via SPHK1/ S1P/ S1PR3 signaling. Oncotarget. 2016; 7(20) :29563-29576.
56. Takabe K, Spiegel S. Export of sphingosine-1-phosphate and cancer progression. J. Lipid Res. 2014; 55:1839-1846.
57. Sarkar S, Maceyka M, Hait NC, et al. Sphingosine kinase 1 is required for migration, proliferation and survival of MCF-7 human breast cancer cells. FEBS Lett. 2005; 579:5313-5317.
58. Chae SS, JH Paik, ML Allende, et al. Regulation of limb development by the sphingosine 1-phosphate receptor S1P (1) /EDG-1 occurs via the hypoxia /VEGF axis. Dev. Biol 2004; 268:441-447.
59. Van Brocklyn JR, Jackson CA, Pearl DK, et al. Prior TW Sphingosine kinase-1 expression correlates with poor survival of patients with glioblastoma multiforme: Roles of sphingosine kinase isoforms in growth of glioblastoma cell lines. J. Neuropathol. Exp. Neurol. 2005; 64:695-705.
60. Quint K, Stiel N, Neureiter D, et al. The role of sphingosine kinase isoforms and receptors S1P1, S1P2, S1P3, and S1P5 in primary, secondary, and recurrent glioblastomas. Tumour Biol. 2014; 35(9):8979-8989.
61. Watters RJ, Wang HG, Sung SS, et al. Targeting sphingosine-1-phosphate receptors in cancer. Anticancer Agents Med Chem. 2011; 11(9):810-817.
62. Sandra Bien-Möller, Sandra Lange, Tobias Holm, et al. Expression of S1P metabolizing enzymes and receptors correlate with survival time and regulate cell migration in glioblastoma multiforme. Oncotarget. 2016; 7(11):13031-46.
63. Bassi R, Anelli V, Giussani P, et al. Sphingosine-1-phosphate is released by cerebellar astrocytes in response to bFGF and induces astrocyte proliferation through G1-protein-coupled receptors. Glia. 2006; 53: 621-630.

64. Anelli V, Gault CR, Cheng AB. Obeid LM Sphingosine kinase 1 is up-regulated during hypoxia in U87-MG glioma cells role of hypoxia-inducible factors 1 and 2. J. Biol. Chem. 2008; 283:3365-3375.
65. Strub GM, Maceyka M, Hait NC, et al. Extracellular and Intracellular Actions of Sphingosine-1-Phosphate. Adv. Exp. Med. Biol. 2010; 688:141-155.
66. Marfia G, Campanella R, Navone SE, et al. Autocrine/ paracrine sphingosine-1-phosphate fuels proliferative and stemness qualities of glioblastoma stem cells. Glia. 2014; 62:1968-1981.
67. Abuhusain HJ, Matin A, Qiao Q, et al. Metabolic Shift Favoring Sphingosine 1-Phosphate at the Expense of Ceramide Controls Glioblastoma Angiogenesis. J. Biol. Chem. 2013; 288:37355-37364.
68. Hla T. Signaling and biological actions of sphingosine 1-phosphate. Pharmacol. Res. 2003; 47:401-407.
69. Yoshida Y, Nakada M, Sugimoto N, et al. Sphingosine-1-phosphate receptor type 1 regulates glioma cell proliferation and correlates with patient survival. Int. J. Cancer. 2010; 126:2341-2352.
70. Bernhart E, Damm S, Wintersperger A, et al. Interference with distinct steps of sphingolipid synthesis and signaling attenuates proliferation of U87-MG glioma cells. Biochem. Pharmacol. 2015; 96:119-130.
71. Kim K, Kim YL, Sacket SJ, et al. Sphingosine 1-phosphate (S1P) induces shape change in rat C6 glioma cells through the S1P2 receptor: Development of an agonist for S1P receptors. J. Pharm. Pharmacol. 2007; 59:1035-1041.
72. Quint K, Stiel N, Neureiter D, et al. The role of sphingosine kinase isoforms and receptors S1P1, S1P2, S1P3, and S1P5 in primary, secondary, and recurrent glioblastomas. Tumour Biol. 2014; 35:8979-8989.
73. Rosen H. Goetzl EJ Sphingosine 1-phosphate and its receptors: An autocrine and paracrine network. Nat. Rev. Immunol. 2005; 5:560-570.
74. Maceyka M, Spiegel S. Sphingolipid metabolites in inflammatory disease. Nature 2014; 10(7503):58-67.
75. Kim RH, Takabe K, Allegood JC, et al. Estradiol induces export of sphingosine 1-phosphate from breast cancer cells via ABCC1 and ABCG2. The Journal of Biological

Chemistry 2010; 285(14):77-86.

76. Sato K, Ui M, Okajima F. Differential roles of Edg-1 and Edg-5, sphingosine 1-phosphate receptors, in the signaling pathways in C6 glioma cells. Brain Res. Mol. Brain Res. 2000; 85:151-160.
77. Okajima F, Tomura H, Sho K, et al. Involvement of pertussis toxin-sensitive GTP-binding proteins in sphingosine 1-phosphate-induced activation of phospholipase C-Ca 2+system in HL60 leukemia cells. FEBS Lett. 1996; 379:260-264.
78. Czajkowski R, Sabala P, Baranska J. Sphingosine modulates Ca signals via phospholipase C dependent pathway in glioma C6 cells. Acta Neurobiol. Exp. 1997; 57:353.
79. Kono M, Proia RL. Imaging S1P1 activation in vivo. Exp Cell Res 2015; 333(2): 178-182.
80. Bradaric MJ, Barua A, Penumatsa K, et al. Sphingosine-1 phosphate receptor (S1P1), a critical receptor controlling human lymphocyte trafficking, is expressed in hen and human ovaries and ovarian tumors. J Ovarian Res. 2011; 4(1):4.
81. You S, Piali L, Kuhn C, et al. Therapeutic use of a selective S1P1 receptor modulator ponesimod in autoimmune diabetes. PLoS One. 2013; 8(10): e77296.
82. Lee H, Deng J, Kujawski M, et al. STAT3-induced S1PR1 expression is crucial for persistent STAT3 activation in tumors. Nat Med. 2010; 16(12):1421-1428.
83. Li M H, Sanchez T, Yamase H, et al. S1P/S1P1 signaling stimulates cell migration and invasion in Wilms tumor. Cancer Lett 2009; 76(2):171-179.
84. Visentin B, Vekich J A, Sibbald B J, et al. Validation of an anti-sphingosine-1-phosphate antibody as a potential therapeutic in reducing growth, invasion, and angiogenesis in multiple tumor lineages. Cancer Cell. 2006; 9(3):225-238.
85. Liu Y, Wada R, Yamashita T, et al. Edg-1, the G proteincoupled receptor for sphingosine-1-phosphate, is essential for vascular maturation. J Clin Invest. 2000; 06(8):951-961.
86. Priceman SJ, Shen S, Wang L, et al. S1PR1 is crucial for accumulation of regulatory T cells in tumors via STAT3. Cell Rep. 2014; 6(6):992-999.
87. Arikawa K, Takuwa N, Yamaguchi H, et al. Ligand-dependent inhibition of B16 melanoma cell migration and invasion via endogenous S1P2 G protein-coupled receptor. Requirement of inhibition of cellular RAC activity. J Biol Chem. 2003; 278(35):32841-32851.
88. Chae SS, JH Paik, ML Allende, et al. Regulation of limb development by the sphingosine

1-phosphate receptor S1P (1)/EDG-1 occurs via the hypoxia /VEGF axis. Dev. Biol. 2004; 268:441-447.

89. Quint K, Stiel N, Neureiter D, et al. The role of sphingosine kinase isoforms and receptors S1P1, S1P2, S1P3, and S1P5 in primary, secondary, and recurrent glioblastomas. Tumour Biol. 2014; 35(9):8979-8989.
90. Watters RJ, Wang HG, Sung SS, et al. Targeting sphingosine-1-phosphate receptors in cancer. Anticancer Agents Med Chem. 2011; 11(9):810-817.
91. Yoshida Y1, Nakada M, Sugimoto N, et al. Sphingosine-1-phosphate receptor type 1 regulates glioma cell proliferation and correlates with patient survival. Int J Cancer. 2010; 126(10):2341-52.
92. Van Brocklyn J1, Letterle C, Snyder P, et al. Sphingosine-1-phosphate stimulates human glioma cell proliferation through Gi-coupled receptors: role of ERK MAP kinase and phosphatidylinositol 3-kinase beta. Cancer Lett. 2002; 181(2):195-204.
93. Young N, Van Brocklyn JR. Roles of sphingosine-1-phosphate (S1P) receptors in malignant behavior of glioma cells. Differential effects of S1P2 on cell migration and invasiveness. Exp Cell Res. 2007; 313(8):1615-27.
94. Van Brocklyn JR, Young N, Roof R. Sphingosine-1-phosphate stimulates motility and invasiveness of human glioblastoma multiforme cells. Cancer Lett. 2003; 199(1):53-60.
95. Gunther Schmidt, Stefan Reber, Martin H. Bolli, et al. Practical and Scalable Synthesis of S1P1 Receptor Agonist ACT-209905. Org. Process Res. Dev. 2012; 16(4):595–604.
96. Soo-Jin Park, Dong-Soon Im. Sphingosine 1-Phosphate Receptor Modulators and Drug Discovery. Biomol Ther (Seoul). 2017; 25(1): 80–90.
97. Bolli MH, Mathys B, Mueller C, et al. AMINO- PYRIDINE Derivatives As S1P1 /EDG1 Receptor Agonists. WO/2008/114157.
98. Bolli MH, Lescop C, Nayler O. Synthetic sphingosine 1-phosphate receptor modulators--opportunities and potential pitfalls. Curr Top Med Chem. 2011; 11(6):726-57.
99. Gallego O. Nonsurgical treatment of recurrent glioblastoma. Curr Oncol. 2015; 22(4): e273-81.
100. Stupp R, Hegi ME, Mason WP, et al. Effects of radiotherapy with concomitant and adjuvant temozolomide versus radiotherapy alone on survival in glioblastoma in a randomised Phase III study: 5 years analysis of the EORTC-NCIC trial. Lancet Oncol. 2009;

10(5):459-66.

101. Liu G, Yuan X, Zeng Z, et al. Analysis of gene expression and chemoresistance of CD133+ cancer stem cells in glioblastoma. Mol Cancer. 2006; 5:67.

102. Kemper K, Sprick MR, de Bree M, et al. The AC133 epitope, but not the CD133 protein, is lost upon cancer stem cell differentiation. Cancer research. 2010; 70(2):719-29.

103. Pallini R, Ricci-Vitiani L, Montano N, et al. Expression of the stem cell marker CD133 in recurrent glioblastoma and its value for prognosis. Cancer. 2011; 117(1):162-74.

104. Kelberman D, Rizzoti K, Lovell-Badge R, et al. Genetic regulation of pituitary gland development in human and mouse[J]. Endocrine reviews. 2009; 30(7):790-829.

105. Jakub Neradil, Renata Veselska. Nestin as a marker of cancer stem cells. Cancer Sci. 2015; 106(7):803–811.

106. Rasper M, Schäfer A, Piontek G, et al. Aldehyde dehydrogenase 1 positive glioblastoma cells show brain tumor stem cell capacity. Neuro Oncol. 2010; 12(10):1024-33.

107. Friedman MD, Jeevan DS, Tobias M, et al. Targeting cancer stem cells in glioblastoma multiforme using mTOR inhibitors and the differentiating agent all-trans retinoic acid. Oncol Rep. 2013; 30(4):1645-50.

108. Broadley KW, Hunn MK, Farrand KJ, et al. Side population is not necessary or sufficient for a cancer stem cell phenotype in glioblastoma multiforme. Stem Cells. 2011; 29(3):452-61.

109. Jisen Huai, Lars Jöckel, Karen Schrader, et al. Role of caspases and non-caspase proteases in cell death. F1000 Biol Rep. 2010; 2: 48.

110. David RM, Thorsten B, Tak WM. Caspase Functions in Cell Death and Disease. Cold Spring Harb Perspect Biol. 2013; 5: a008656

111. Ryan AV Bell, Lynn A Megeney. Evolution of caspase-mediated cell death anddifferentiation: twins separated at birth. Cell Death and Differentiation. 2017; 24:1359–1368

112. Reya T, Morrison SJ, Clarke MF, et al. Stem cells, cancer, and cancer stem cells. Nature. 2001; 414:105-11.

113. Huff CA, Matsui WH, Smith BD, et al. Strategies to eliminate cancer stem cells: Clinical implications. Eur J Cancer. 2006; 42(9):1293-7.

114. Bayin NS, Modrek AS, Placantonakis DG. Glioblastoma stem cells: Molecular characteristics and therapeutic implications. World J Stem Cells. 2014; 6(2): 230–238.

115. Atique U Ahmed, Brenda Auffinger, Maciej S Lesniak. Understanding glioma stem cells: rationale, clinical relevance and therapeutic strategies. Expert Rev Neurother. 2013; 13(5):545–555.

116. Baranowski M, Gorski J. Heart sphingolipids in health and disease. Adv Exp Med Biol. 2011; 721:41-56.

117. Estrada-Bernal A, Palanichamy K, Ray Chaudhury A, et al. Induction of brain tumor stem cell apoptosis by FTY720: a potential therapeutic agent for glioblastoma. Neuro Oncol. 2012; 14(4):405-15.

118. Takuwa N, Du W, Kaneko E, et al. Tumor-suppressive sphingosine-1-phosphate receptor-2 counteracting tumor-promoting sphingosine-1-phosphate receptor-1 and sphingosine kinase 1-Jekyll Hidden behind Hyde. Am. J. Cancer Res. 2011; 1:460-481.

119. Sonoda Y, Yamamoto D, Sakurai S, et al. FTY720, a novel immunosuppressive agent, induces apoptosis in human glioma cells. Biochem Biophys Res Commun. 2001; 281(2):282-8.

120. Zhang L, Wang H, Zhu J, et al. FTY720 reduces migration and invasion of human glioblastoma cell lines via inhibiting the PI3K/AKT/mTOR/p70S6K signaling pathway. Tumour Biol. 2014; 35(11):10707-14.

121. Beretta F, Bassani S, Binda E, et al. The GluR2 subunit inhibits proliferation by inactivating Src-MAPK signalling and induces apoptosis by means of caspase 3/6-dependent activation in glioma cells. Eur. J. Neurosci. 2009; 30:25-34.

122. Pyne NJ, Ohotski J, Bittman R, et al. The role of sphingosine 1-phosphate in inflammation and cancer. Adv. Biol. Regul. 2014; 54:121-129.

123. Malchinkhuu E, Sato K, Maehama T, et al. S1P (2) receptors mediate inhibition of glioma cell migration through Rho signaling pathways independent of PTEN. Biochem. Biophys. Res. Commun. 2008; 366:963-968.

124. Gulati N, Karsy M, Albert L, et al. Involvement of mTORC1 and mTORC2 in regulation of glioblastoma multiforme growth and motility. Int. J. Oncol. 2009; 35:731-740.

125. Van Brocklyn J, Letterle C, Snyder P, et al. Sphingosine-1-phosphate stimulates human glioma cell proliferation through Gi-coupled receptors: Role of ERK MAP kinase

and phosphatidylinositol 3-kinase beta. Cancer Lett. 2002; 181:195-204.

126. Hu WM, Li L, Jing BQ, et al. Effect of S1P5 on proliferation and migration of human esophageal cancer cells. World J. Gastroenterol. 2010; 15:1859-1866.

127. Nagahashi M, Takabe K, Terracina KP, et al. Sphingosine-1-phosphate transporters as targets for cancer therapy. Biomed Res Int. 2014; 2014:651727.

128. Kubiatowski T, Jang T, Lachyankar MB, et al. Association of increased phosphatidylinositol 3-kinase signaling with increased invasiveness and gelatinase activity in malignant gliomas. J Neurosurg. 2001; 95(3):480-8.

129. Reya T, Morrison SJ, Clarke MF, et al. Stem cells, cancer, and cancer stem cells. Nature. 2001; 414:105-11.

130. Huff CA, Matsui WH, Smith BD, et al. Strategies to eliminate cancer stem cells: Clinical implications. Eur J Cancer. 2006; 42(9):1293-7

131. Mimeault M, Hauke R, Mehta PP, et al. Recent advances in cancer stem/progenitor cell research:therapeutic implications for overcoming resistance to the most aggressive cancers. J Cell Mol Med. 2007; 11(5):981-1011.

132. Dean M, Fojo T, Bates S. Tumour stem cells and drug resistance. Nat Rev Cancer. 2005; 5(4):275-284.

133. Raaijmakers MH. ATP-binding-cassette transporters in hematopoietic stem cells and their utility as therapeutical targets in acute and chronic myeloid leukemia. Leukemia. 2007; 21(10):2094-102.

134. Zeppernick F, Ahmadi R, Campos B, et al. Stem cell marker cd133 affects clinical outcome in glioma patients. Clin Cancer Res. 2008; 14(1):123-9.

135. Sakariassen PA, Immervoll H, Chekenya M. Cancer stem cells as mediators of treatment resistance in brain tumors: status and controversies. Neoplasia. 2007; 9(11):882-92.

136. Chambers I, Colby D, Robertson M, et al. Functional expression cloning of Nanog, a pluripotency sustaining factor in embryonic stem cells. Cell. 2003; 113(5):643-55.

137. Mitsui K, Tokuzawa Y, Itoh H, et al. The homeoprotein Nanog is required formaintenance ofpluripotency inmouse epiblastand ES cells. Cell. 2003; 113(5):631-42.

138. Rodda DJ, Chew JL, Lim LH, et al. Transcriptional regulation of nanog by OCT4 and SOX2. J Biol Chem. 2005; 280(26):24731-7.

139. Wernig M, Meissner A, et al. In vitro reprogramming of fibroblasts into a pluripotent ES-cell-like state. Nature. 2007; 448(7151):318-24.

140. Okita K, Ichisaka T, Yamanaka S. Generation of germline-competent induced pluripotent stem cells. Nature. 2007; 448(7151):313-7.

141. Singh SK, Clarke ID, Terasaki M, et al. Identification of cancer stem cell in human brain tumors. Cancer Res. 2003; 63(18):5821-28.

142. Tohyama T, Lee VM, Rorke LB, et al. Nestin expression in embryonic human neuroepithelium and in human neuroepithelial tumor cells. Lab Invest. 1992; 66(3):303-13.

143. Rutka JT, Ivanchuk S, Mondal S, et al. Co-expression of nestin and vimentin intermediate filaments in invasive human astrocytoma cells. Int J Dev Neurosci. 1999; 17(5-6):503-15.

144. Schiffer D, Manazza A, Tamagno I. Nestin expression in neuroepithelial tumors. Neurosci Lett. 2006; 400(1-2):80-5.

145. Singh SK, Hawkins C, Clarke ID, et al. Identification of human brain tumour initiating cells. Nature. 2004; 432(7017):396-401.

146. Joo KM, Kim SY, Jin X, et al. Clinical and biological implications of CD133 - positive and CD133 - negative cells in glioblastomas. Lab Invest. 2008; 88(8):808-15.

147. Wang J, Sakariassen PO, Tsinkalovsky O, et al. CD133 - negative glioma cells from tumors in nude rats and give rise to CD133 - positive cells. Int J Cancer. 2008; 122(4):761-768.

148. Bien-Möller S, Balz E, Herzog S, et al. Association of Glioblastoma Multiforme Stem Cell Characteristics, Differentiation, and Microglia Marker Genes with Patient Survival. Stem Cells Int. 2018; 2018:9628289.

149. Hossain M, Banik NL, Ray SK. Synergistic anti-cancer mechanisms of curcumin and paclitaxel for growth inhibition of human brain tumor stem cells and LN18 and U138MG cells. Neurochem Int. 2012; 61(7):1102-13.

150. Wu B, Sun C, Feng F, et al. Do relevant markers of cancer stem cells CD133 and Nestin indicate a poor prognosis in glioma patients? A systematic review and meta-analysis. J Exp Clin Cancer Res. 2015; 34:44.

151. Ogden AT, Waziri AE, Lochhead RA, Identification of A2B5+CD133- tumor-initiating

cells in adult human gliomas. Neurosurgery. 2008; 62(2):505-14; discussion 514-5.

152. Kim KJ, Lee KH, Kim HS, et al. The presence of stem cell marker-expressing cells is not prognostically significant in glioblastomas. Neuropathology. 2011; 31(5):494-502.

153. Griguer CE, Oliva CR, Gobin E, et al. CD133 is a marker of bioenergetic stress in human glioma. PLoS One. 2008; 3(11): e3655.

154. Choy W, Nagasawa DT, Trang A, et al. CD133 as a marker for regulation and potential for targeted therapies in glioblastoma multiforme. Neurosurg Clin N Am. 2012 Jul; 23(3):391-405.

155. Bradshaw A, Wickremsekera A, Tan ST, et al. Cancer Stem Cell Hierarchy in Glioblastoma Multiforme. Front Surg. 2016; 3:21.

156. Chen R, Nishimura MC, Bumbaca SM, et al. A hierarchy of serfrenewing tumorinittiating cell types in glioblastoma. Cancer Cell, 2010, 17(4):362-75.

157. Tchoghandjian A, Baeza-Kallee N, Beclin C, et al. Cortical and subventricular zone glioblastoma-derived stem-like cells display different molecular profiles and differential in vitro and in vivo properties. Ann Surg Oncol. 2012; 19(3): 608-19.

158. Cattaneo E, McKay R. Proliferation and differentiation of neuronal stem cells regulated by nerve growth factor. Nature. 1990; 347(6295):762-5.

159. Tohyama T, Lee VM, Rorke LB, et al. Nestin expression in embryonic human neuroepithelium and in human neuroepithelial tumor cells. Lab Invest. 1992; 66(3):303-13.

160. Kleeberger W, Bova GS, Nielsen ME, et al. Roles for the stem cell associated intermediate filament Nestin in prostate cancer migration and metastasis. Cancer Res. 2007; 67(19):9199-206.

161. Zhang M, Song T, Yang L, et al. Nestin and CD133: valuable stem cell-specific markers for determining clinical outcome of glioma patients. J Exp Clin Cancer Res. 2008; 27:85.

162. Sankar A, Thomas DG, Darling JL. Sensitivity of short-term cultures derived from human malignant glioma to the anti-cancer drug temozolomide. Anticancer Drugs. 1999; 10(2):179-85.

163. Pardal R, Clarke MF, Morrison SJ. Applying the principles of stem-cell biology to cancer. Nat Rev Cancer. 2003; 3(12):895-902.

164. Herzog S, Fink MA, Weitmann K, et al. Pim1 kinase is upregulated in glioblastoma

multiforme and mediates tumor cell survival. Neuro Oncol. 2015; 17(2):223-42.

165. De Sousa E Melo F, Vermeulen L, Fessler E, et al. Cancer heterogeneity - a multifaceted view. EMBO Rep. 2013; 14(8):686-95.

166. Marjanovic ND, Weinberg RA, Chaffer CL. Cell plasticity and heterogeneity in cancer. Clin Chem. 2013; 59(1):168-79.

167. Navin NE. Tumor evolution in response to chemotherapy: phenotype versus genotype. Cell Rep. 2014; 6(3):417-9.

168. Gerlinger M, Horswell S, Larkin J, et al. Genomic architecture and evolution of clear cell renal cell carcinomas defined by multiregion sequencing. Nat Genet. 2014; 46(3):225-233.

169. Sottoriva A, Spiteri I, Piccirillo SG, et al. Intratumor heterogeneity in human glioblastoma reflects cancer evolutionary dynamics. Proc Natl Acad Sci USA. 2013; 110(10):4009-14.

170. Almendro V, Marusyk A, Polyak K. Cellular heterogeneity and molecular evolution in cancer. Annu Rev Pathol. 2013; 8:277-302.

171. Patel AP, Tirosh I, Trombetta JJ, et al. Single-cell RNA-seq highlights intratumoral heterogeneity in primary glioblastoma. Science. 2014; 344(6190):1396-401.

172. Lee E, Yong RL, Paddison P, et al. Comparison of glioblastoma (GBM) molecular classification methods. Semin Cancer Biol. 2018; 53:201-211.

173. Navin N, Kendall J, Troge J, et al. Tumour evolution inferred by single-cell sequencing. Nature. 2011; 472(7341):90-4.

174. Hyman DM, Puzanov I, Subbiah V, et al. Vemurafenib in multiple nonmelanoma cancers with BRAF V600 mutations. N Engl J Med. 2015; 373(8):726-36.

175. Schwaederle M, Daniels G A, Piccioni D E, et al. On the road to precision cancer medicine: analysis of genomic biomarker actionability in 439 patients. Mol Cancer Ther. 2015; 14(6):1488-94.

Eidesstattliche Erklärung

Hiermit erkläre ich, dass ich die vorliegende Dissertation selbständig verfasst und keine anderen als die angegebenen Hilfsmittel benutzt habe.

Die Dissertation ist bisher keiner anderen Fakultät, keiner anderen wissenschaftlichen Einrichtung vorgelegt worden.

Ich erkläre, dass ich bisher kein Promotionsverfahren erfolglos beendet habe und dass eine Aberkennung eines bereits erworbenen Doktorgrades nicht vorliegt.

Datum: 24.08.2020
Unterschrift: Yong Xiao

Acknowledgements

Before concluding this thesis, my deepest gratitude goes first and foremost to my supervisor, Prof. Henry Schroeder who have leaded me into a challenging yet fascinating field of academic research. The profit that I gained from them will be of everlasting significance to my future research.

I would like to express my utmost gratitude to my research supervisor. Prof. Bernhard H. Rauch for his sincere and selfless support, prompt and useful advice during my research. He has walked me through all the stages of the writing of this thesis. He gives me a lifetime unforgettable memory of benevolence, patience, intelligence, diligence and erudition.

I would like to express my heartfelt gratitude to Dr. Sascha Marx, who help me in the most difficult time of my life. Meanwhile, during the past two and half years, he also provided me with valuable suggestions about study and life which may benefit me in my whole life.

I would like to express my sincere gratitude to Dr. Sandra Bien-Möller, who led me into the world of Pharmacology. Profound and intelligent, she endowed me with new insights towards my study. Special thanks she've put considerable time and effort into her ments on the draft. Without her consistent and illuminating instruction, this thesis could not have reached its present form.

I am also greatly indebted to all the faculty and staff at the Department of Neurosurgery and Pharmacology: Dr. Markus Grube, Ms. Tina Sonnenberger, Ms. Elke Rösel, etc., who have instructed and helped me a lot in the past two years. You've made me feel warm in a foreign country.

Finally, I'd like to extend my thanks to my family, significant other, and my friends who often give me care and encouragement in the process of my study. Under their love, I can go with strong motivation and power and that now I can be here, completing my postgraduate study smoothly.